POTENTIALLY TSUNAMIGENIC EVENT LAYER IN LATE HOLOCENE GREAT SOUTH BAY, LONG ISLAND, NEW YORK: CONSTRAINTS ON ORIGINS, PROCESSES, AND EFFECTS

By

Sarah Krentz

Thesis

Submitted to the Faculty of the

Graduate School of Vanderbilt University

in partial fulfillment of the requirements

for the degree of

MASTER OF SCIENCE

in

Earth and Environmental Sciences

August 2009

Nashville, Tennessee

Approved:

Professor Steven Goodbred, Jr.
Professor Molly Miller

ACKNOWLEDGEMENTS

This work could not have been undertaken without the financial support of NY Sea Grant for funding the initial 2004-2005 REU program to collect the Long Island Data as well as the Vanderbilt Department of Earth and Environmental Sciences and my advisor, Dr. Steve Goodbred Jr., for continued support. Thanks also go to my entire advisory committee for their guidance.

I am grateful to Roberta Challener, the crew of the RV Peconic, and Sarah Koehler, Yugo Nakai, Zach Tessler, and Zac Duval for all their tireless, volunteered assistance in Great South Bay June 2008 fieldwork. The core data could not have been recovered without their perseverance. Thanks also to those who performed the many previous fieldwork and analyses related to the project, particularly Philip LoCicero. And my sincere apologies go to those who had the misfortune of working in the lab while the cores were being analyzed, it is a smell that is not easily forgotten.

I am also incalculably grateful to my partner, Heather for her love and encouragement. She has been my cheerleader, sounding board, proofreader, and has provided endless hugs and twizzlers throughout this process. Most importantly, I would like to thank Dr. Steve Goodbred Jr. for his endless insights, enthusiasm, and always keeping his lab door open to me. It has been an amazing opportunity to be able to work with him for the past 5 years.

TABLE OF CONTENTS

LIST OF TABLES

LIST OF FIGURES

INTRODUCTION

It is widely recognized that high-energy events such as storms and tsunami have significant effects on coastal systems over short timescales. While many of these systems show a recovery to the pre-event dynamic equilibrium, longer term impacts to the coastal zone are less well known. A recent study of late Holocene history in the Great South Bay estuary, Long Island, New York shows evidence for a high-energy deposit emplaced between 2200-2400 yr BP coincident with a permanent change of the estuarine system from its pre-event depositional environment. This deposit is referred to as the Major Depositional Event (or MDE), however as will be discussed in the study, its presence may result from instantaneous or ongoing geologic processes.

With significant human population and real estate located on the mainland shores and barrier island, stability and susceptibility of the Great South Bay system to reorganization is a major concern. Much effort has gone into understanding recent dynamics of the barrier and its inlets (Rampino 1980; Bonisteel 2004), and even effort into curtailing significant changes in them (Kraus 2003). However, less is known about the frequency and longer term impact that a high-energy event would have on the system as a whole. The anomalous MDE deposit seen in the sediment record and its potential influence in the area will be investigated in this study.

The current Great South Bay back-barrier lagoonal system is approximately 30 km long and bounded by Long Island to the north and the Fire Island barrier complex to the south (Fig. 1). The estuary is relatively shallow with a mean depth of 2.3 meters and a small tidal range of 0.3 meters(Schubel 1991). In contrast, 20,000 years ago at the Last Glacial Maximum, much of northeastern North America and most of Long Island were covered by the Laurentide ice sheet (Figure 2 from Dyke 2002). Sea level was approximately 120 meters lower than present, subaerially exposing the present day continental shelf of the New York-New Jersey bight. As climate warmed,

the ice sheet melted and sea levels rose, transgressing the shelf to initially form a paludal environment that subsequently developed into the current estuarine environment and surrounding topography of Long Island (Rampino 1980).

Questions to be investigated

Vibracores and shallow seismic surveys of Great South Bay backbarrier lagoon reveal an anomalous sedimentary deposit. These 20-30 cm-thick units are composed of either gravel-based sands or reworked shell deposits and are traceable over 100s of meters in the seismic record. Radiocarbon dates well constrain the age of these horizons between 2100-2400 yBP. The deposit is anomalous in the sedimentary record and its large grain size indicates a high energy formation. The date of the deposits formation also coincides with an abrupt transition into the modern estuarine depositional regime of the bay.

What mechanism or process formed the Major Depositional Event (MDE) layer?

Competing, plausible modes for the deposit's formation are (i) a storm/hurricane event, (ii) a transgressive lag layer resulting from rising sea levels, or (iii) a tsunami event. Storms and hurricanes presently influence Long Islandand are also recorded in the backbarrier sediments as deposits of overwash sand (Scileppi 2007). However, as the estuary's formation is a result of sea-level rise and coastal transgression, a sand and gravel layer could also be formed by waves at the transgressing shoreface (Varekamp 1991). Last, while tsunami events are rare along the passive Atlantic margin, they are not unheard of. For example the 1929 Grand Banks tsunami occurred further up the east coast from Long Island and resulted from sediment slumping caused by an offshore earthquake (Heezen and Ewing 1952). The mid-Atlantic margin has also been recognized as vulnerable to

tsunami events (Driscoll, 2000), and both tsunami monitoring systems and hazard assessment are currently under investigation by US and Canadian agencies (Geist and Parsons 2009; O'Reilly 2007).

How does the MDE deposit fit into the geologic history of the Great South Bay during late Holocene transgression?

Once the mechanism of deposition is further constrained, it is also important to understand how the event or processes have affected the estuary throughout its evolution during the late Holocene. Understanding such influences or response of the modern coastal system is of particular concern for potentially recurring events such as storm or tsunami.

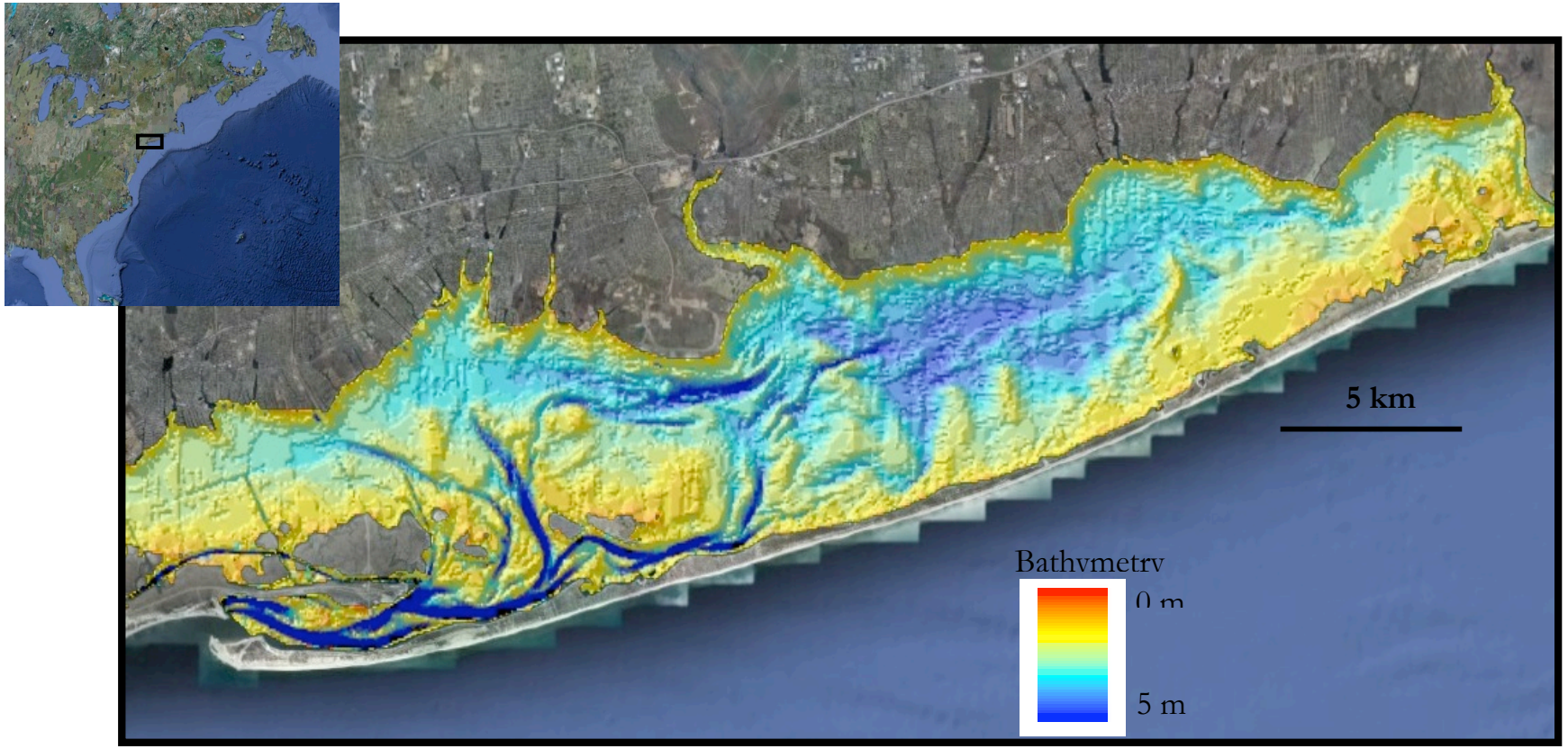

Figure 1: Locaation and bathymetry of Great South Bay (data courtesy of NOAA, plotted in Google Earth)

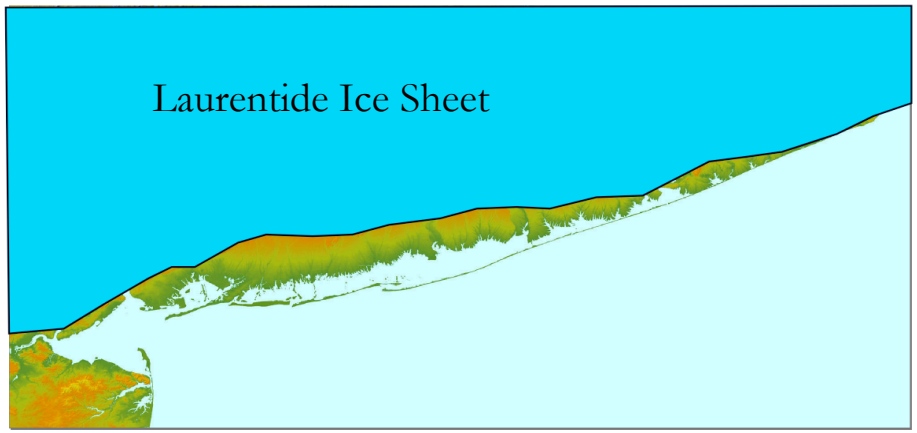

Last Glacial Maximum

Present

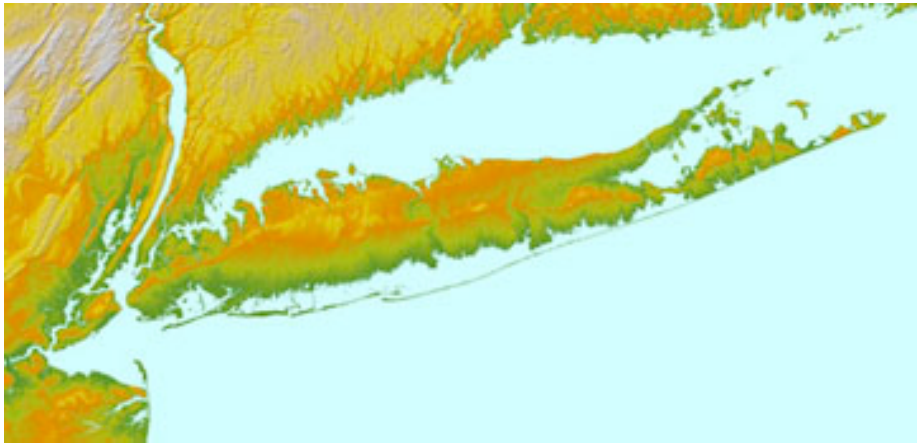

Figure 2: Maps of Long Island, New York showing maximum extent of the Laurentide Ice Sheet (above; based on Dyke 2002) and the present day shoreline and topography (below; digital elevation model courtesy of Bret Bennington, Hofstra University, NY.)

METHODS

During the summers of 2004 and 2005, 34 vibracores and ~200 km of high-resolution sub-bottom profiling data were collected (Fig. 3). Sub-bottom data were collected with an Edgetech CHIRP sonar unit using a 2-12 kHz swept frequency at a sampling rate of 50 ms, giving 1-10 m of acoustic penetration into sediments with a vertical resolution of approximately 6 cm. Data was viewed in the native Edgetech software and post-processed in Seismic UNIX as well as Triton Sub-Bottom Interpreter software in order to remove seismic noise and artifacts. Major sub-bottom acoustic reflectors were traced and exported using the Triton program and plotted in ArcGIS software and Microsoft Excel.

The 34 core locations were chosen based on results from the acoustic profiles, targeting a variety of observed stratigraphic sequences, including many infilled channel sequences, near-barrier locations and mainland-proximal locations (Fig. 3). In June of 2008, 8 additional vibracores (GSB 101 – GSB 108) were collected specifically targeting the MDE deposit. While initial coring and processing was performed as part of the NY Sea Grant Study (which will be detailed in the following section), additional core analyses, sonar data processing with Triton software, and the acquisition and processing of cores 101-108 were all performed as part of this thesis research.

All cores ranged from 1-5 m in length. After being split, one half of each core was sealed and archived while the other half was visually examined, photographed, in some cases X-radiographed, and sampled for sediment analyses. These analyses were performed to establish criteria for identifying major and minor facies, including their physical and lithological characteristics and spatial distribution. That information was then used to determine the depositional environments in which the facies were formed, in order to characterize different phases of the Great

South Bay's geologic history. Much of the initial facies identification was done in the 2004-2005 NY Sea Grant study as detailed in the results section.

Physical characteristics

After each core was split, it was visually examined and logged for color, lithology, major facies, organic remains, bedding, burrows, and sedimentary structures. Molluskan fauna were also sampled, categorized, and identified, as part of another study (LoCicero 2006).

Core sediments were sampled at 5-10 cm intervals and weighted before and after 12 hours in a drying oven to determine water content, which is in part related to porosity, compaction, and sedimentation rates. The dried sediments were then weighed before and after 6 hours in a combustion oven at 450° C to determine bulk organic conent.

Sediment grain-size distributions were also measured for each major facies and the MDE deposit using a Malvern laser-diffraction size analyzer (Mastersizer 2000E). Data were exported and normalized to the sand fraction in order to compare samples within and among the different facies. As the analytical range for the instrument is 0.001 - 1.7 mm, larger particles were dry-sieved and massed in order to be incorporated in the grain-size distribution profiles.

Radiocarbon dating

In addition to constraining the facies' physical boundaries, identifying their age is also crucial to understanding the estuary's history. 38 samples from 16 different cores were radiocarbon dated by Accelerator Mass Spectrometry (AMS) at the National Ocean Sciences AMS facility in Woods Hole, MA. Radiocarbon ages were calibrated and corrected for reservoir effects (Appendix A) using the online Calib 5.0 program (Stuiver et al. 2005). These dates were then used to temporally

constrain facies as well as calculate various accretion rates. All ages are reported here as calibrated yr BP.

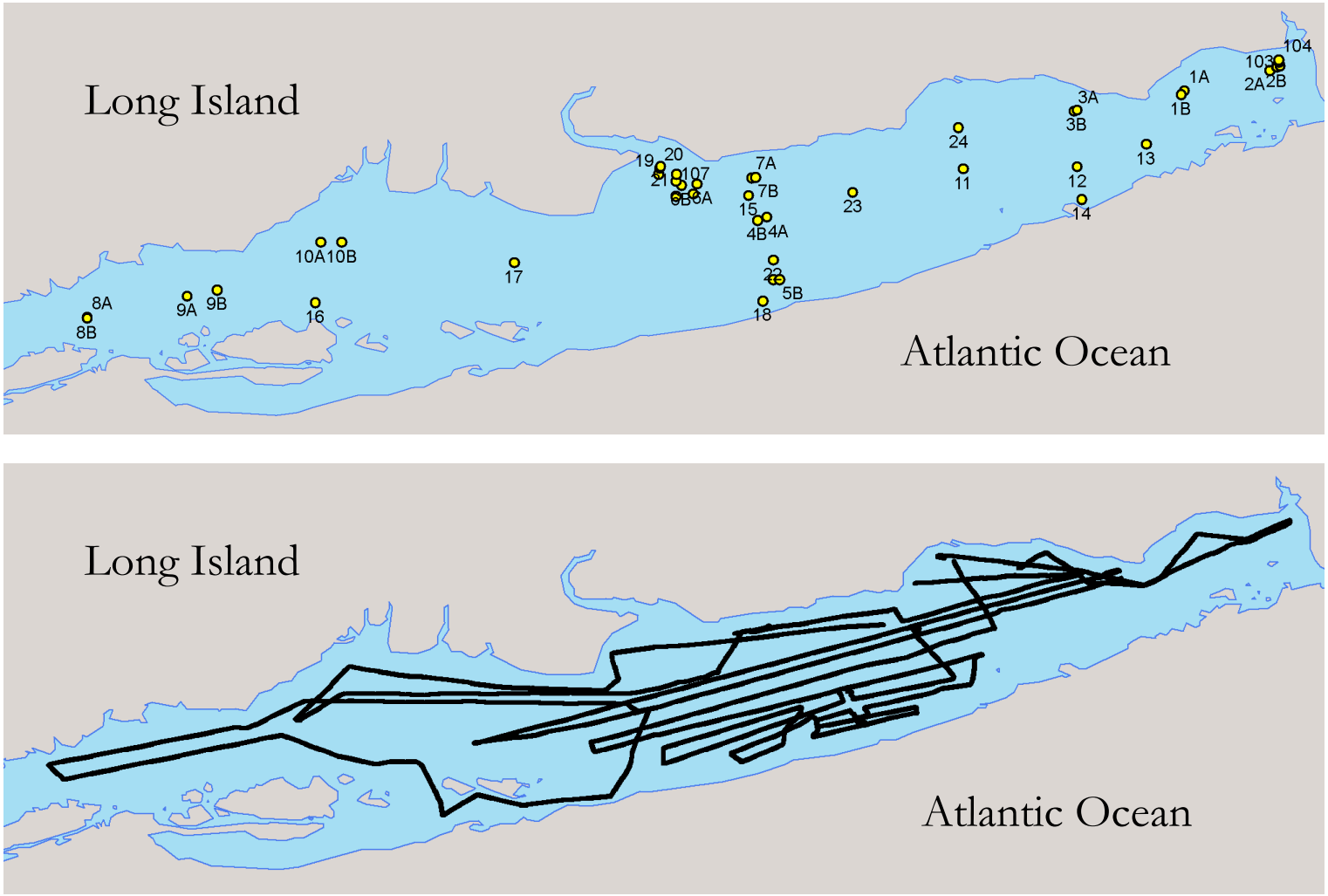

Figure 3: Core locations (top) and seismic survey tracklines (bottom) in Great South Bay, Long Island, New York.

RESULTS

Description of major facies

Previous results from Great South Bay describefour main facies within the late Quaternary stratigraphy (Goodbred 2007; Fig. 4; Table 1). Descriptions of the facies are detailed below.

Glacial Outwash

Core and acoustic records show the entire estuary to be underlain by sands and gravels expelled from the melting and retreating Laurentide ice sheet (Figs. 5, 6). Based on the known geologic and climate history of the region, the outwash is assumed to have been emplaced during the deglaciation of the area, approximately 15,000-18,000 yr BP (Rampino 1980).

These sands and gravel create a strong acoustic reflector, allowing the deposit to easily be traced in the seismic record (Fig. 5). The exception to this is close to the barrier island, where the modern estuary bottom consists of sandy, acoustically reflective deposits, allowing very little penetration into the underlying sediments. The outwash deposits are generally massive, and in several cores the upper portion of the deposit appears to have been subaerially exposed and reworked by during the late Holocene trangsression. In acoustic records, the outwash surface is seen to define complex sub-bottom incised channel complexes, many of which align with current rivers and creeks of Long Island. The glacial outwash outcrops in one portion of the bay, and the rest of this basal topography has been infilled and covered by the more recent facies of the estuary.

Table 1: Facies table of late Holocene Great South Bay stratigraphy (modified from Goodbred 2007)

Facies	Lithology	Sedimentary Structure	Organic Matter	Shells	Acoustic Character	Period of Deposition	Environmental Interpretation
Glacial Outwash	poorly sorted sands and gravel with occasional small mud subcomponent, particularly at top of unit	Massive	primarily none, occasional woody roots near top of unit	none	widespread, prominent basal reflector in the estuary; surface frequently incised; shows topography ranging from 10m depth to outcropping in modern seabed	estimated ~15,000 to 20,000 yr BP	glacial and post-glacial braided outwash plain
Vegetated Intertidal Clays	brown to blackish clays with abundant organic matter; no sands or silt	well-defined planar laminae to parallel bedded muds and organic-rich muds	LOI=5-30%, up to 60%	none	generally acoustically transparent	~3900 to ~2300 yr BP from 6 dates	fresh to oligohaline tidal marsh
Estuarine Muds	gray muds with variable sand content (5-30% weight)	little to no preserved structure; occasional mud-filled burrow or bioturbated sand horizons	LOI <5%; occasional laminae of sea-grass detritus	Common estuarine molluscan fauna and occasional shell beds	occasional weak internal reflectors; stronger and more frequent reflectors where muds alternate with sand units in seaward portions of the bay	~3900 yr BP to present from 20 dates	subtidal estuarine lagoon; basin settings typically more distal (>2 km) to barrier
Estuarine Sands	tan to gray sands and muddy sands	Little to no structure; occasional coarse bedding or interbedded sandy muds	None	sporadic shell hash; rarely concentrated in beds	Strong reflectore, generally with little acoustic penetration particularly near barrier	~1900 yr BP to present from 12 dates	Subtidal estuarine lagoon; flood-tidal delta complex or breach/overwash, typically more proximal (<2 km) to barrier
Major Depositional Event (MDE)	Sands, sands and gravel, or densely packed shell (*Gemma gemma*) beds	Rough fining up pattern in sand and gravel, units, no structure in shell beds or sand units; erosive basal contact with diffuse, often bioturbated, upper contact	none	None in sand or sand and gravel units; dense shell beds composed of *Gemma gema*	prominent and baywide reflector; drapes over existing topography with depth ranges from .1-4.5 m below surface; acoustic character is consistent baywide	2200 to 2400 yr BP from 7 dates	(see text)

Vegetated Intertidal Clays

Above the glacial outwash facies in the stratigraphic record is a series of fine-grained (<10 μm) organic-rich clays. The facies is rich with organic matter, showing thin laminae and often beds of roots and woody-plant fragments. No shell material is found in any instance of this facies. Based on the abundance of terrestrial plant material and absence of marine or estuarine shells, the deposit is interpreted to be a fresh to brackish tidal marsh. Where present, the deposit overlies glacial outwash sands and gravels at was recovered in 30% of the cores. The facies was generally absent from deeper outwash channels, where the organic-rich clay unit is absent. In these cases facies shift from glacial to subtidal estuarine with no freshwater or intertidal phase. Due to their deeper depths, it is assumed that the sites with no intertidal facies became flooded as estuarine environments earlier in GSB's history than other locations. These deeper channel thalwegs infilled first while their shallower banks became vegetated marsh environments before sea level eventually transgressed the entire channel feature. Radiocarbon dates (Appendix A) of roots and grasses from this facies were sampled from the basal glacial outwash contact of several cores and the upper contact with MDE or estuarine muds. These dates constrain deposition of the Vegetated Intertidal Clay facies from 4400-2300 yr BP.

Estuarine Muds

Gray estuarine muds are the most pervasive facies found in the Great South Bay, being recovered in 95% of the cores. Though the facies sediments vary in sand, organic, and shell content, they occur in every area of the estuary at some time during the late Holocene. Radiocarbon dates of estuarine shells near the basal contact with the glacial outwash surface show the facies ot have been deposited in the deepest portions of the estuary as early as 3900 yr BP, possibly even 4100 yr BP using extrapolation from accretion rates (2.3 mm/yr). In several cores, the muddy facies persists for

several thousand years to the present. It can be assumed, then, that the facies appears to correspond to the modern environment in which it occurs – relatively low-energy portions of the estuarine system away from active reworking by barrier inlet and overwash processes.

Estuarine Sands

Like the estuarine muds, sandy estuarine deposits are common throughout the modern estuary and within the stratigraphy, being recovered in 69% of the cores. The facies is generally thick (20-150 cm), massive, and tend to comprise clean sand, particularly in areas adjacent to the barrier island. While many examples of the estuarine sands are found in cores <2 km from the current barrier island, and assumed to represent periods of barrier breaching or inlet activity, they also occur closer to Long Island and are also likely associated with inlet processes. The lower contact of these deposits tends to be sharp, though not erosive, representing an abrupt change in depositional processes or an event related deposit. Several near-barrier cores also show repeated layers of these clean sands, possibly reflecting repeated barrier breaches or inlet formations. Radiocarbon dates of articulated bivalve shells in these sands place the deposits as old as 1900 yr BP, and these facies persist through to the present.

Major Depositional Event (MDE) – Samples of the facies recovered in: 2A, 2B, 3A, 3B, 6A, 7A, 19, 20, 21, 101, 102, 104, 105 (13 of 42 cores)

An anomalous fifth facies was also recognized from previous research in Great South Bay, being comprised mainly of sands and gravels with a rip-up basal contact with the underlying fine-grained sediments. The deposit was found in 30% of the cores. While these deposits were initially termed the MDE, this study will investigate whether it formed from an event or process.

The MDE facies is variable and comprised of 3 subfacies that include (i) sand and gravel, (ii) sand, and (iii) a densely packed, articulated shell bed. All 3 types display an irregular rip-up basal surface and a diffuse, often bioturbated, upper contact. At least one example also contains rip-up clasts. These findings are suggestive of a high-energy process. The MDE layer overlies glacial outwash, freshwater, and estuarine mud facies but is always overtopped by an estuarine mud to sandy mud.Radiocarbon dates from the basal contact of the MDE deposits are nearly contemporaneous (<200 years), and their calibrated 2-sigma age ranges are statistically indistinguishable.

Sand and gravel MDE – Samples of the facies recovered in: 2B, 3A, 6A, 7A, 102, 104, 105 (7 of 13 MDE cores)

The most common manifestation of the MDE facies are coarse sands, gravels, and small cobbles (Fig. 7A). The deposit is 5-25 cm thick and exhibits some modest upward and landward fining (see Grain Size section). Stratigraphically, the sand and gravel unit is always bound on top by the estuarine mud facies, whereas its basal contact lies on top of freshwater organic-rich muds, glacial outwash, or estuarine muds.

Sand MDE – Samples of the facies recovered in: 2A, 101, 102 (3 of 13 MDE cores)

Several of the cores containing the MDE facies display similar characteristics to the sand and gravel deposit, but lack the gravel fraction (Fig. 7b). This manifestation of the deposit is also 5-25 cm thick with little to no fining. As in the sand and gravel deposit, the sand-only variety of the MDE is consistently overlain by the estuarine facies but lies on top of freshwater organic-rich muds.

Shell bed MDE – Samples of the facies recovered in: 19, 20, 21 (3 of 13 MDE cores)

This third variety of the MDEfacies consists of dense, articulated shell beds of the bivalve *Gemma gemma (Fig. 7c)*. The approximately 30 cm deposit consists of articulated shells and muds, with little to no sand. Gemma gemma is a small (<5 mm), common species throughout the late Holocene stratigraphy (LoCicero 2006), but it dwells in high energy, sandy substrates such as inlets (Schubel 1991). Therefore, their presence in muddy substrates suggests that they were transported and emplaced en masse.

Despite lithologic differences, the three MDE subfacies are well correlated in the seismic record (Fig. 8). In these data a relatively strong, acoustic boundary corresponding to the MDE is seen to be draped on top of the strong basal glacial-outwash reflector. The MDE reflector also mimics the existing glacial outwash topography and is unique in this characteristic. Other reflectors seen in the seismic record, even those corresponding to the relatively large changes between facies, are modest reflectors in comparison to those formed by the MDE deposits.

Spatial and temporal characteristics of the MDE layer

Spatial extent of the MDE layer

The MDE deposit is widely distributed throughout the bay (Figure 9), with the majority of it found in the northern third of the estuary, nearest to the mainland. While the deposit was not identified closer to the barrier island, the high acoustic reflectivity of the sandy bottom may be masking the deposit in this area. In very sandy stratigraphy it also may be difficult to distinguish the deposit from other sands deposited by storms or barrier-related processes. Nevertheless, cores and seismic data showing the MDE deposit are robust and widespread.

Comparisons of MDE thickness, depositional depth, and distance to current shoreline show trends of thinning and shallowing landward, assuming a paleoshoreline orientation similar to today's (Figures 10-12). There also appears to be a correlation between thickness of deposit and depth of deposition, with thinner deposits emplaced at higher paleoelevations.

In addition to MDE's geographic distribution (Figure 9), mapping of the MDE reflector from the seismic record also allows its the deposit's depth distribution to be observed (Figure 13), demonstrating variable and significant relief. In several sonar records with a continuous MDE reflector , the depth of the deposit varies as much as 2.5 meters in less than a kilometer. Other reflectors, such as those associated with facies transitions, tend to be more planar in character, as they are emplaced by environmental conditions that are directly related to sea level rise. The MDE deposit, by contrast, is unique in its physical character and spatial distribution (Table 2).

Table 2: Major characteristics of the MDE layer and its surrounding facies.

Core	thickness (cm)	depth of MDE basal contact (cm below sea level)	MDE sediment type	Overlying facies	underlying facies	latitude	longitude	seismic file containing core	perpendicular distance from modern shoreline (m)
2A	12	325	sand	estuarine muds	organic-rich mud	40.751600	-72.900020	P4	860
2B	15	230	sand and gravel	sandy estuarine muds	organic-rich mud	40.752780	-72.897460	P4	761
3A	14	397	sand and gravel	estuarine sands	estuarine muds	40.736600	-72.971800	P23	937
3B	25	360	sand and gravel	estuarine muds	organic-rich mud	40.736900	-72.970630	P23	874
6A	24	379	sand and gravel	sandy estuarine muds	organic-rich mud	40.709970	-73.110233	P19	984
7A	22	327	sand and gravel	sandy estuarine muds	sandy glacial outwash	40.712283	-73.090067	P19	1041
20	25	425	*gemma gemma* and gravel	estuarine muds	estuarine muds	40.715683	-73.123717	P64	
101	12	228	sand	sandy estuarine muds	organic-rich mud	40.752800	-72.897217	offline	760
102	9	214	sand and gravel	sandy estuarine muds	organic-rich mud	40.753150	-72.896200	offline	727
104	14	169	sand and gravel	sandy estuarine muds	estuarine muds	40.755400	-72.896700	offline	478
105	~30	455	sand and gravel	sand and gravelly estuarine muds	glacial outwash	40.705517	-73.117867	offline	

Age of the MDE layer

With the exception of the dense shell bed, the MDE deposit itself tends to be fairly sparse in radiocarbon-dateable material. However, one radiocarbon date within the deposit and 5 others immediately beneath the MDE layer are well-correlated (Table 3). This correlation, even with analytical and calibration errors factored in, suggests the MDE deposit to be rapidly emplaced as an event layer rather than by a longer-term time-transgressive estuarine process.

Table 3: Calibrated radiocarbon dates of basal contact of the MDE layer

Core	Calibrated age (yr BP)	Stratigraphic Position
2A	**2403**	1 cm below MDE in freshwater organics
3A	**2267**	articulated *Gemma gemma* shell at base of MDE
3B	**2829**	3 cm below MDE contact into freshwater muds
6A	**2451**	1 cm below MDE in freshwater sediments
20	**2323**	base of MDE, articulated shell
20	**2456**	2 cm below MDE in estuarine muds below MDE

Chronostratigraphic context

In order to determine the impact, if any, of the MDE on the rest of the estuary and its evolution, the deposit must be put in a chronostratigraphic context. With this aim, the bay was divided into 13 geographic zones, based on core data. The boundaries and facies within each zone were then converted from depth (below sea level) to time (yr BP) in order to allow comparison. Despite the Great South Bay occupying a relatively small area, the estuary is a dynamic and heterogeneous environment; thus these 13 sectors are highly variable.

The depth-time relationships and rates of sedimentation for chronostratigraphy were determined from 38 radiocarbon dates processed and calibrated from the cores (Appendix A). These rates are critical to determine ages of facies within the cores that may not have been dated. In each particular zone, a specific accretion rate was calculated for that geographic area based on the calibrated radiocarbon ages, however, baywide the rates should be reasonably well constrained. By plotting these calibrated dates against the depth below mean sea level from which the dated samples are recovered (Figure 14), these baywide average accretion rates can be seen. The plot shows a consistent general trend of 1.5 mm/yr as the current estuarine sedimentation rate. This accretion nearly doubles to 2.4 mm/yr for some old, deep infilled estuarine sequences in incised channels and is roughly halved, at .75 mm/yr, in the equally old freshwater marshes.

Figure 15 shows the geographic locations and cores that comprise the 13 zones. The main facies and characteristics of these zones will be detailed below. For all units, the outwash sands and gravels are assumed to have been emplaced 15,000-20,000 yr BP based on the known climate and ice sheet changes (Rampino 1980). Any material dated from this unit indicates a time when the outwash was subaerially or subaqueously exposed post deposition. All radiocarbon dates have been calibrated to correct for reservoir effects.

Zone A

Zone A lies in the westernmost part of the Great South Bay and currently has a muddy to sandy mud bottom in this region (Figure 16). Sea grass fragments in estuarine muds from 185 cm in core 8A were radiocarbon dated and calibrated to 1236 yr BP, giving an estuarine accretion rate for this zone of 1.5 mm/yr. The estuarine facies sits immediately atop a clean sand unit that is atop mud, sand and gravel outwash. A soft bark piece from near the top of this glacial unit at 335 cm has a calibrated radiocarbon date of 3921 yr BP.

Estuarine muds extend from 0-290 cm in the dated core and were of similar magnitude in the undated core 8B. Using the 1.5 mm/yr estuarine accretion rate and also assuming an order of magnitude accretion of the sands of 1 cm/yr there is a gap of roughly 2000 years. As there is appears to be a sharp unconformity between the estuarine unit and the sands, the missing time is most likely between these facies either eroded or never deposited.

Zone B

Zone B is also in the western portion of the bay and is characterized by modern muds, sandier than zone A with several small sand layers (Figure 17). Within the sandy muds at 185 cm from core 9B a fragment of a *Crepidula* mollusk has a calibrated date of 1134 yr BP giving an estuarine accretion rate of 1.6 mm/yr. Below the estuarine facies lie organic-rich mud deposits which extend to the end of the cores. A radiocarbon date of these organic sediments from 278 cm in core 9B calibrates to 3624 yr BP. Using an accretion rate of .75 mm/yr for this facies, the age of the bottom of this core is about 4400 yr BP. Estuarine deposits extend from 0-260 cm within the cores with the freshwater facies beginning at this point. However, these accretion rates only account for a portion of this 4400-year record. From approximately 1800 to 3500 yr BP no lithologic record exists, either due to non-deposition or erosion.

Zone C

Zone C, while still in the western third of the estuary, differs from the previous two in the area (Figure 18). The two cores in the zone are from a deeper part of the basin and are comprised entirely of estuarine muds with varying sand and shell content throughout. 5 radiocarbon dates from core 10B give a very steady sedimentation rate of 1.2 mm/yr for the

past 4,000 years in this area (Figure 19). The cores show that Zone C transitioned into an estuarine environment early in the bay's history and this environment has persisted through to the present. While no distinct deposit is visible, acoustic data in Zone D shows a clear but faint reflector corresponding to a 20-cm section of lower density muds in core 10B.

Zone D

As in the previous region, zone D also transitioned into an estuarine environment early in the evolution of the bay (Figure 19). Core 17 shows an estuarine sequence from 0-98 cm, with a thick clean sand unit from 98-240 cm. The base of the core comprises glacial outwash deposits. A sea-grass fragment from near the top of the clean sand unit dates to 1890 yr BP. Assuming an order of magnitude accretion rate of 1 cm/yr for the clean sands, the thick deposit was emplaced over roughly 140 years, most likely related to inlet processes. Muddy sands and a glacial outwash unit underlie the clean sand unit with the glacial unit showing evidence of oxidation, indicating subaerial exposure at some point in time.

Zone E1

Zone E, while small in geographic size, shows some key differences and therefore has been subdivided further into subzones E1 and E2 (Figure 20). Cores from sub-zone E1 were taken in deep, infilled channels, with estuarine muds dating as old as 3370 yr BP. In the middle of these estuarine muds lies the dense, articulated *Gemma gemma* bed identified as the MDE deposit. Radiocarbon dates from articulated shells from the top and bottom of the deposit in core 20 date to 2309 and 2323 yr BP, respectively, with a sea-grass fragment 15 cm below the deposit dating to 2456 yr BP. The narrow age range of the 15-cm thick deposit indicates emplacement by a single event rather than an ongoing process. 150 cm of

estuarine muds lie above the shell layer. Using an estuarine accretion rate of 1.5 mm/yr, these muds account for 1000 years of sediment accretion. As the top of the shell bed dates to 2309 yr BP, there is an approximately 1300 year gap in sedimentation following emplacement of the MDE deposit.

As there are neither visible unconformities nor other seismic reflectors above the MDE in the acoustic record, it is likely that a period of non-deposition immediately followed the MDE event. Using the same 1.5 mm/yr accretion rate, the estuarine muds in the bottom of the core can be extrapolated back to approximately 3370 yr BP. Similar to Zones C and D, Zone E1 contains a deeper infilled outwash channel. This portion of E1 is aligned with the current Great River on mainland Long Island, suggesting that this valley was an estuarine environment early in the bay's evolution with a depositional hiatus from approximately 2300 to 1000 yr BP.

Zone E2

In contrast to Zone E1 within the deeper paleochannel, Zone E2 encompasses the edges of the paleo Great River channel *(Figure 21)*. The modern environment in this area consists of sandy muds, whichpersist for the upper 60 cm of the core and account for approximately 400 years of deposition using a 1.5 mm/yr sedimentation rate. Underlying these muds is the 25-cm thick MDE deposit, containing sands and large gravels and cobbles. A wood fragment from organic-rich muds immediately below the MDE layer in core 6A dates to 2451 yr BP, and this organic mud facies persists to the bottom of the cores. Using a modest accretion rate of 0.75 mm/yr for this 87-cm thick deposit shows the fresh to brackish tidal marshes being established by at least 3600 yr BP, if not earlier. Assuming a maximum erosion of 100 years of sediment associated with emplacement of the MDE

deposit, there is an almost 2000-year sedimentation hiatus following its emplacement in this region of the estuary.

Zone F

Zone F lies in the northern portion of the bay, east of Zone E (Figure 22). Like zone E, it contains sandy muds and a well-defined sand and gravel MDE facies. No radiocarbon dates were taken from the 2 cores that comprise this zone, however using a 1.5 mm/yr accretion rate shows the estuarine sandy muds to have existed and deposited in the bay for the past 730 years. The MDE layer underlies these estuarine deposits and sits atop thick, clean sands. Based on dated and seismic correlation of all other MDE deposits, it is assumed that the MDE facies in zone F was also emplaced in an event approximately 2300 yr BP, giving a depositional hiatus of 1600 years following the event.

Zone G

Zone G is in the middle of the bay, encompassing cores near the barrier as well as close to the modern shoreline of Long Island (Figure 23). Core deposits consist of estuarine muds with several sand layers immediately atop glacial sands and gravels. A wood fragment from the top of the glacial outwash dates to 2909 yr BP, indicating that the outwash surface was exposed at this time. A mollusk from core 18 at 90 centimeters dates to 660 yr BP giving a local accretion rate of 1.4 mm/yr. Another mollusk from a sandier deposit in core 4B at 280 cm dates to 1911 yr BP. Using the 1.4 mm/yr accretion rate, the sandier deposit was deposited from approximately 1360 to 2180 yr BP with a gap in sedimentation from 1360 to 660 yr BP as well as from 2909 to 2180 yr BP. While no MDE deposit is seen in the lithology in this zone, there is a gap in sedimentation at the 2300 yr BP point. Or the

deposit may be present but the sandy MDE facies may not be distinguishable amid other sand-dominated facies.

Zone H

Zone H lies in the southeastern portion of the estuary quite close to the current barrier island (Figure 24). Deposits consist of muddy sands, thin sand lenses, and massive clean sand units relating to barrier island dynamics. As in other zones, the sands and muds have accretion rates differing by an order of magnitude. Three dates from cores 12 and 14 show the estuarine environment existing by at least 1875 yr BP. These dates are plotted in Figure 24 against their depth below sea level. The graph shows that the average accretion rate during this period was 0.37 mm/yr. As 0.37 mm/yr is slower than expected for an estuary higher average rates of 1.5 mm/yr and 1 cm/yr in muds and sands, respectively, the lithologically varying deposits in Zone H also likely include depositional hiatuses, although they are difficult to constrain.

Zone I

Like Zone H, all cores from Zone I consist of estuarine facies, showing the current estuarine environment was established in this mid-bay area at least 2620 yr BP (Figure 25). Cores from this zone consist of varying estuarine muds and sands interspersed with thin sand lenses, as well as thicker clean sand units related to overwash events and inlet processes in this active portion of the estuary. Figure 25 shows a plot of the 10 radiocarbon dates from cores 11, 22, and 23. However as in Zone H, the cores contain such a variety of deposits with accretion rates that are likely an order of magnitude apart, the 0.45 mm/yr is not necessarily a good average to use. This relatively slow sedimentation rate suggests that

there are likely gaps in deposition during the period investigated, although these are difficult to constrain without additional information. The oldest radiocarbon date from this zone records the estuarine environment being established there by at least 2620 yr BP, and likely prior as the 2620 yr BP date comes from the middle of a shelly unit that extends deeper into the core.

Zone J

Zone J lies near the modern shoreline of Long Island in the eastern portion of the bay, just west of a headland separating Bellport and Patchogue bays (Figure 26). The current setting and topmost deposit in the cores in this area consist of muddy sands. Also prominent in the seismic record and core from this area is the sand and gravel MDE deposit. The MDE layer lies atop vegetated marsh facies that in turn sit on top glacial outwash, much of which appears to be oxidized, indicating previous subaerial exposure. A small twig in the upper third of the organic deposits dates to 2829 yr BP. Using an average accretion rate of 0.75 mm/yr for the paludal sediments, vegetated marsh environment persisted for approximately 1000 years from 3620 to at least 2730 yr BP. A shell from the base of the MDE deposit dates to 2267 yr BP, and it is likely the 300-year gap is accounted for by slightly different rates of accretion as well as minor erosion by the MDE layer. A shell from the base of the estuarine muds and sands that overlie the MDE deposit dates to 782 yr BP, indicating a 1600-year gap in sedimentation between the MDE deposit's emplacement and the modern estuarine regime.

Zone K

Zone K also lies in the eastern portion of the Great South Bay, just east of the headland that divides Patchogue from Bellport bay (Figure 27). No radiocarbon dates were taken from the two cores that comprise this zone, all dates are estimated using accretion rates. The modern estuary sediments in this zone are mostly muds. The core record shows this depositional environment to have been established approximately 1600 yr BP in this area, using an accretion rate of 1.5 mm/yr. A thin (15 cm) section of organic muds are also seen in core 1B, and portions of zone K may have contained short-lived paludal environments prior to the estuary. While no MDE deposit was recovered from the cores, the MDE reflector is apparent and can be correlated with the deposit cored in zones J and L and therefore assumed to be from the same 2400-2200 yr BP interval. As the estuarine sequence only extends back 1600 years, the same long-lived depositional hiatus beginning at approximately 2200 yr BP also occurred in this area. As in most of the bay, glacial outwash underlies the estuarine sequence.

Zone L

Zone L lies the furthest east in the estuary, near the mouth of the modern Carmans River (Figure 28). As in Zone E, the MDE deposit is particularly abundant in this location as well as clear in the seismic record. In June of 2008 this zone, along with Zone E, was targeted and 4 new cores were taken in the area in order to further sample the deposit. Sediments from cores in this location show the uppermost units to be muds and sandy muds with a radiocarbon date from core 2A at 125 cm core depth dating to 1559 yr BP giving a modest accretion rate of 0.8 mm/yr. Immediately underlying the muds sits the 10-20 cm thick sand and gravel MDE deposit. Vegetated marsh organics from immediately below the

MDE deposit date to 2403 yr BP and the base of these thick organic-rich paludal muds dates to 3931 yr BP, showing the tidal marshes to be long lived in this region. However, after the MDE was emplaced, there is a depositional hiatus of approximately 300-500 years and the system does not transition back to intertidal marsh but to the modern subtidal estuarine environment.

Bay wide chronostratigraphy

These sequences, while locally variable, begin to reveal a coherent baywide history for the last 5,000 years (Figure 29). The progression from glacial outwash to fresh/brackish tidal marshes to open estuary is evident, as is the bay wide MDE deposit formed approximately 2300 yr BP. Also clear is a prominent gap in sedimentation that occurs post-MDE emplacement. Not only do depositional patterns prior to the MDE fail to reappear, but the deposit is succeeded in most cases by a distinct gap in sedimentation that persists for hundreds of years, indicating the event or process that formed the MDE was influential in the geologic history of the estuary. Possible origins for the MDE unit and its effects will be discussed in the following section.

Grain-size analyses of the MDE

In addition to its spatial, temporal, and stratigraphic context, capturing the physical characteristics of the MDE deposit itself is crucial in understanding the mechanism and environment under which it was emplaced. Grain-size analyses were performed on all MDE deposits recovered in the cores as well as from glacial outwash, other sand deposits, and the modern southern Long Island shore for comparison (Figures 30-32).

The MDE deposit mainly consists of medium to coarse sands with an addition component of gravel in some areas. With the exception of the muddy sands sampled in core 102, the fractions

of medium and coarse sand found in paleo and modern sand samples throughout the estuary tend to mirror those found in the MDE layer. This indicates the same material comprises both modern and ancient deposits and that the MDE deposit was very locally sourced. The deposit also shows slight fining in the sand fraction (Figure 30) and strong to no fining in the sand and gravel fractions (Figure 31), depending upon the core.

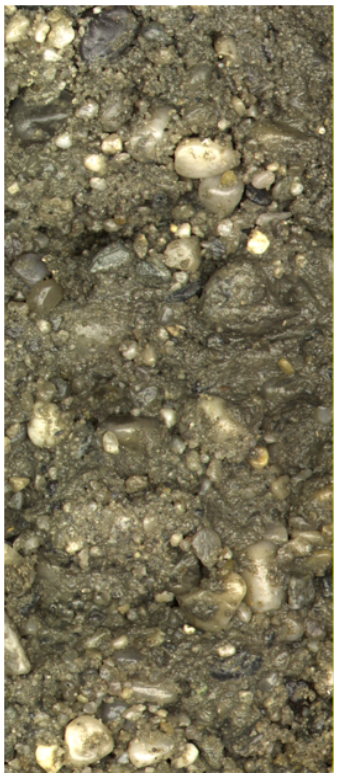

Outwash

Core GSB105

Fresh Water

Core GSB101

Estuarine Muds

Estuarine Sands

Core GSB101

Figure 4: Major facies units in Holocene Great South Bay sediments through transgression from the Last Glacial Maximum through the present. A summary of the facies can be found as in Table 1 on the following page.

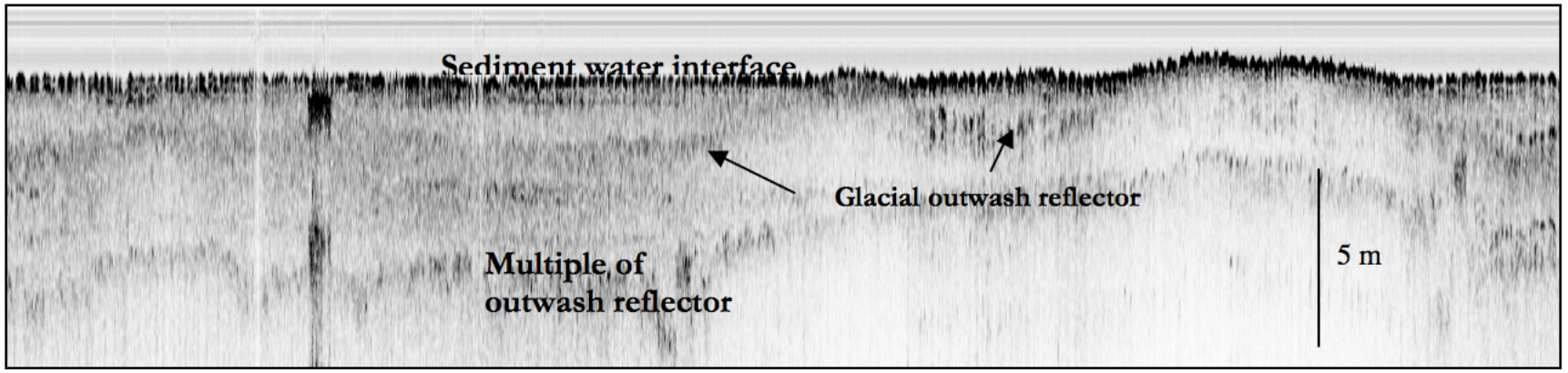

Figure 5: Example of acoustic record showing the prominent glacial-outwash reflector that encompasses meters of sub-bottom relief and locally outcrops at the seabed.

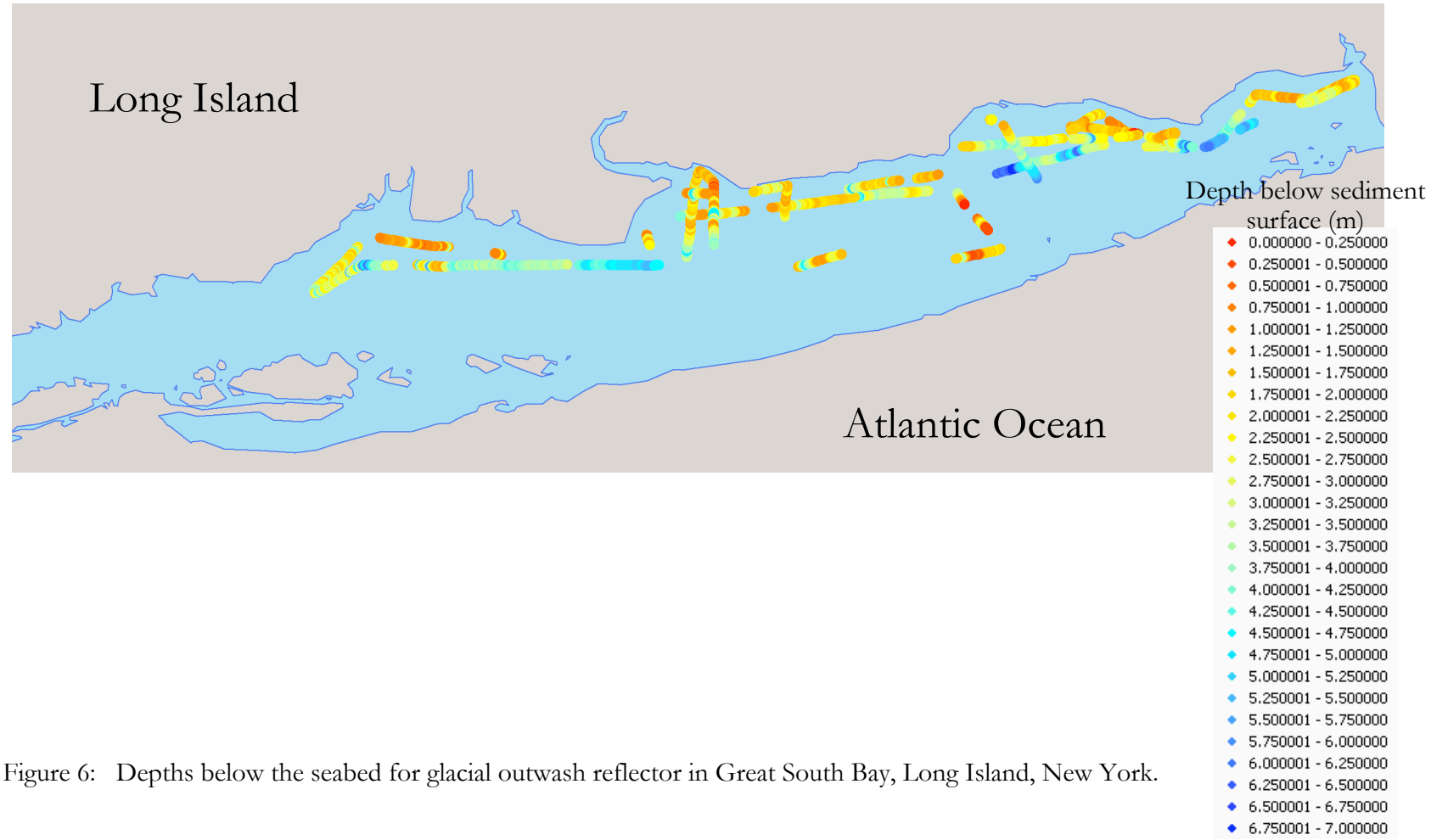

Figure 6: Depths below the seabed for glacial outwash reflector in Great South Bay, Long Island, New York.

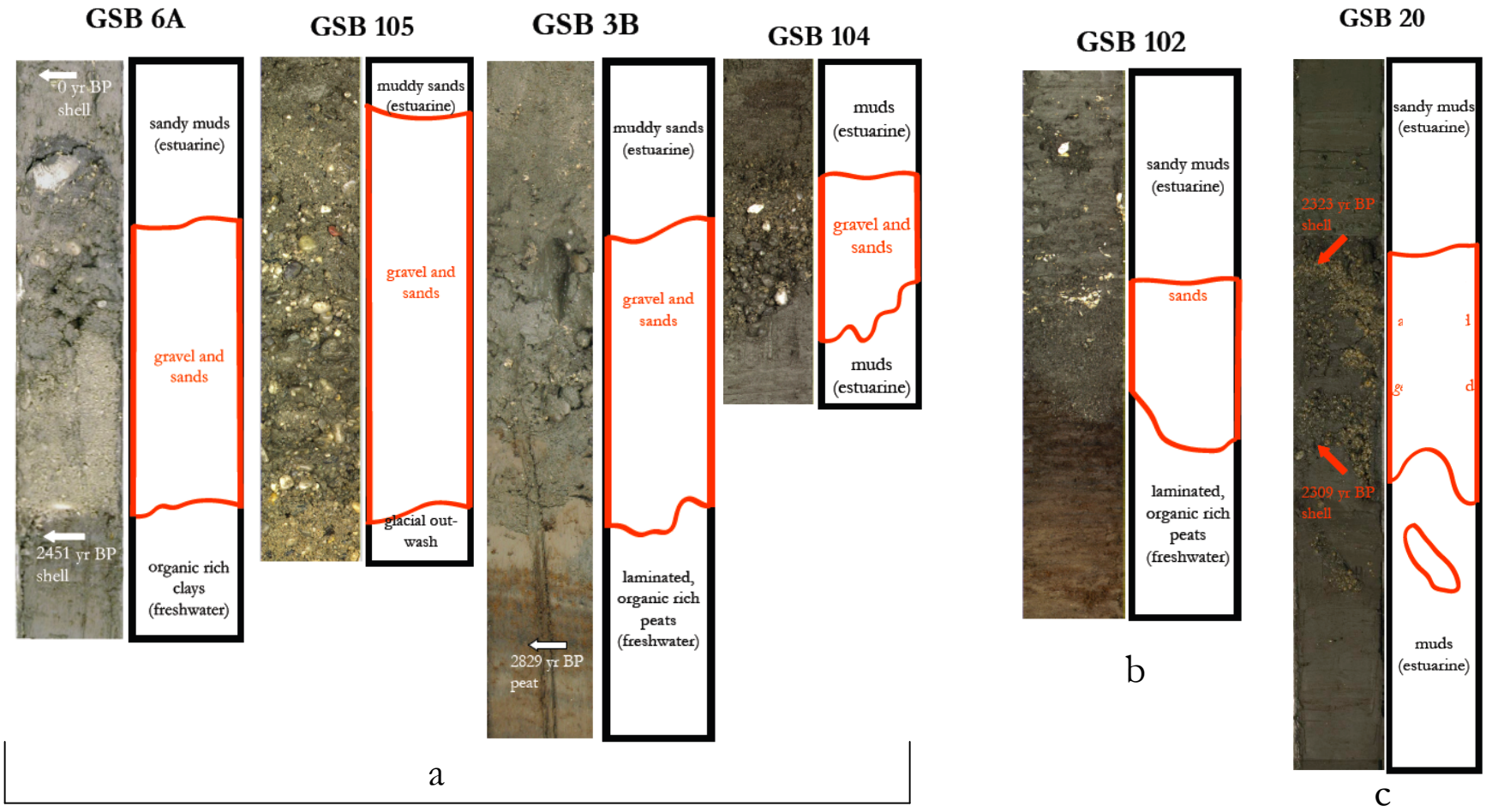

Figure 7: Examples of Major Depositional Event (MDE) facies comprised of sand and gravel (a), sands (b), and dense, articulated *Gemma gemma* bivalves (c).

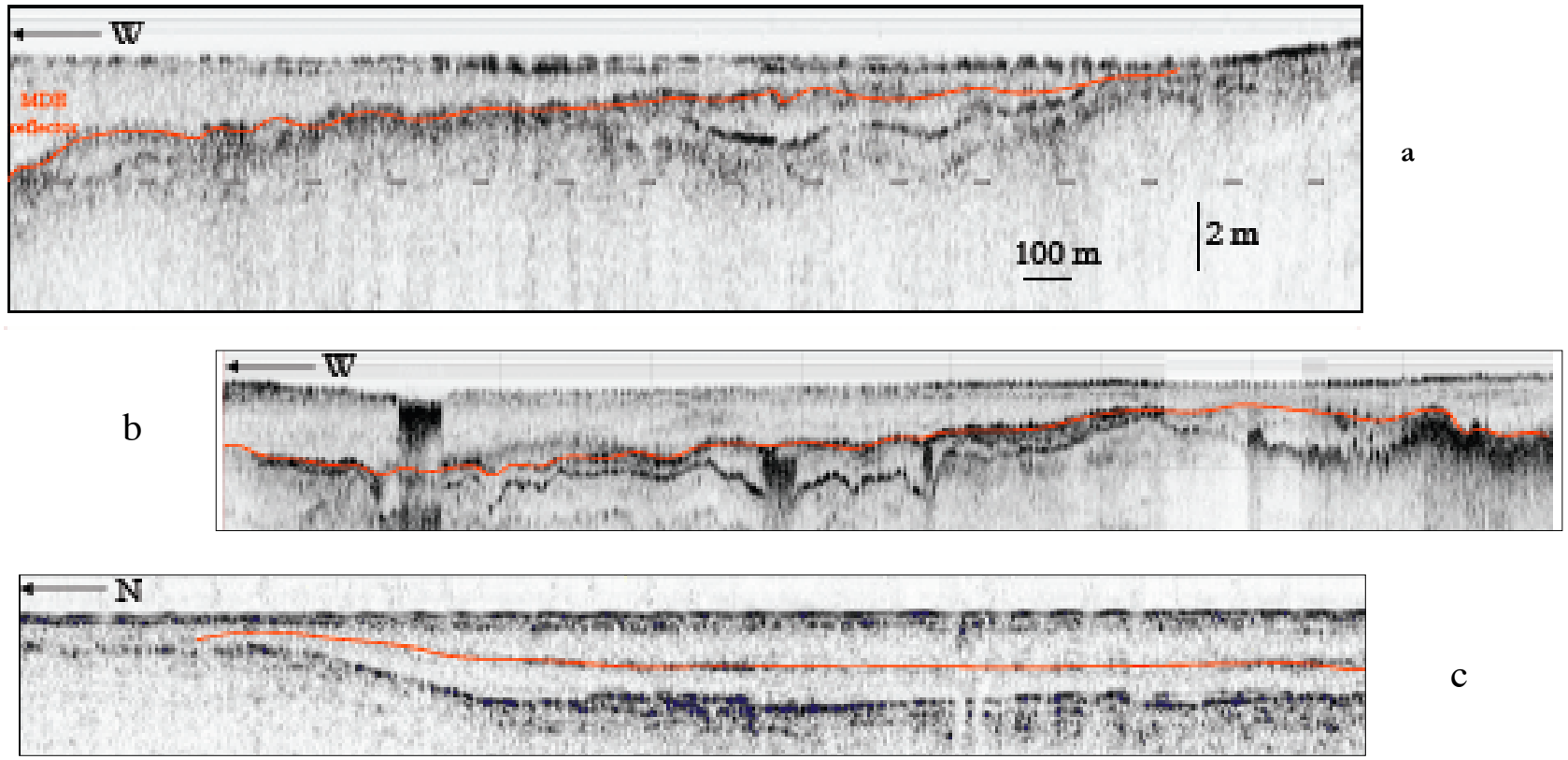

Figure 8: MDE reflector seen in the acoustic record. As in figure 7, the facies is comprised of sands and gravels (a), sands (b), and a dense shell bed (c). The acoustic reflector is prominent and unique within the seismic data in the estuary. Scale is the same for all profiles.

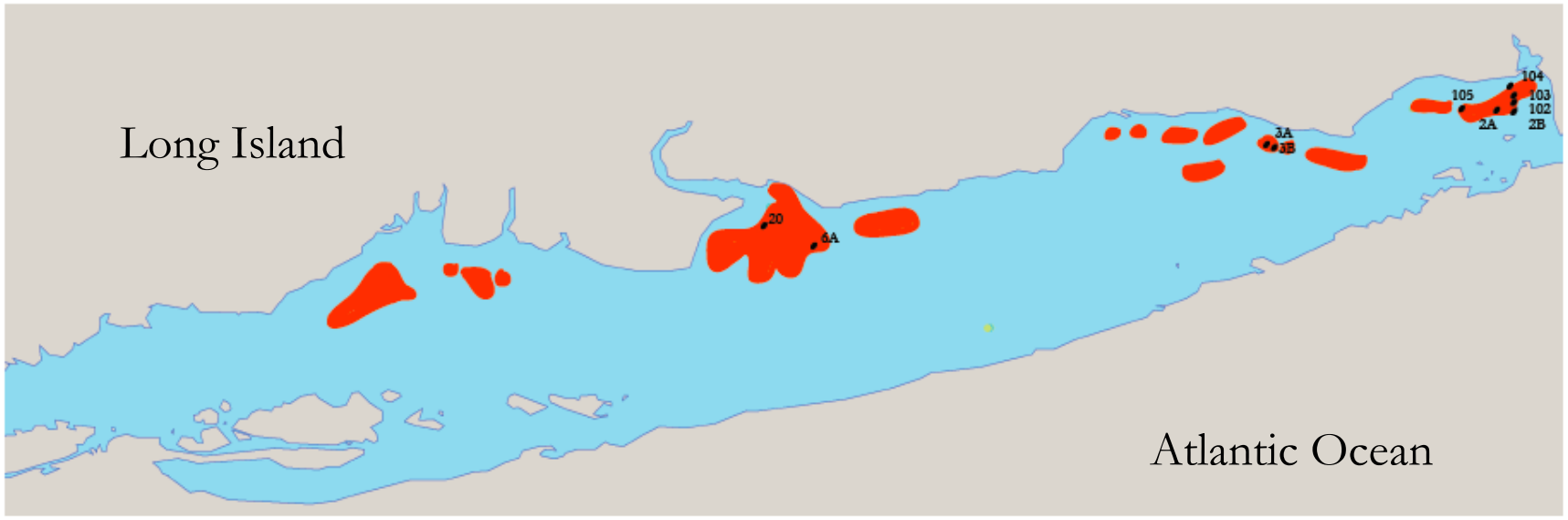

Figure 9: Geographic extent of the MDE deposit in Great South Bay as derived from seismic record. MDE extent is highlighted in red. Geographic position of cores shown in Figure 7 is also labeled.

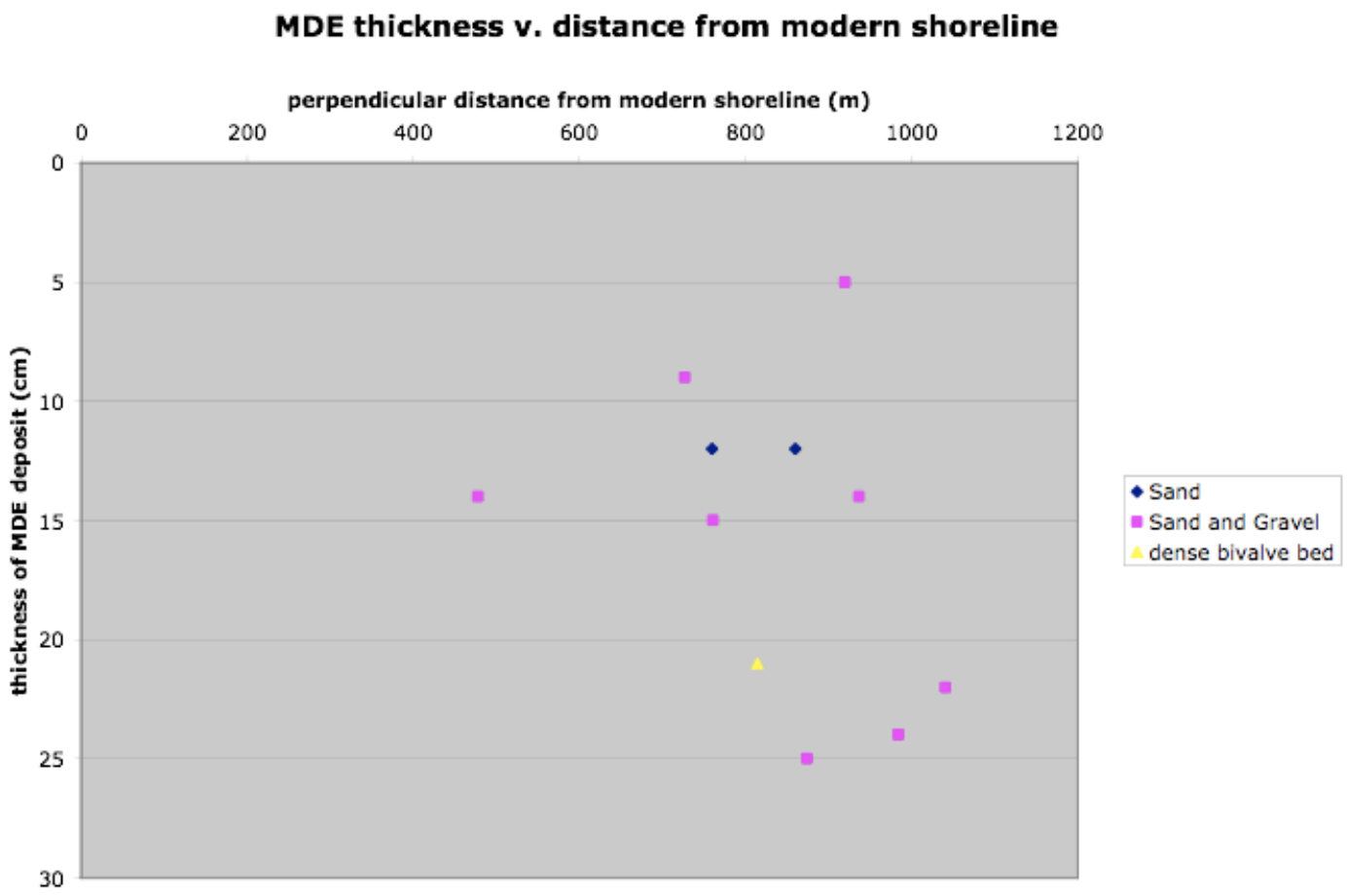

Figure 10: Thickness of MDE deposit relative to its distance from the modern shoreline showing general thinning landward.

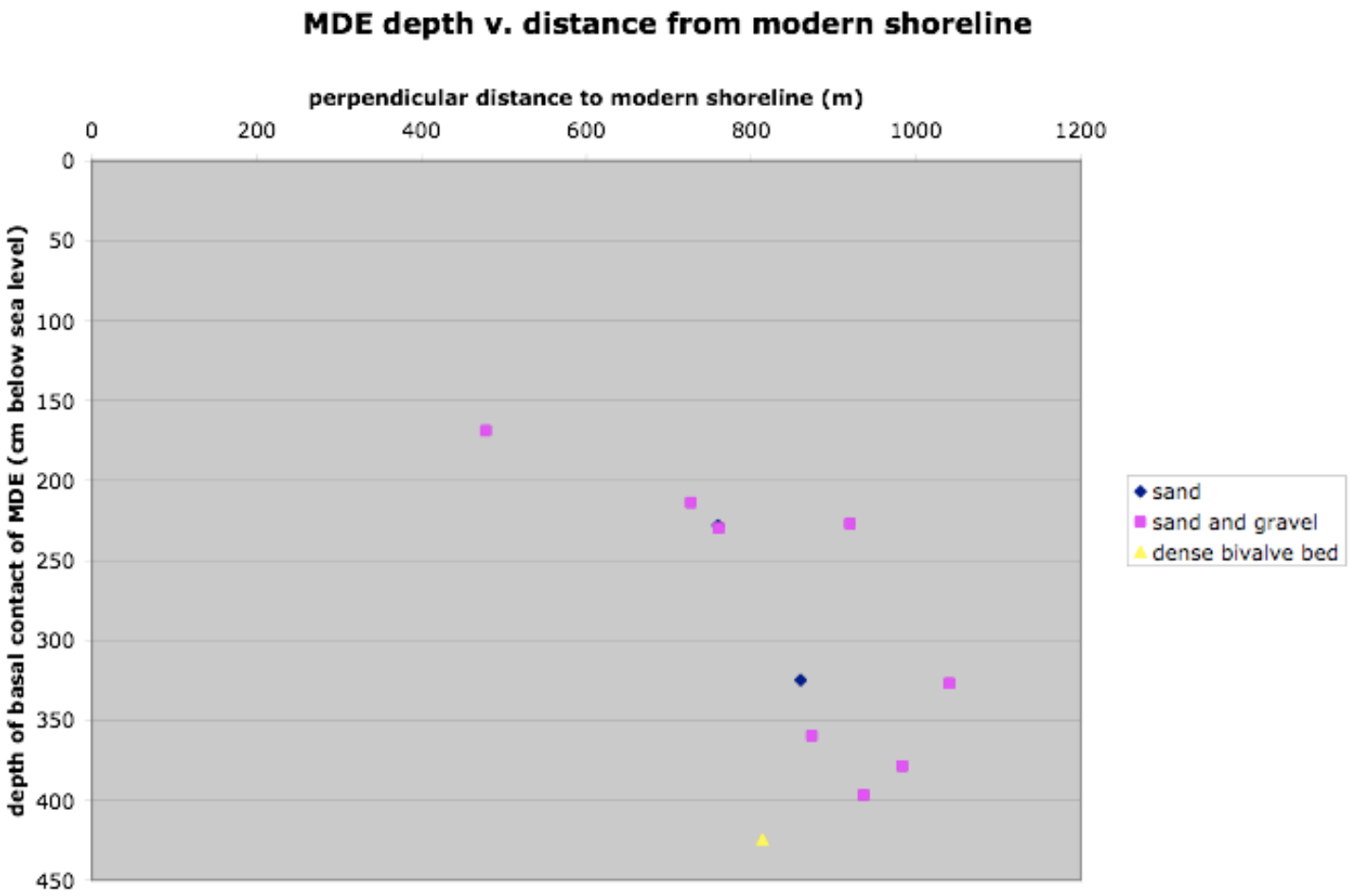

Figure 11: Depth of basal contact of MDE deposit, in cm below sea level, compared to distance from modern shoreline, showing general landward shallowing of the deposit.

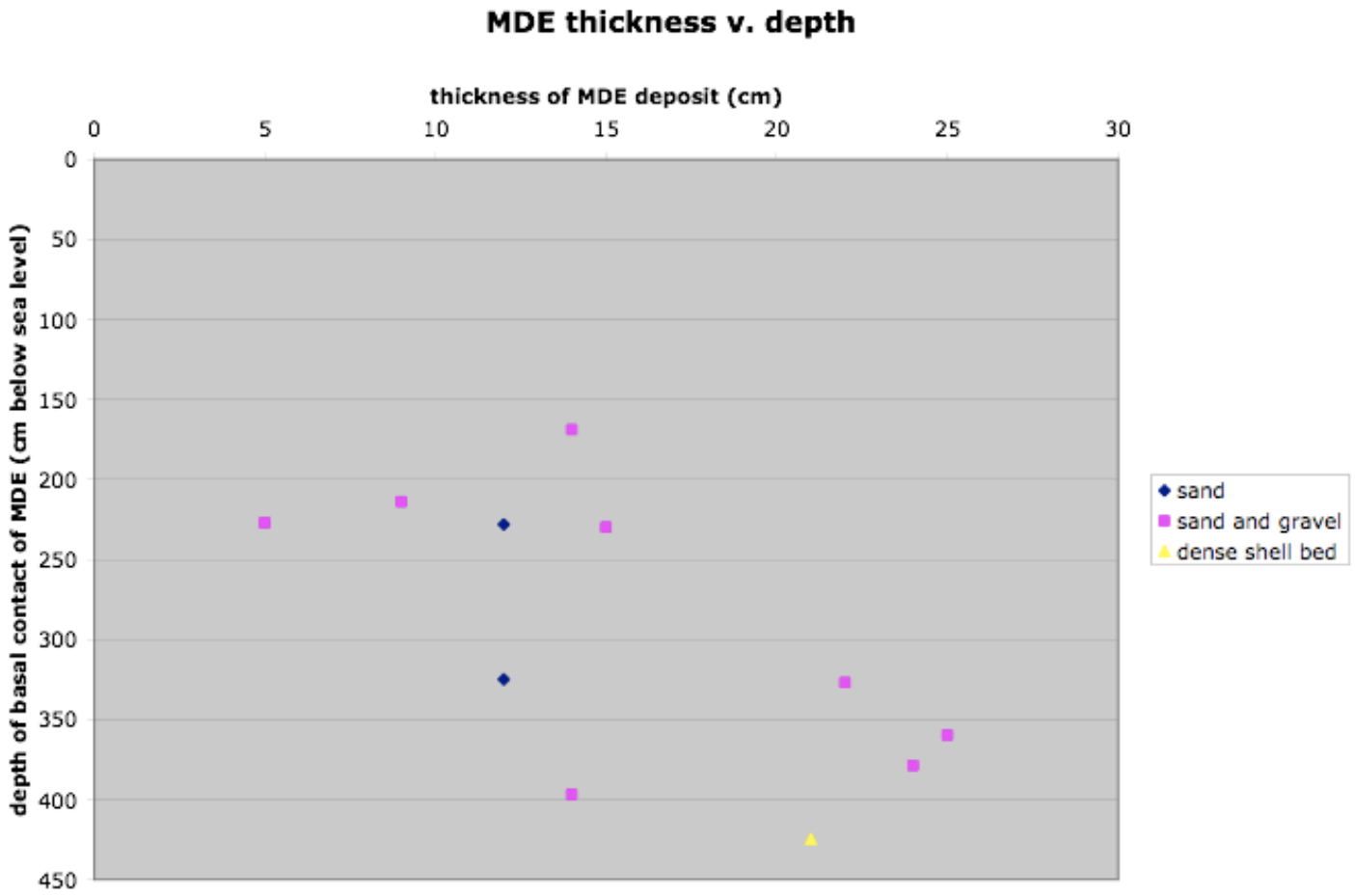

Figure 12: Comparison of thickness of MDE deposit and depth of basal contact in centimeters below sea level, suggesting a coarse trend of landward thinning.

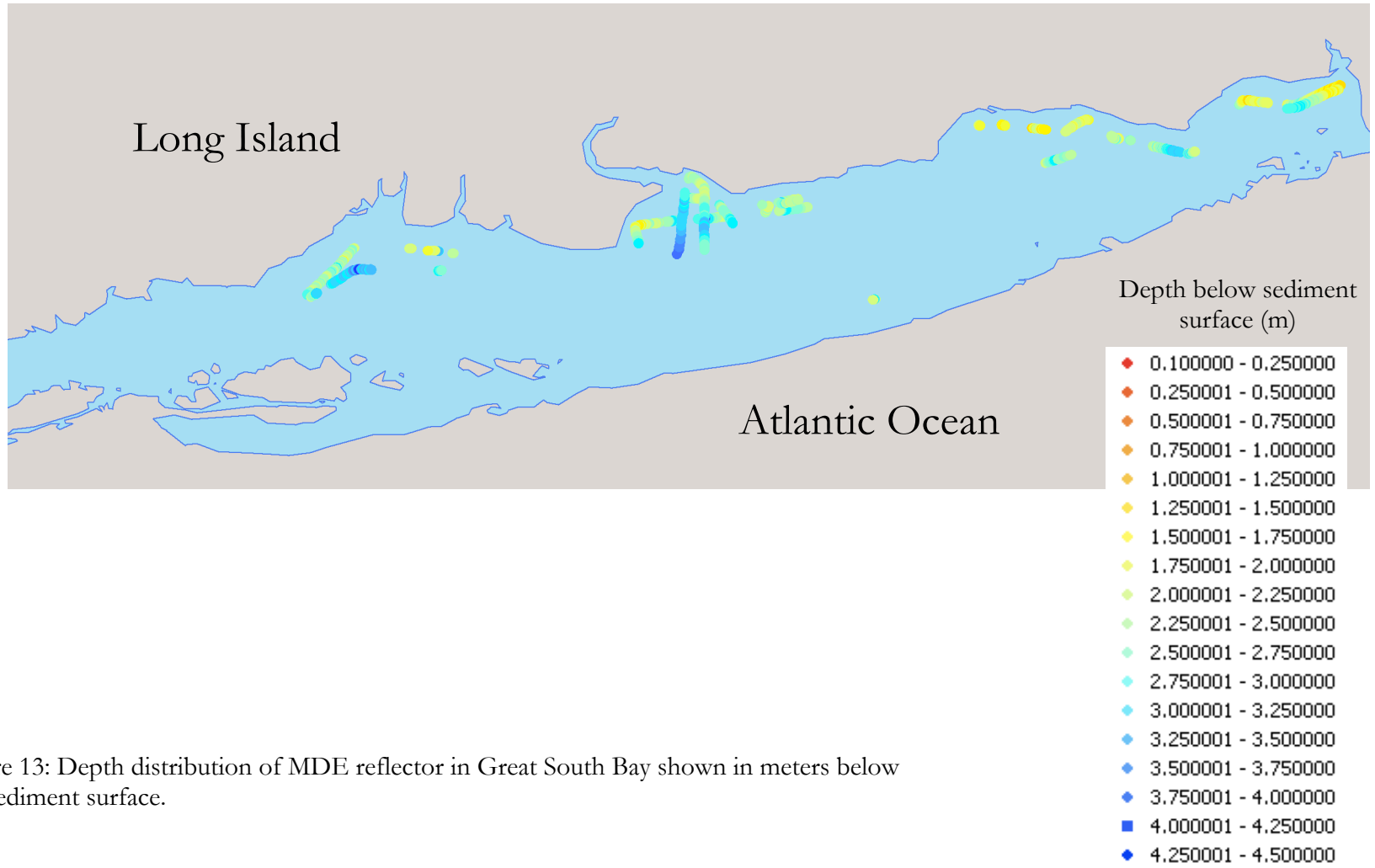

Figure 13: Depth distribution of MDE reflector in Great South Bay shown in meters below the sediment surface.

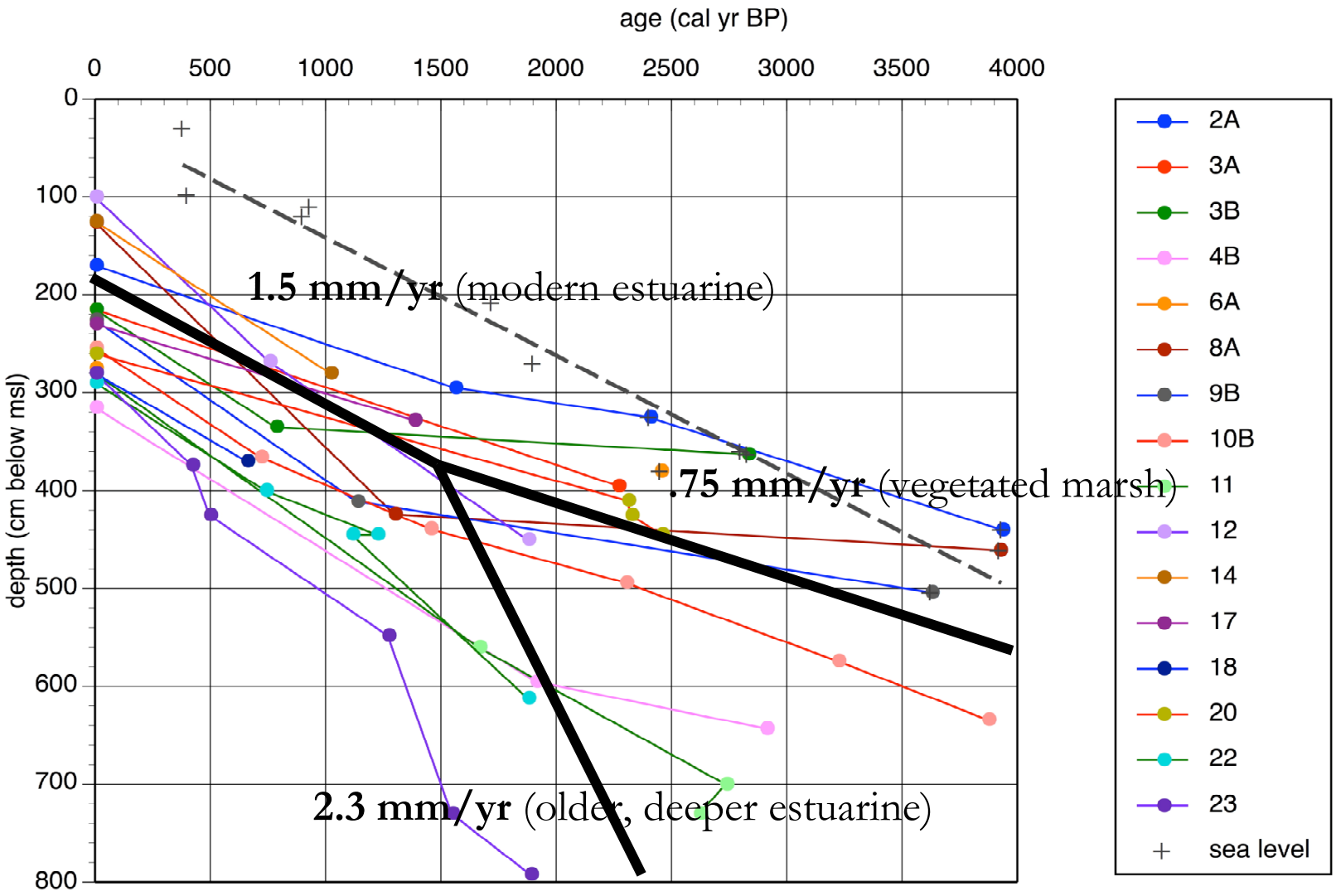

Figure 14: Radiocarbon dates sampled from cores compared to depth in centimeters below sea level. Thick black lines and annotations show average accretion ratesfor the major lithologic units

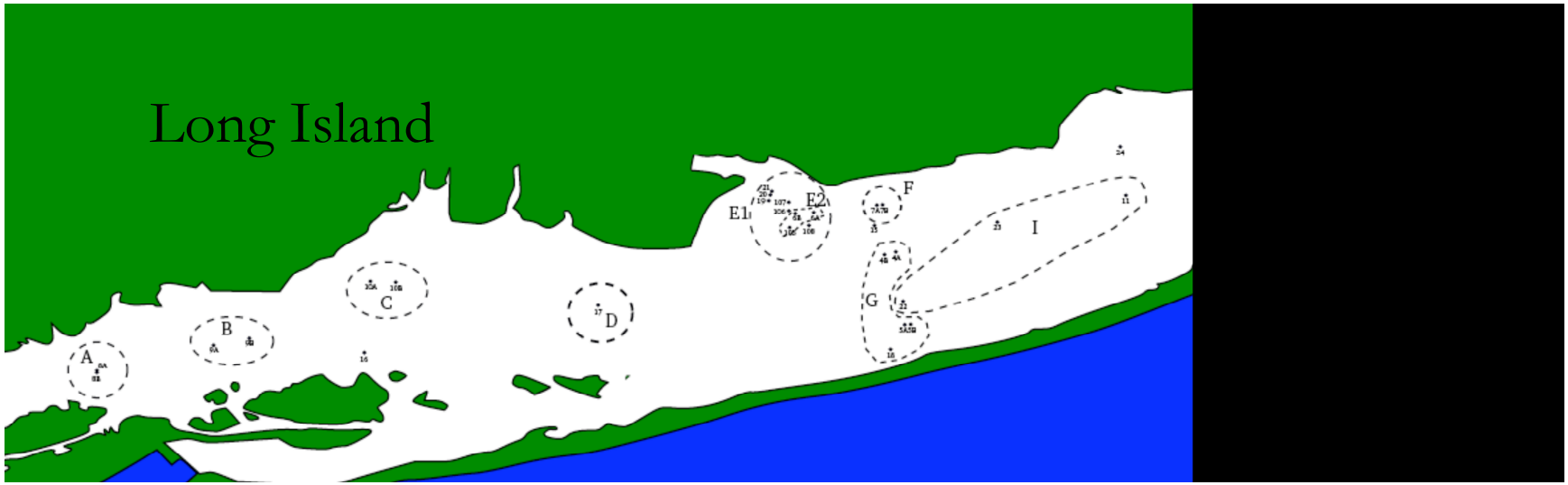

Zone A	B	C	D	E1	E2	F	G	H	I	J	K	L
8A	9A	10A	17	19	6A	7A	4A	14	11	3A	1A	2A
8B	9B	10B		20	6B	7B	4B	12	22	3B	1B	2B
				21	105		5A		23			101
				106			5B					102
				107			18					103
				108								104

Key

MDE

14C Date

MDE and 14C

Figure 15: Distribution of the 13 core zones defined for Great South Bay stratigraphy. Zones were determined based on geographic location as well as similarity of lithology. Cores highlighted in red contain the MDE layer, yellow have been radiocarbon dated, and orange have both been radiocarbon dated and contain the MDE layer.

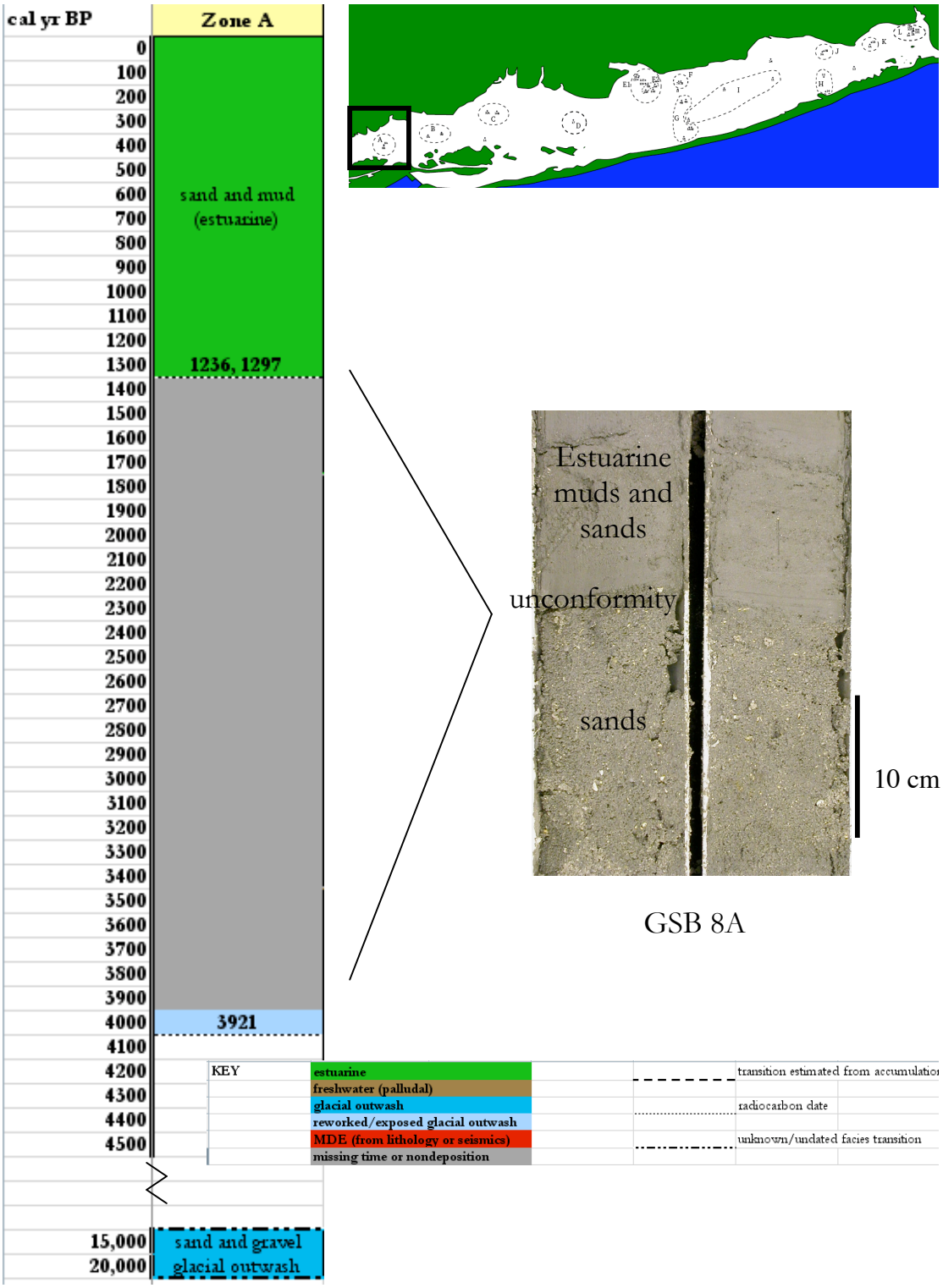

Figure 16: Zone A chronostratigraphy and core image. Key refers to all chronostratigraphy diagrams in this section.

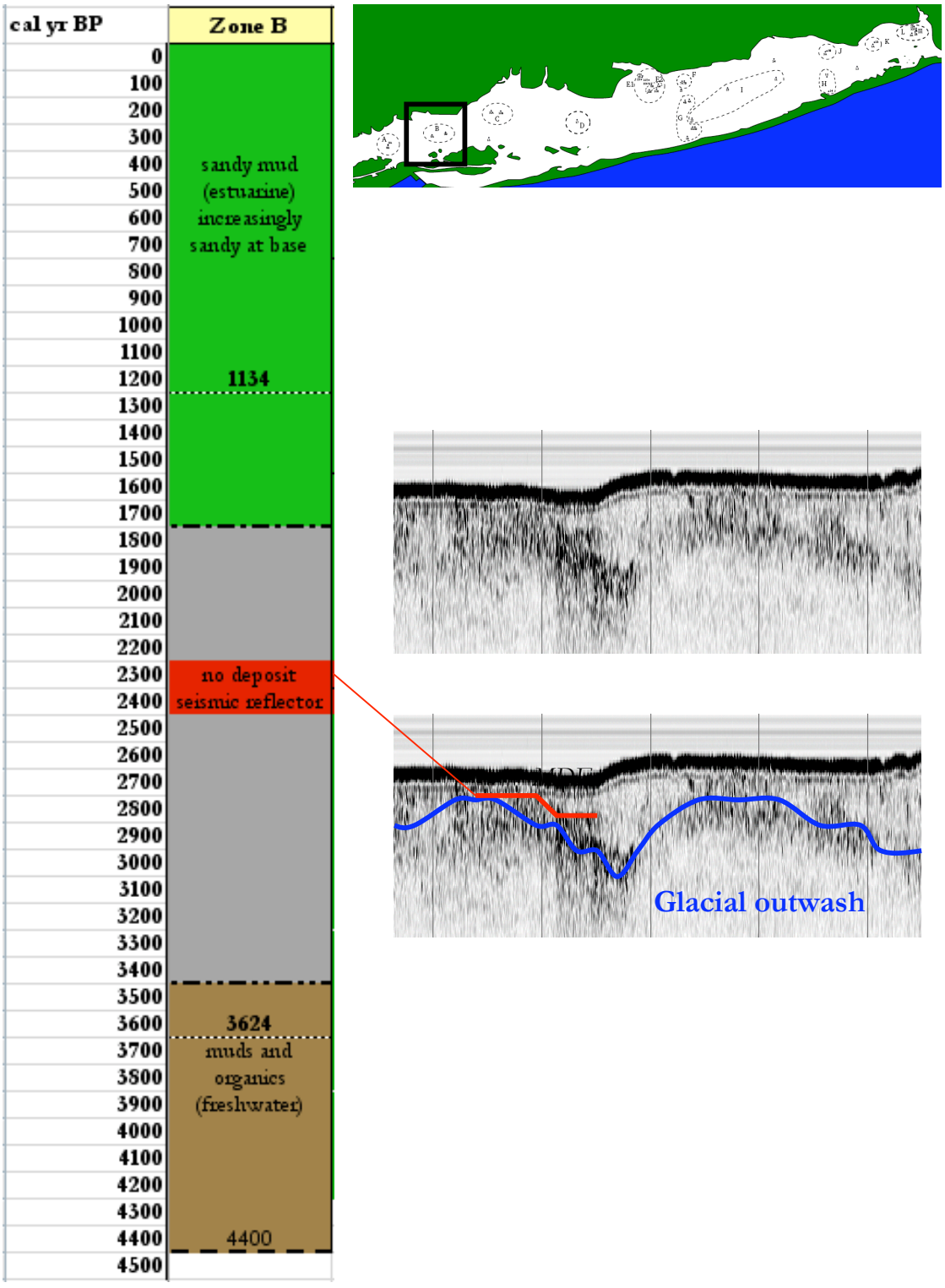

Figure 17: Zone B chronostratigraphy and core images. The deposit is not seen in cores taken from this location, however the MDE reflector is faintly seen in zone B and corresponds to slight density changes in sediment rather than a sand or gravelly deposit.

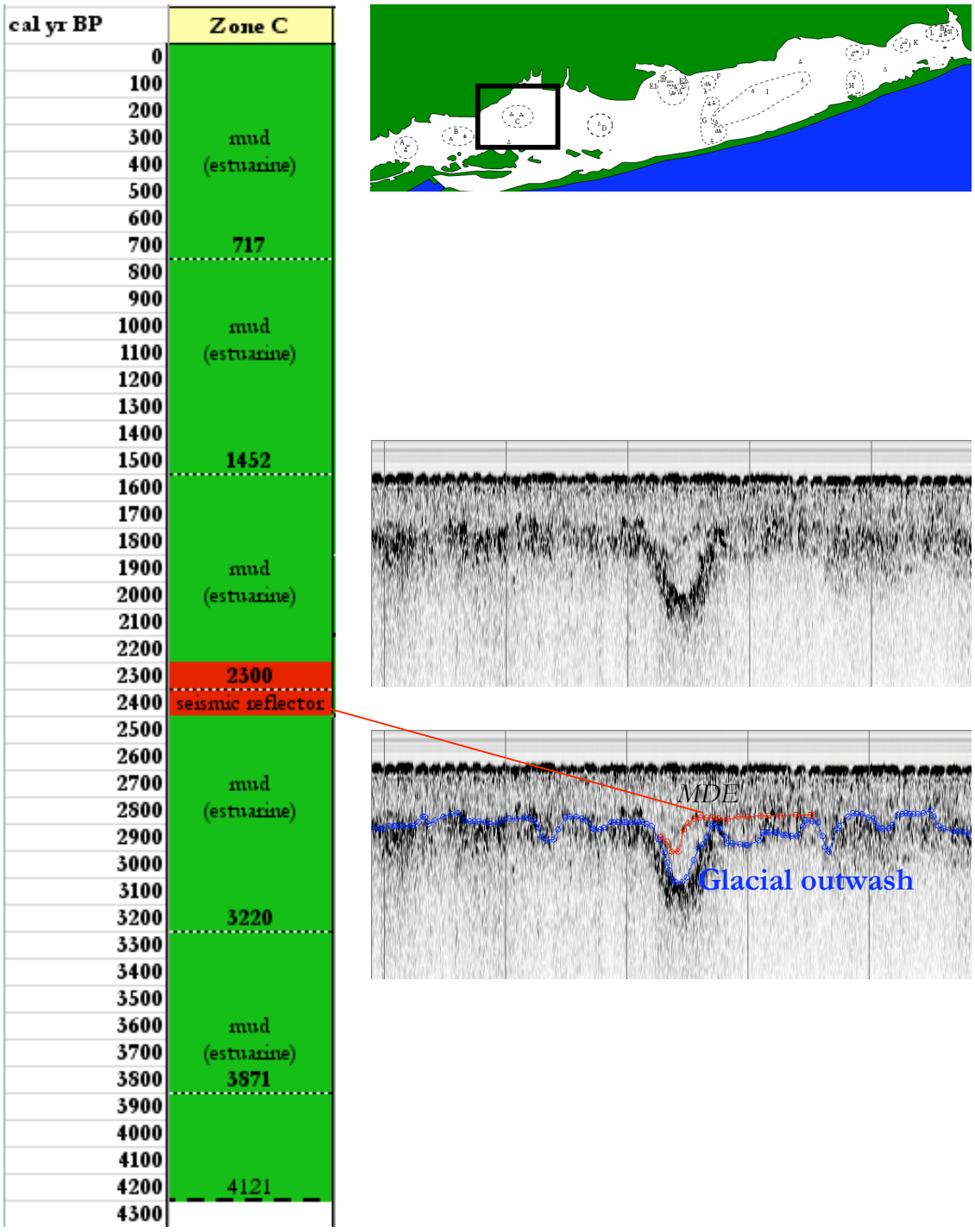

Figure 18: Zone C chronosgratigraphy and seismic image. Although no deposit is found in the two cores taken in this zone, the MDE reflector is seen in zone C, indicating the deposit may be found in portions of zone C not cored.

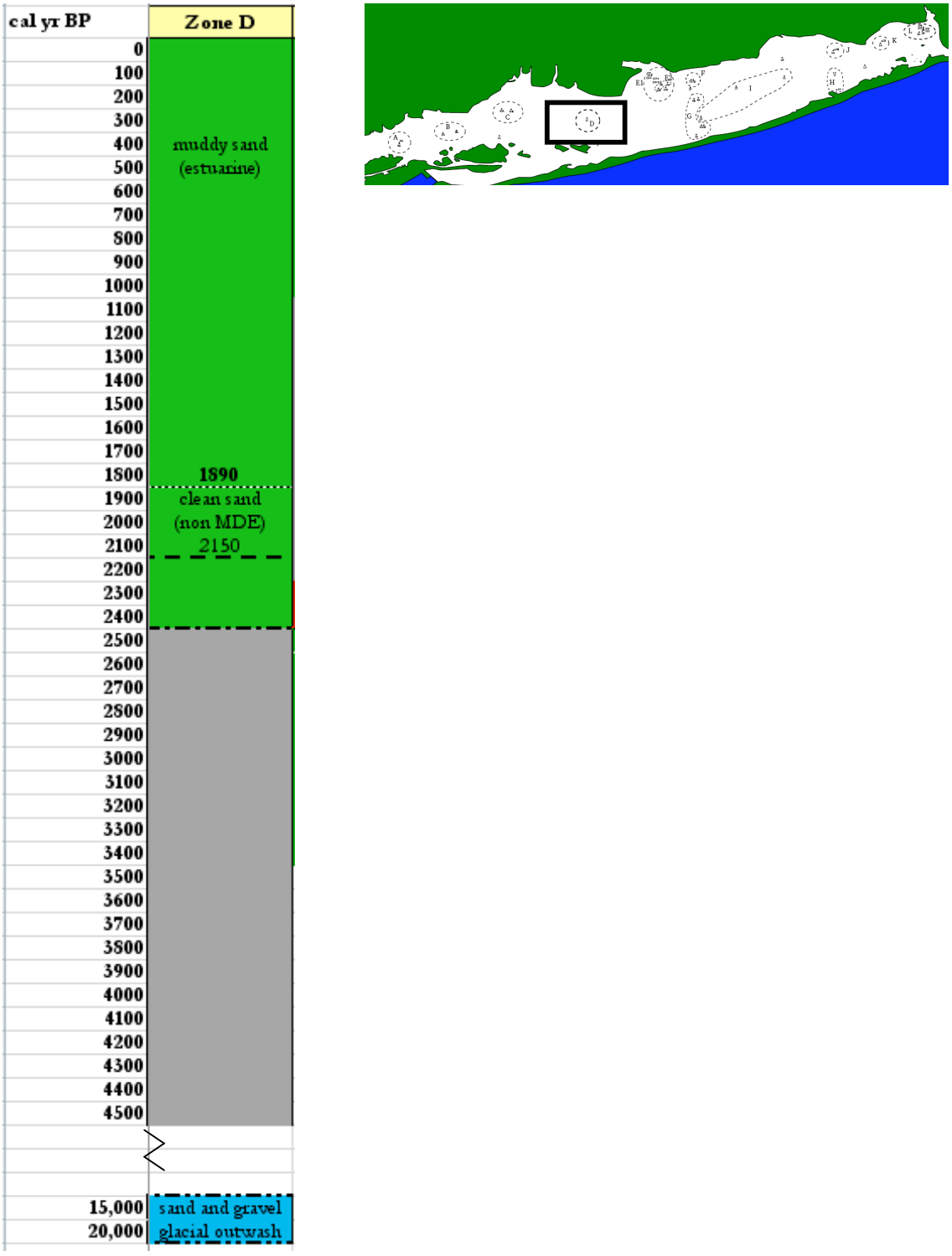

Figure 19: Zone D chronostratigraphy

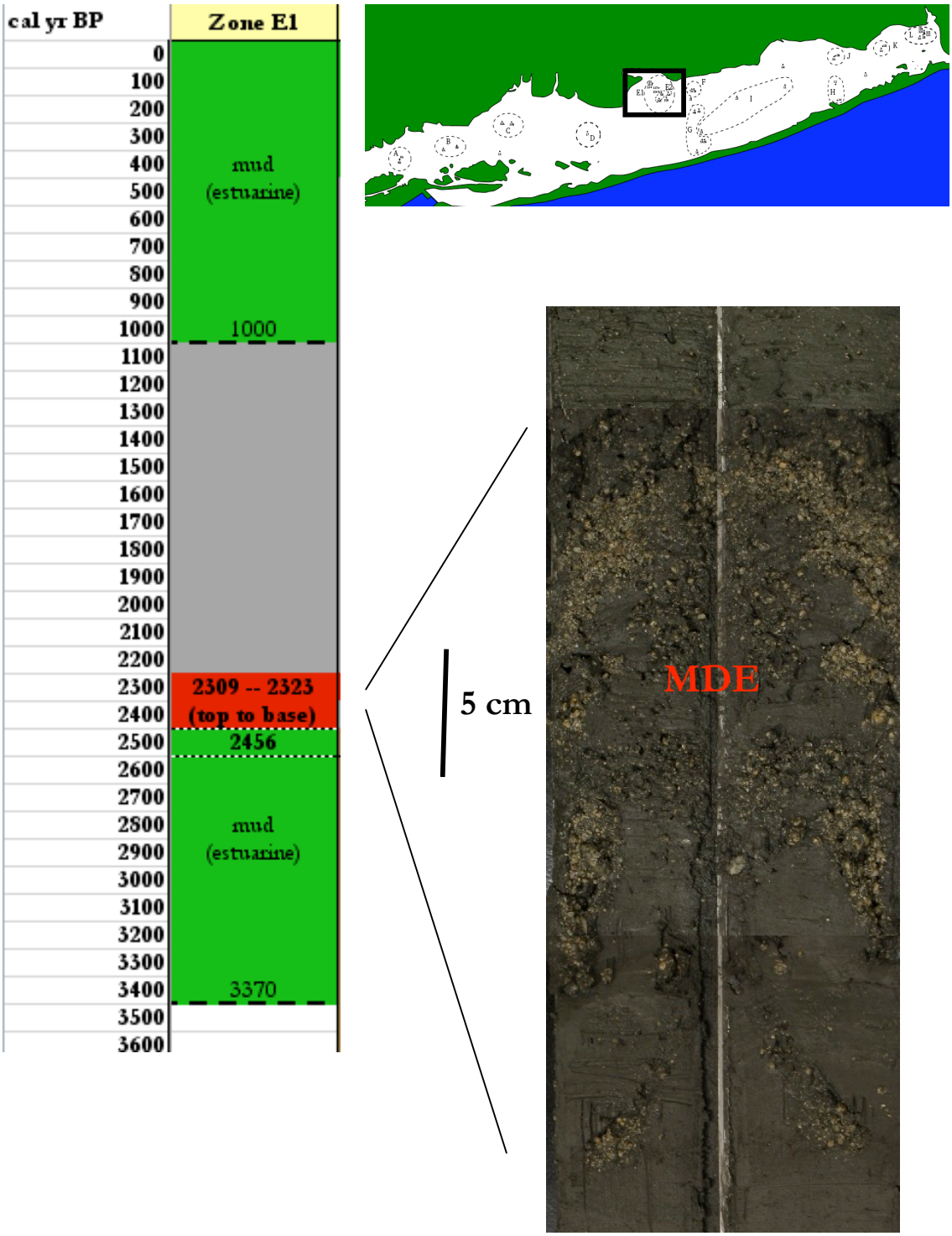

Figure 20: Zone E1 and image of dense, articulated, sand-dwelling *Gemma gemma* bivalves in a matrix of estuarine muds.

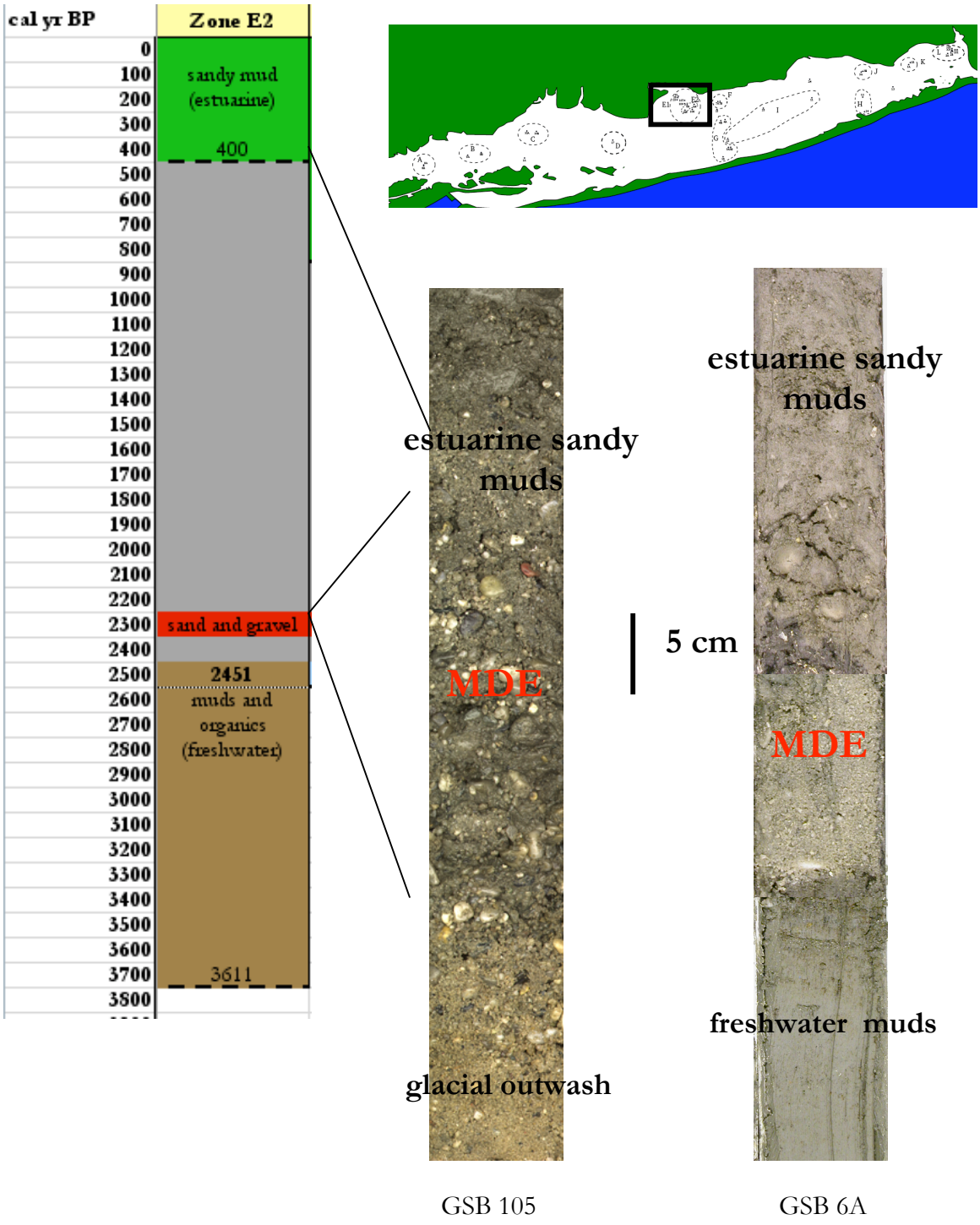

Figure 21: Zone E2 chronostratigraphy and images of the sand and gravel MDE layer from cores 6A and 106. As can be seen in the photograph, core 105, does not contain the long-lived freshwater environment. The MDE deposit in this core sits at a higher elevation and closer to the modern shore, indicating it was likely a subaerial rather than subaqueous environment at the time the MDE layer was deposited.

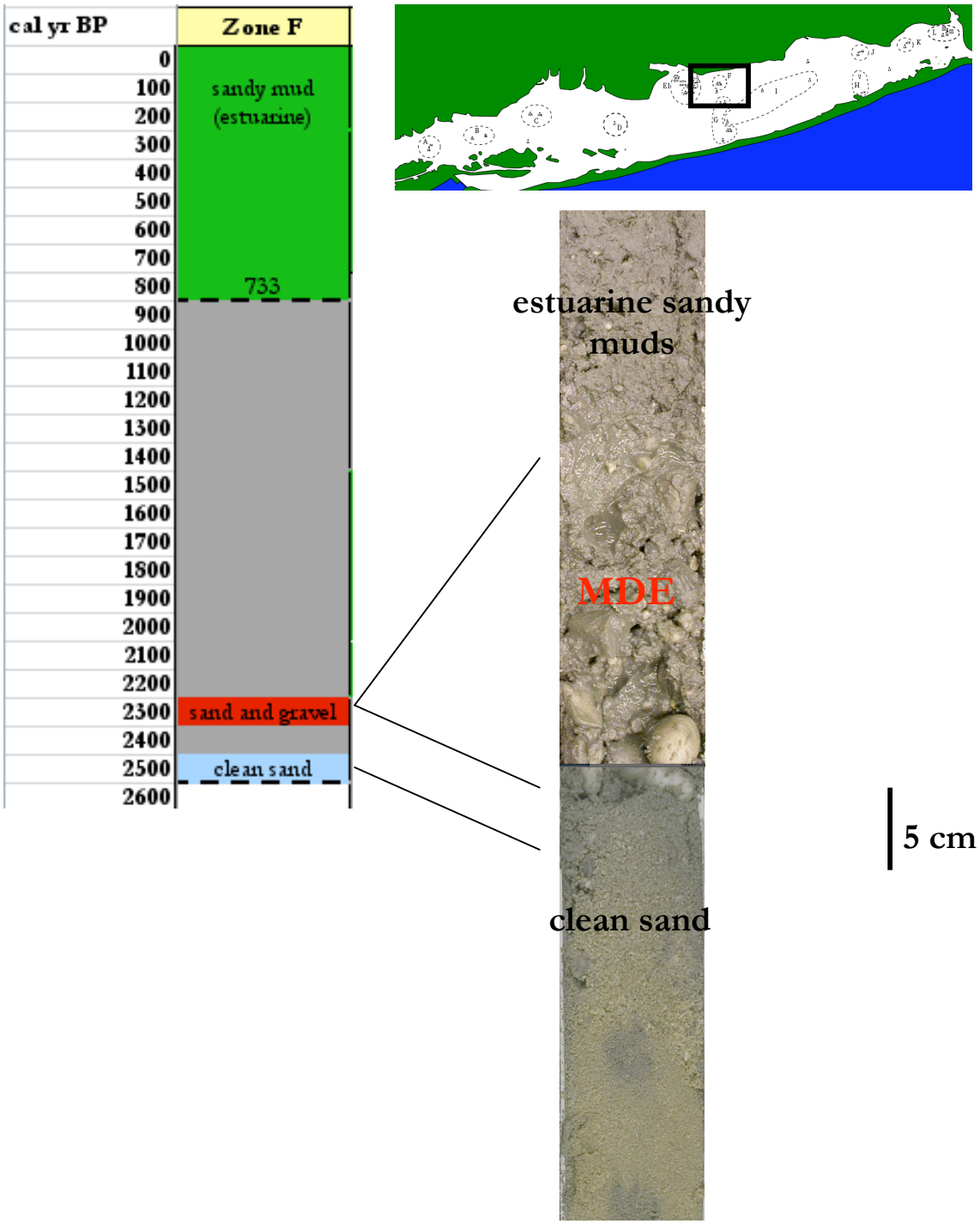

Figure 22: Zone F chronostratigraphy and image of sand and gravel MDE layer from core 7A.

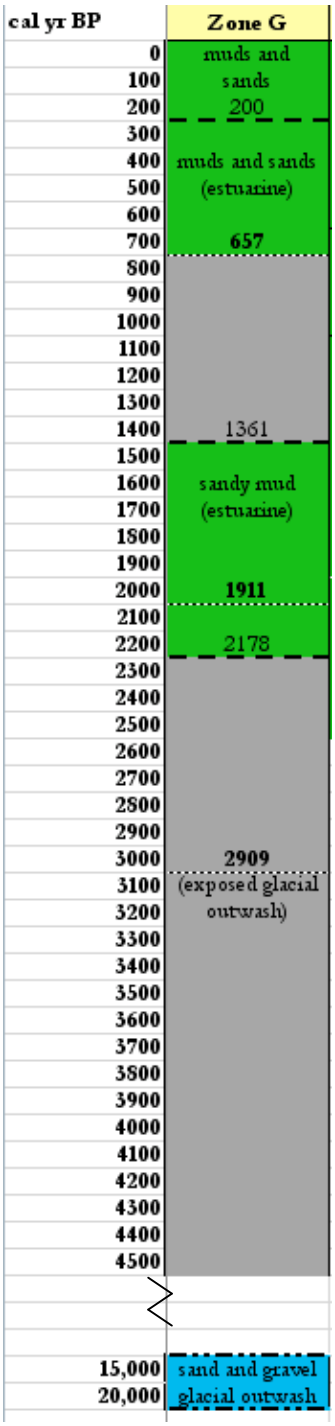

Figure 23: Zone G chronostratigraphy.

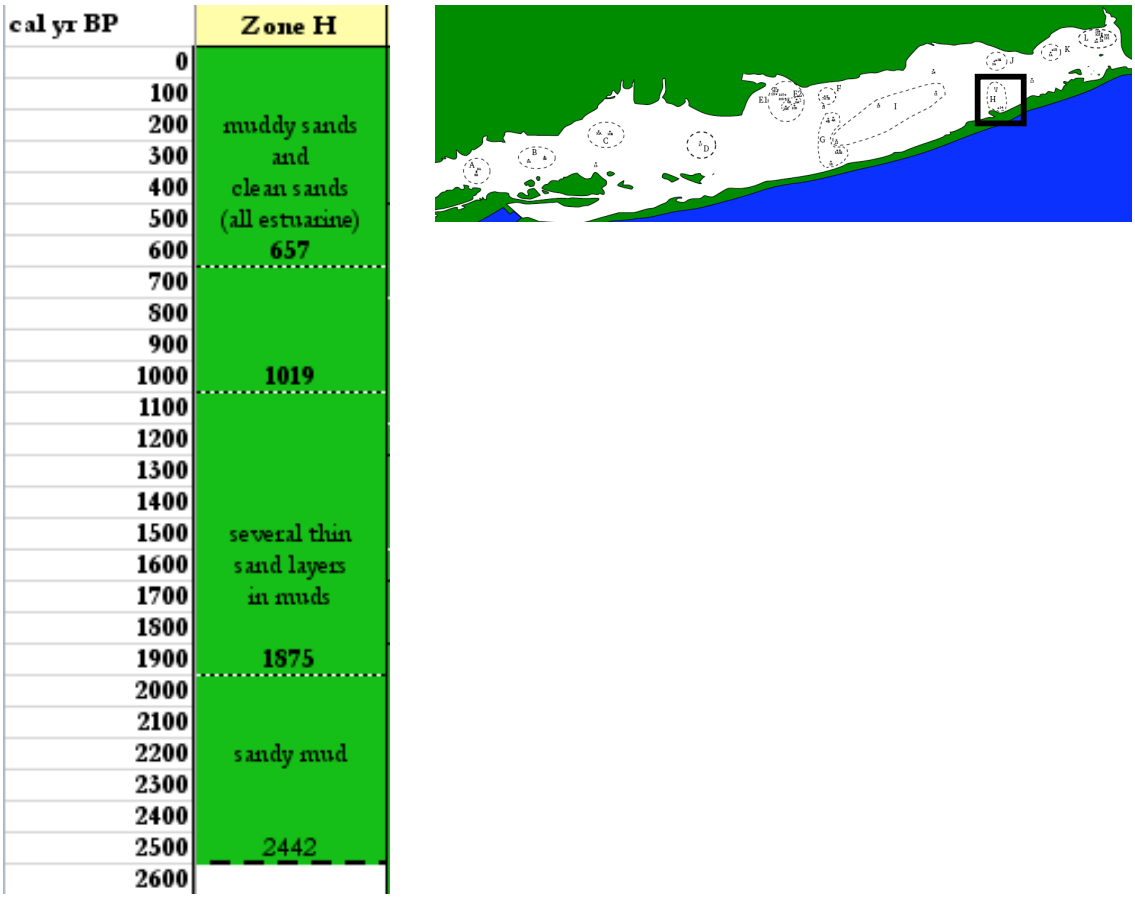

Figure 24: Zone H chronostratigraphy. 3 calibrated radiocarbon dates from the zone show a .37 mm/yr net accretion rate.

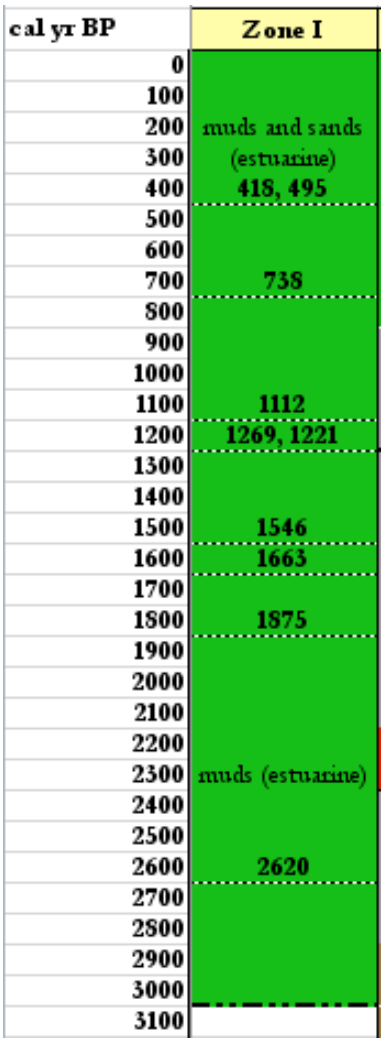

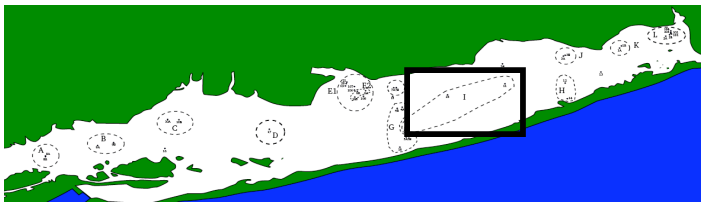

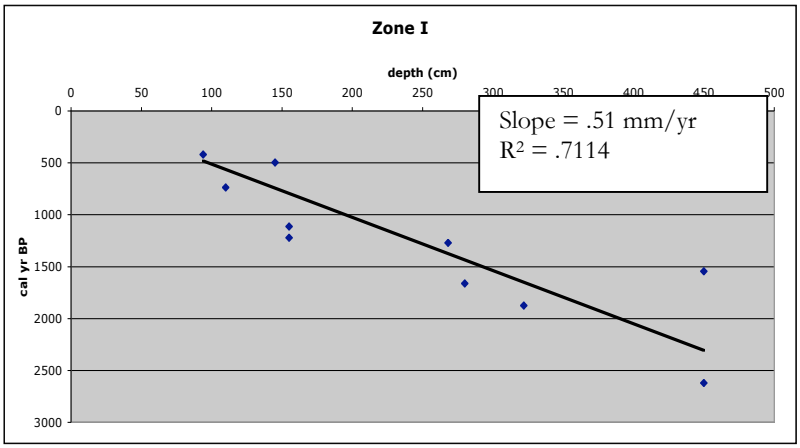

Figure 25: Zone I chronostratigraphy. The diagram shows a continuous estuarine environment throughout the past 3,000 years, however accretion rates indicate there may have been significant gaps in sedimentation during this time period that cannot be resolved.

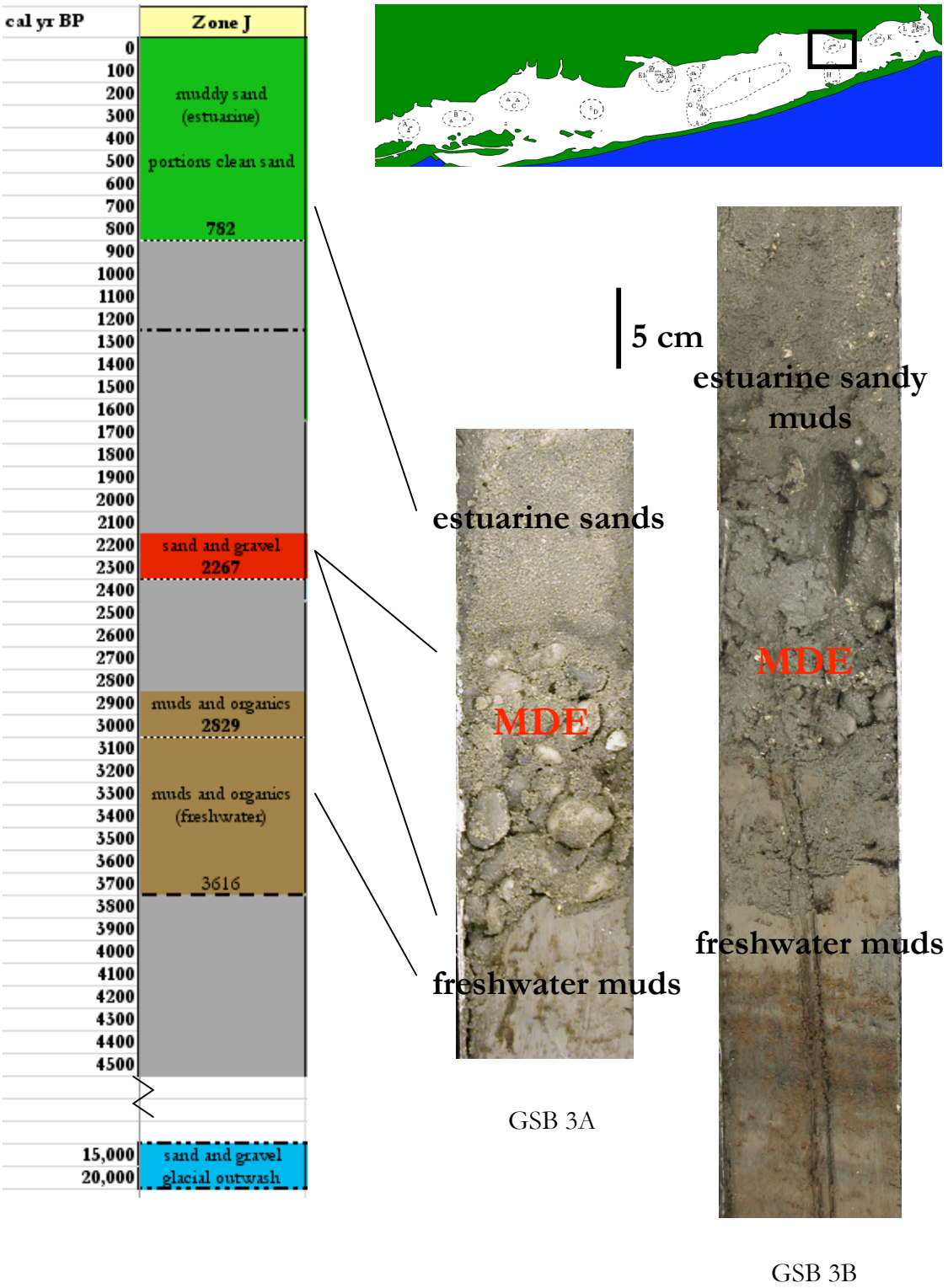

Figure 26: Zone J chronostratigraphy and core images.

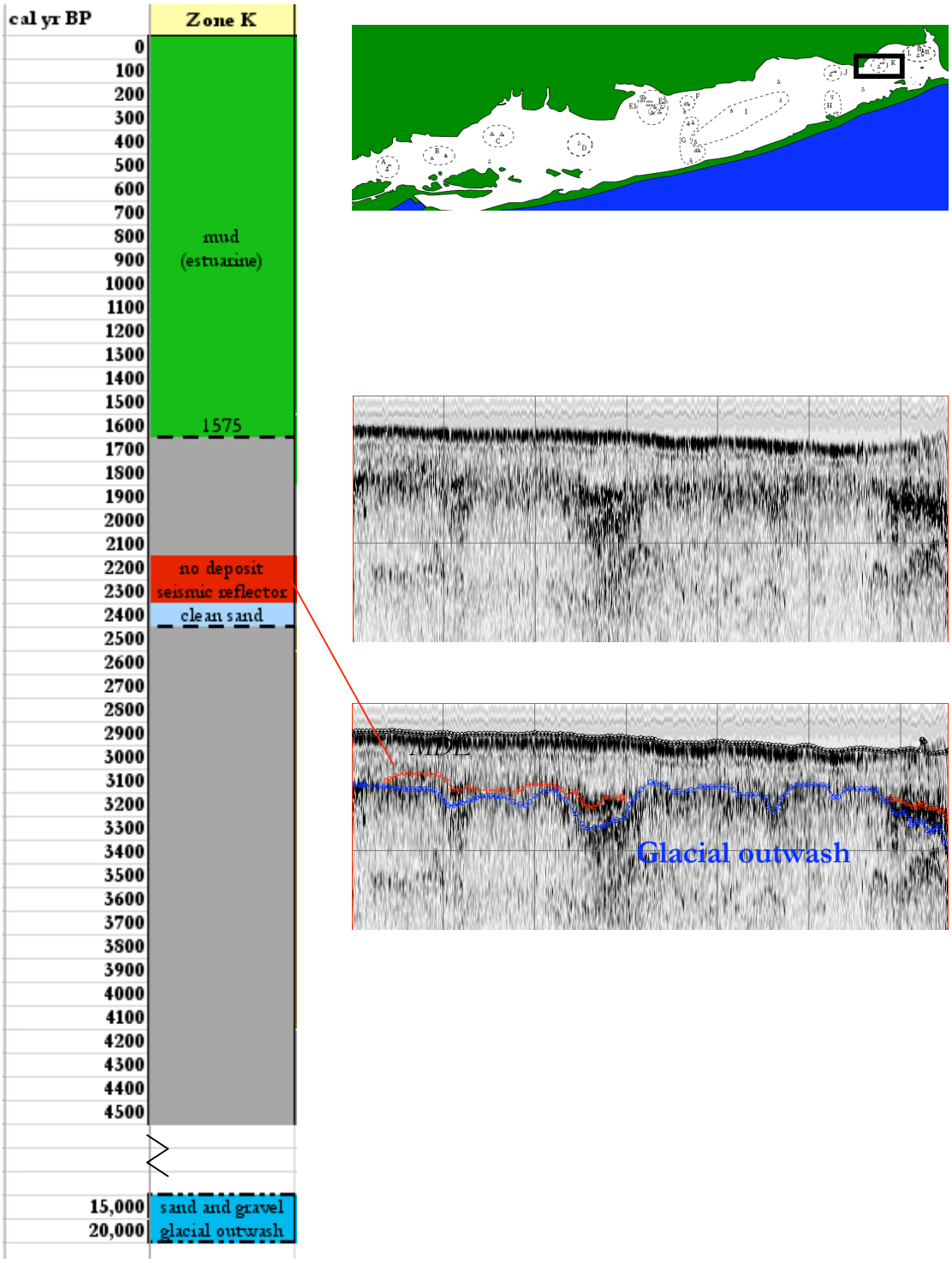

Figure 27: Zone K chronostratigraphy.

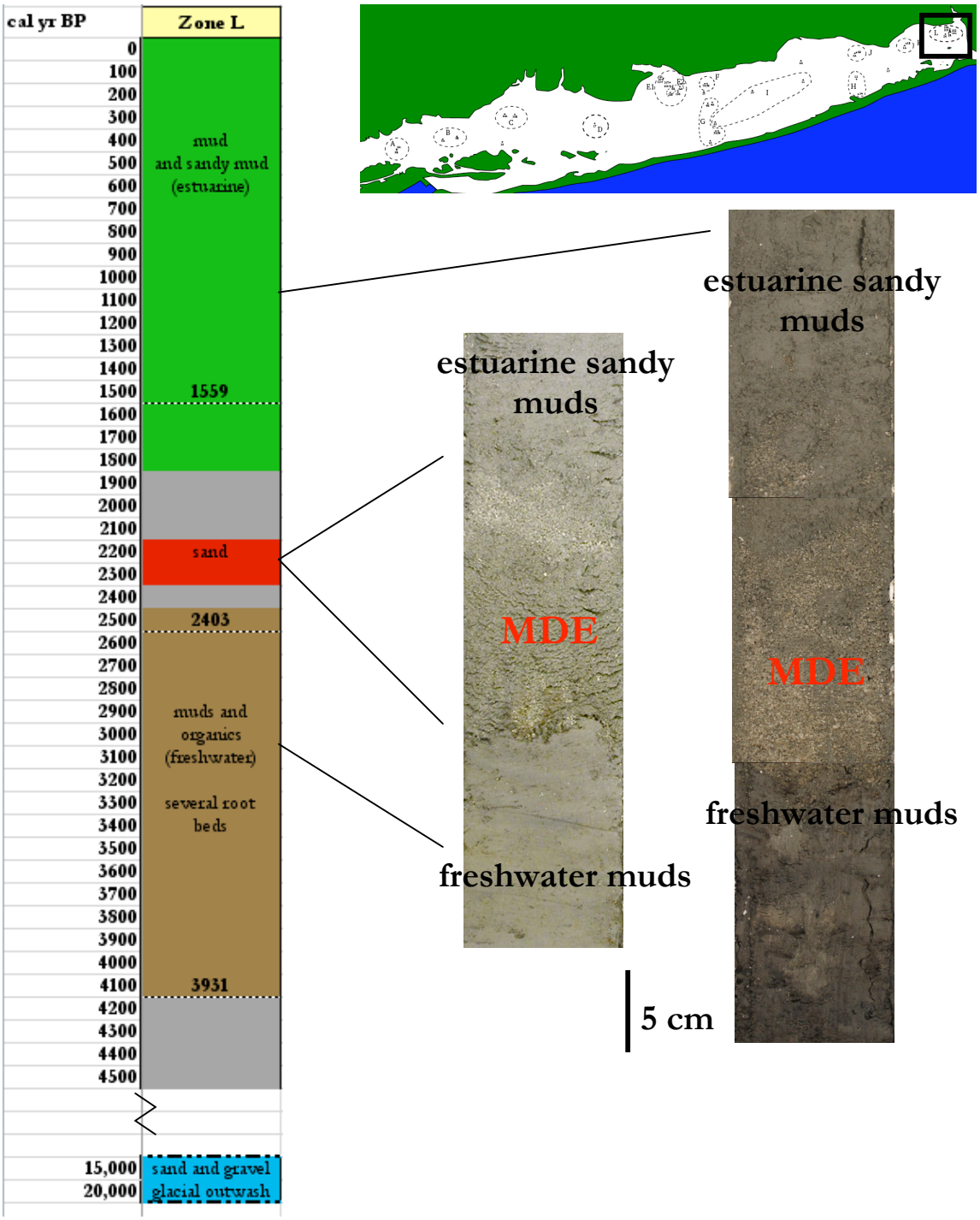

Figure 28: Zone L chronostratigraphy and images of the sandy MDE deposit from cores 2A and 2B. Slight color difference in portions of the core is a camera artifact. As in zones E2 and J, the freshwater environment was established early in the estuary's history in this area. Cores 102 and 104 also are located in zone L, contain the MDE layer and can be seen in Figure 7.

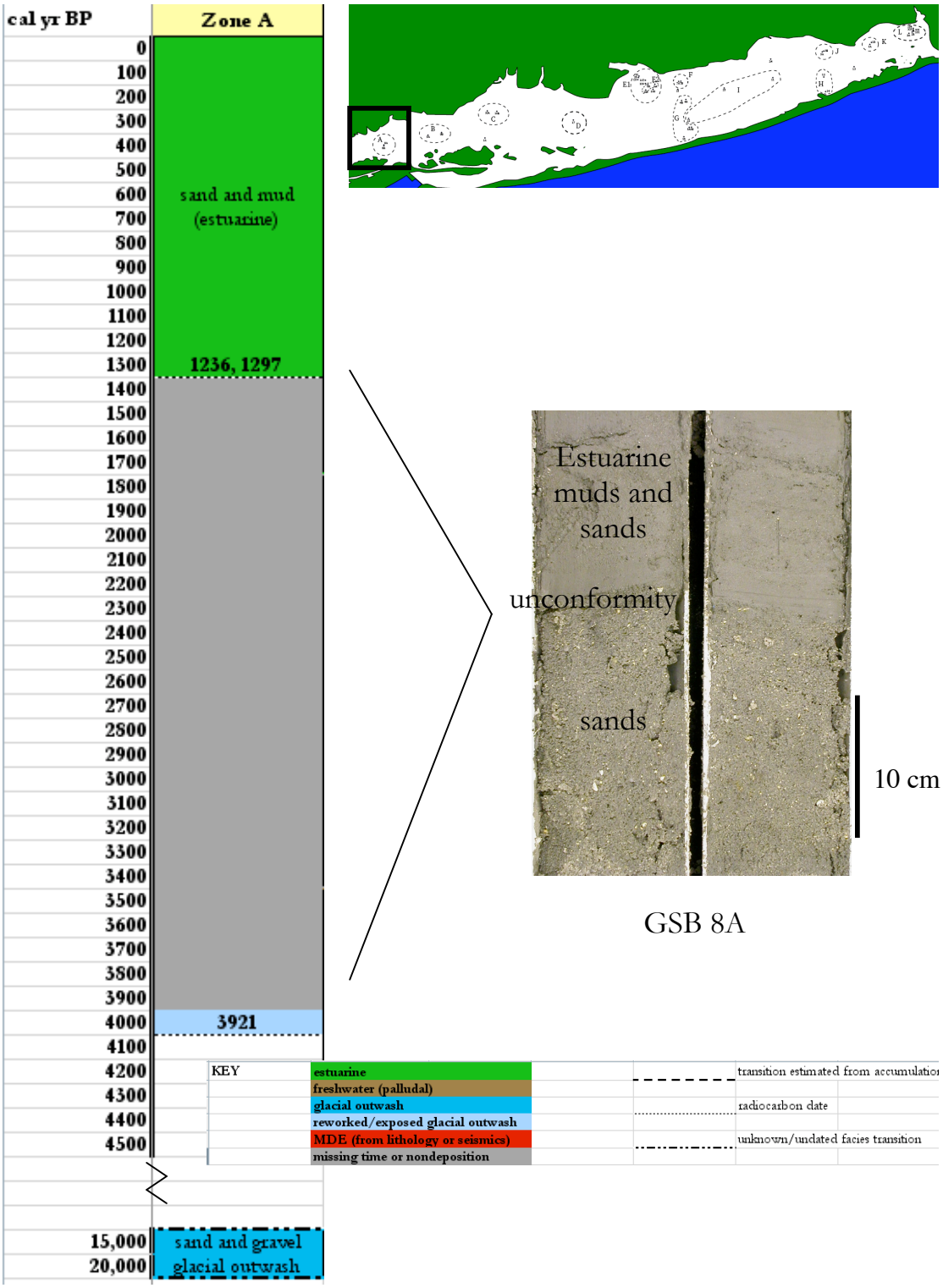

Figure 16: Zone A chronostratigraphy and core image. Key refers to all chronostratigraphy diagrams in this section.

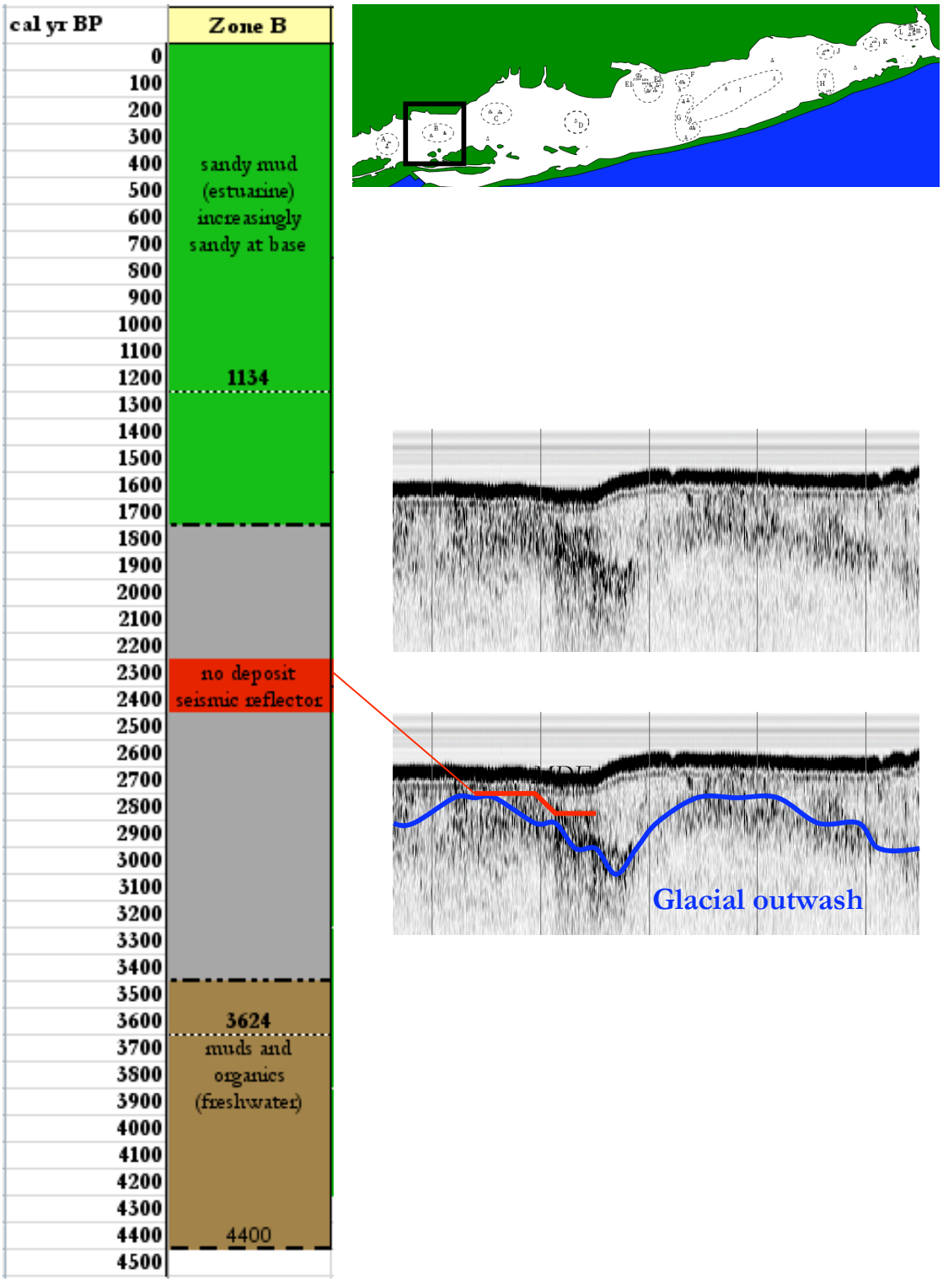

Figure 17: Zone B chronostratigraphy and core images. The deposit is not seen in cores taken from this location, however the MDE reflector is faintly seen in zone B and corresponds to slight density changes in sediment rather than a sand or gravelly deposit.

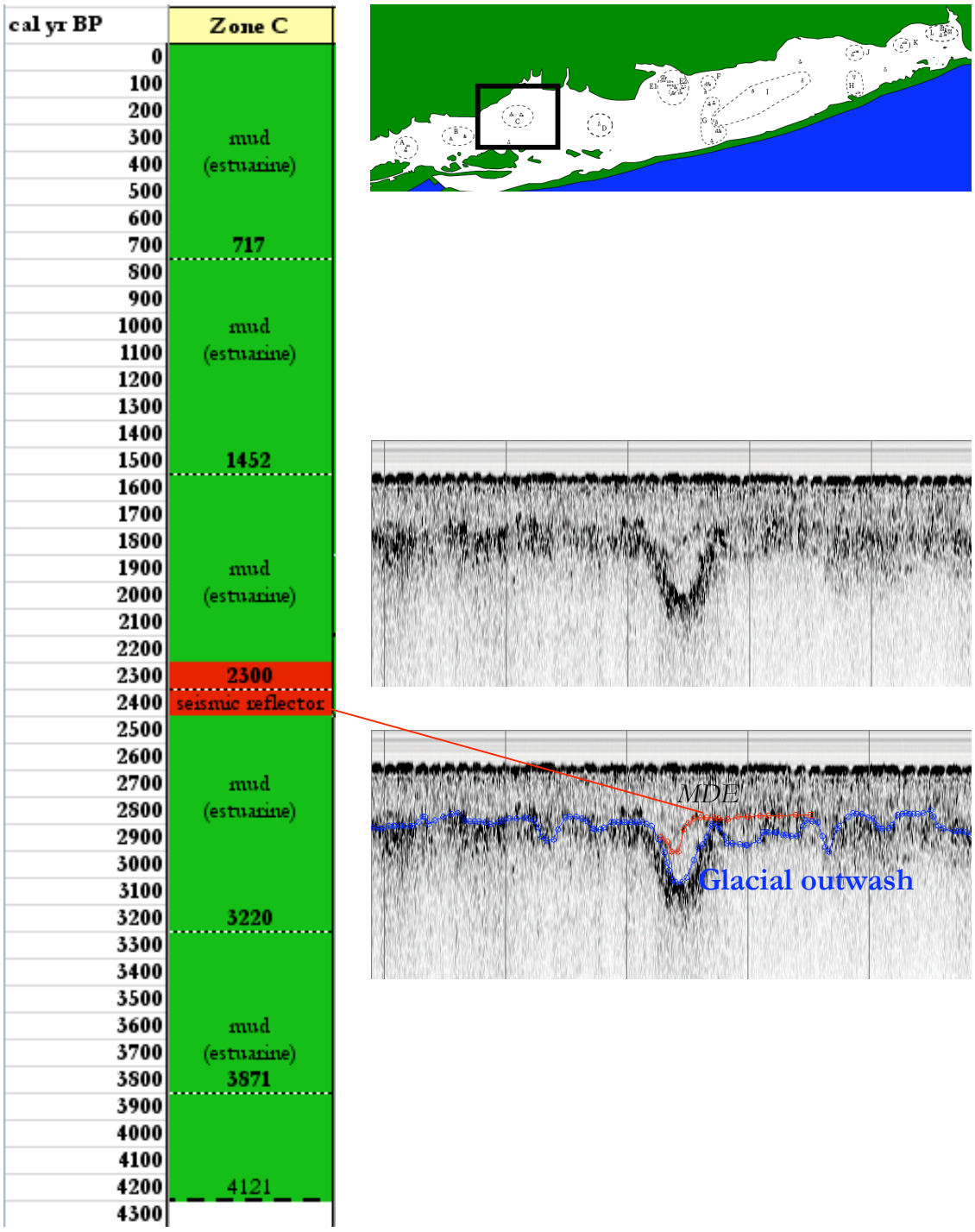

Figure 18: Zone C chronosgratigraphy and seismic image. Although no deposit is found in the two cores taken in this zone, the MDE reflector is seen in zone C, indicating the deposit may be found in portions of zone C not cored.

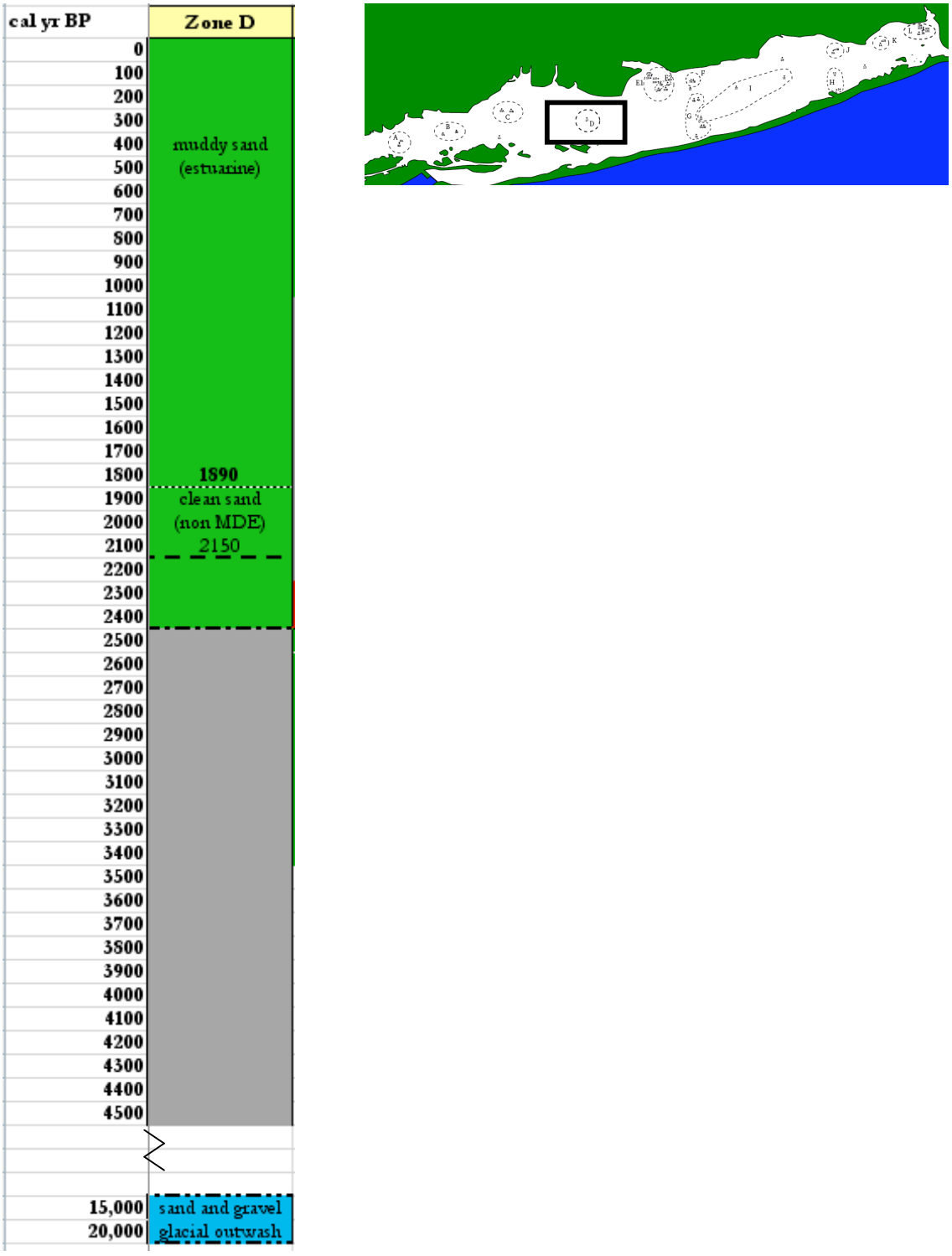

Figure 19: Zone D chronostratigraphy

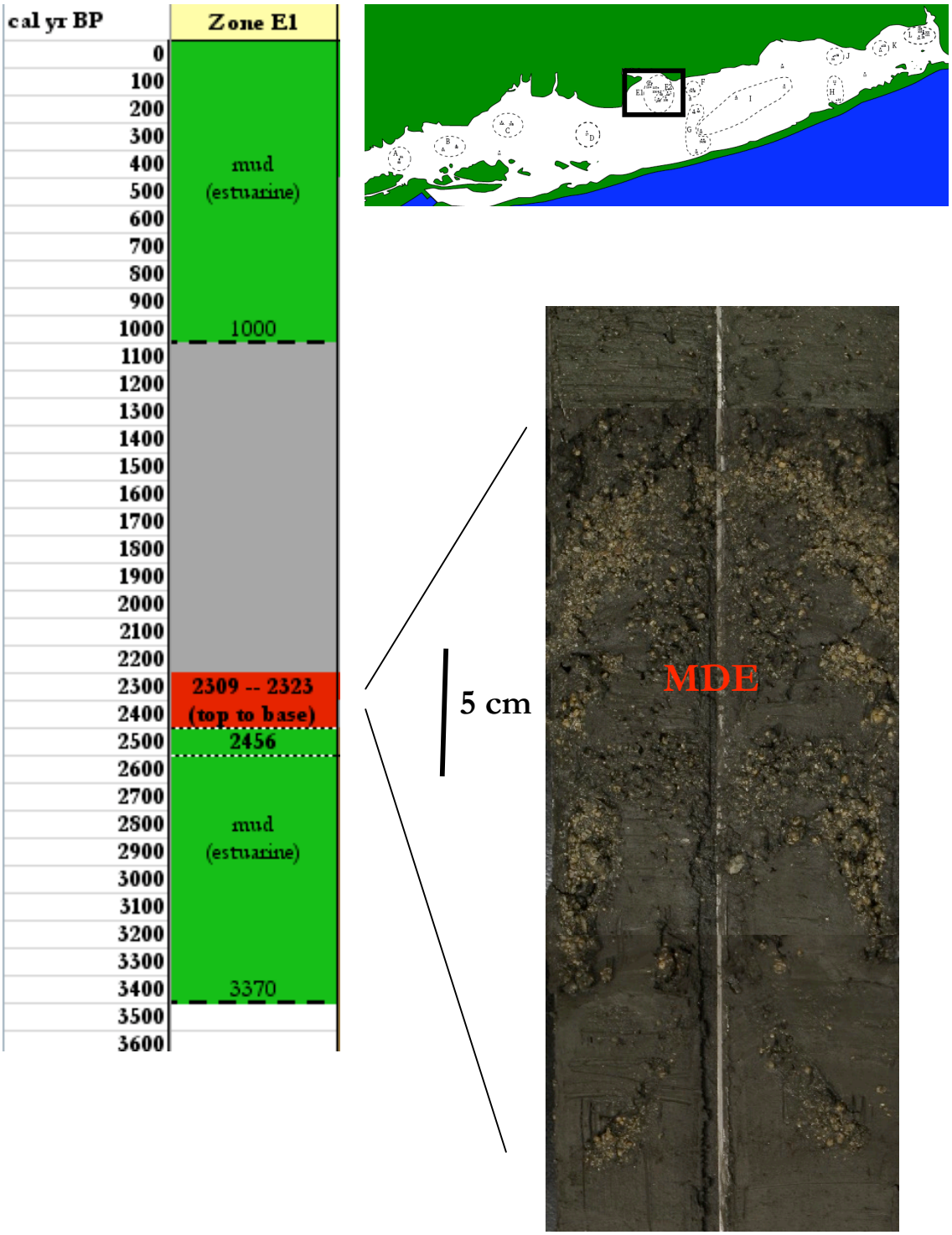

Figure 20: Zone E1 and image of dense, articulated, sand-dwelling *Gemma gemma* bivalves in a matrix of estuarine muds.

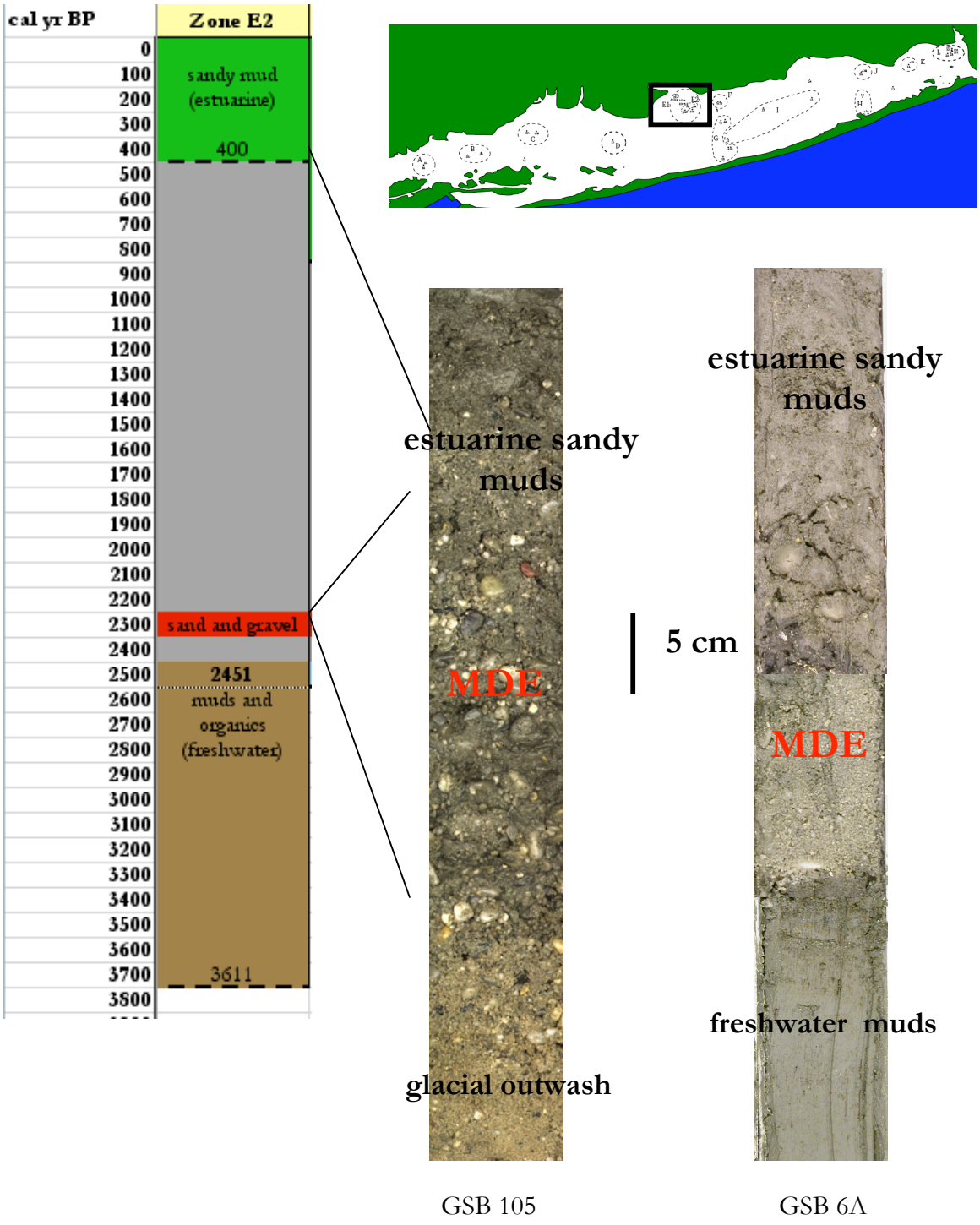

Figure 21: Zone E2 chronostratigraphy and images of the sand and gravel MDE layer from cores 6A and 106. As can be seen in the photograph, core 105, does not contain the long-lived freshwater environment. The MDE deposit in this core sits at a higher elevation and closer to the modern shore, indicating it was likely a subaerial rather than subaqueous environment at the time the MDE layer was deposited.

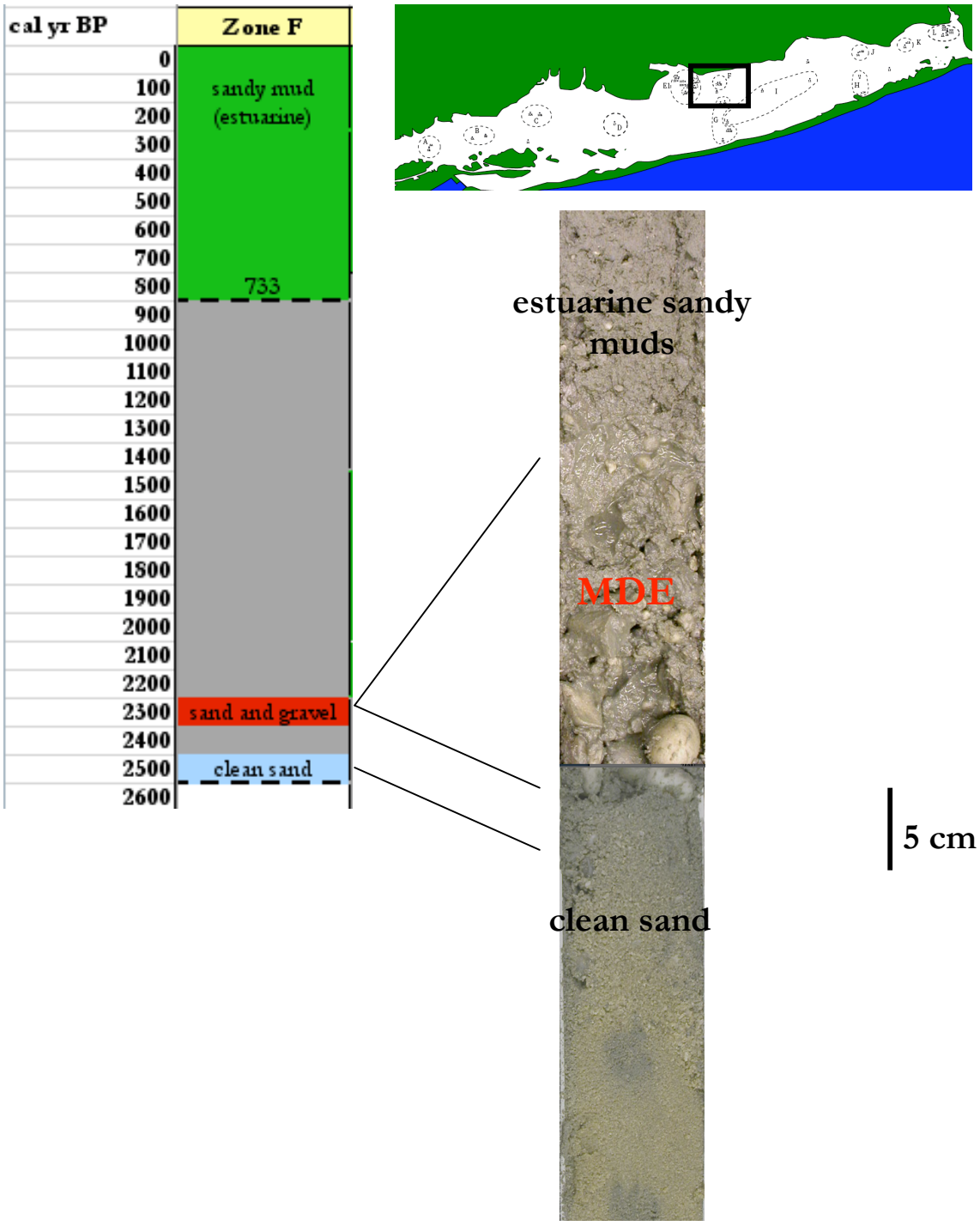

Figure 22: Zone F chronostratigraphy and image of sand and gravel MDE layer from core 7A.

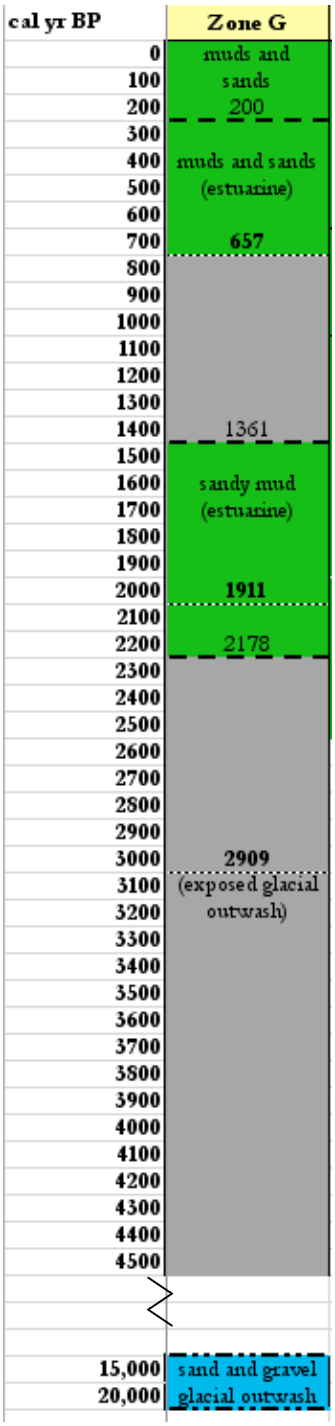

Figure 23: Zone G chronostratigraphy.

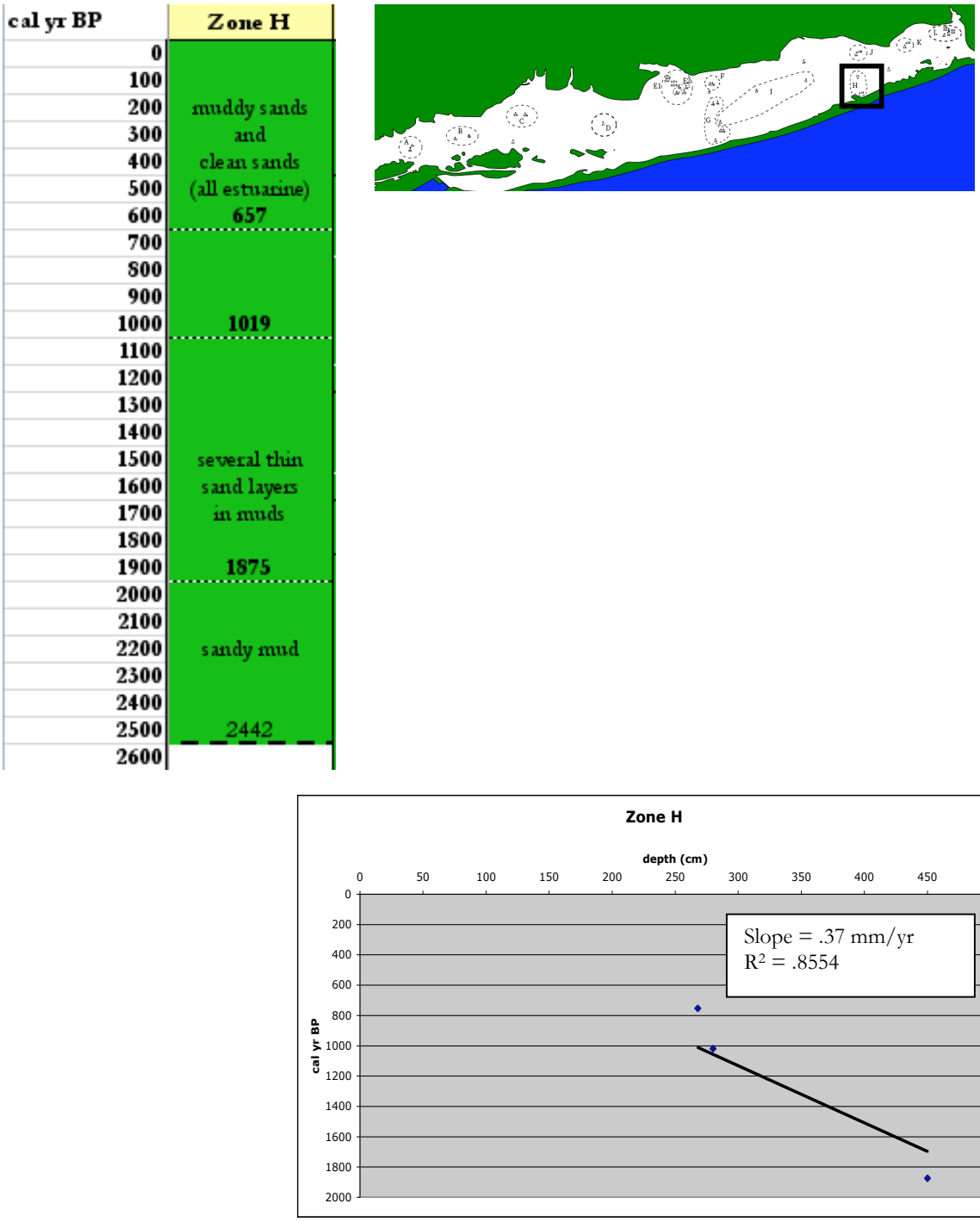

Figure 24: Zone H chronostratigraphy. 3 calibrated radiocarbon dates from the zone show a .37 mm/yr net accretion rate.

cal yr BP	Zone I
0	
100	
200	muds and sands (estuarine)
300	
400	418, 495
500	
600	
700	738
800	
900	
1000	
1100	1112
1200	1269, 1221
1300	
1400	
1500	1546
1600	1663
1700	
1800	1875
1900	
2000	
2100	
2200	
2300	muds (estuarine)
2400	
2500	
2600	2620
2700	
2800	
2900	
3000	
3100	

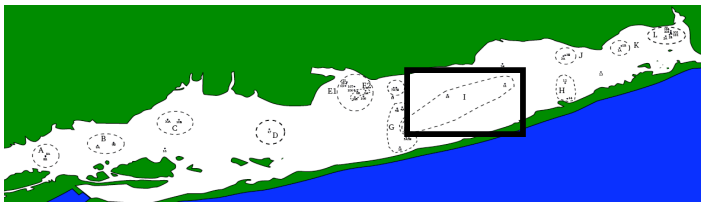

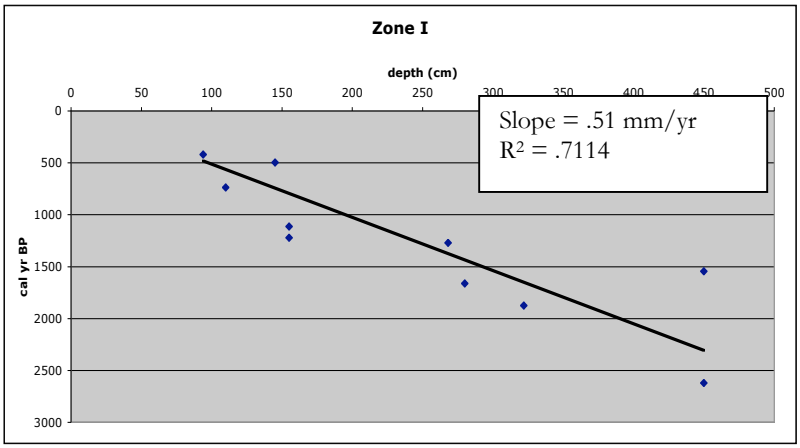

Figure 25: Zone I chronostratigraphy. The diagram shows a continuous estuarine environment throughout the past 3,000 years, however accretion rates indicate there may have been significant gaps in sedimentation during this time period that cannot be resolved.

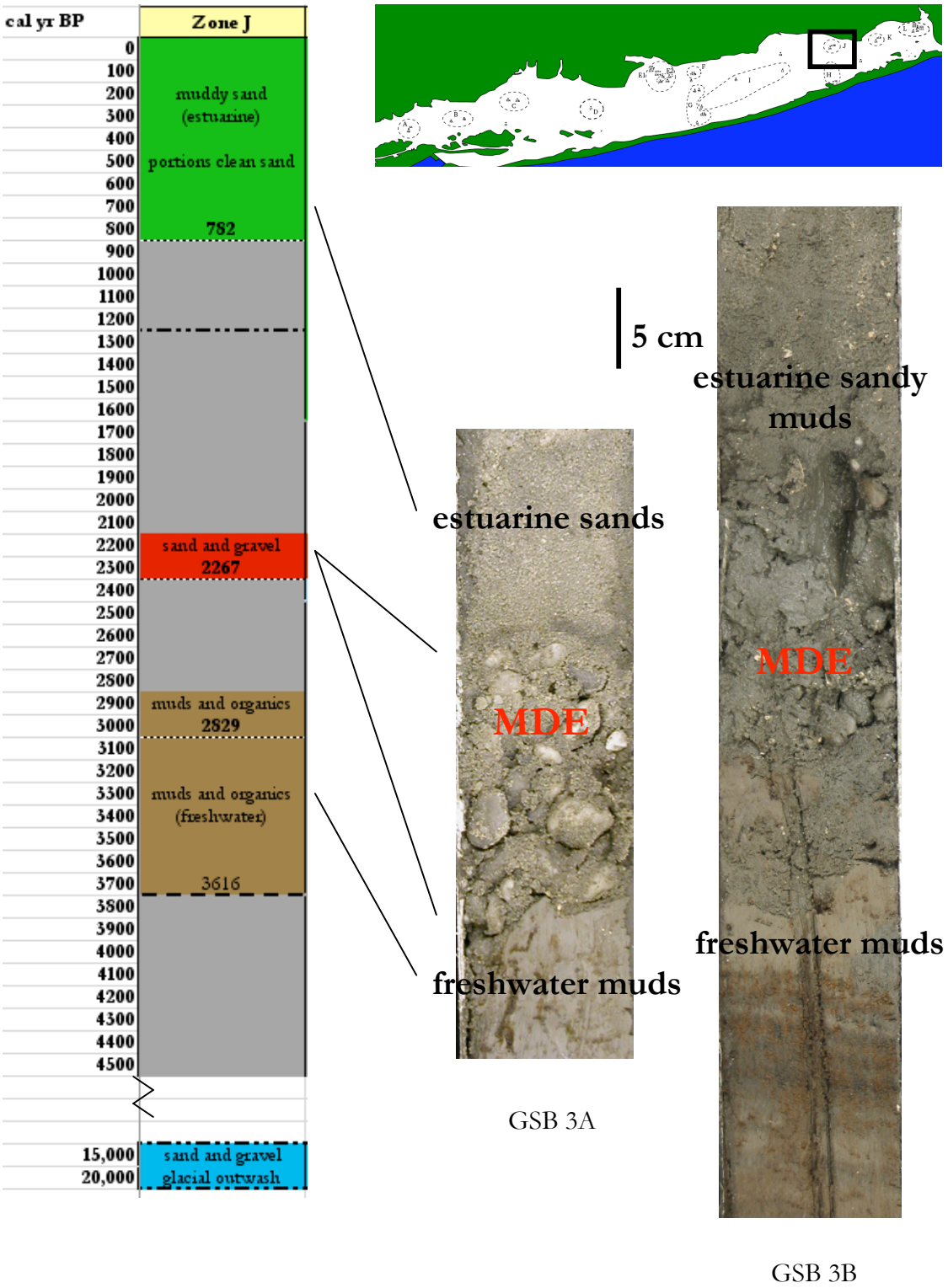

Figure 26: Zone J chronostratigraphy and core images.

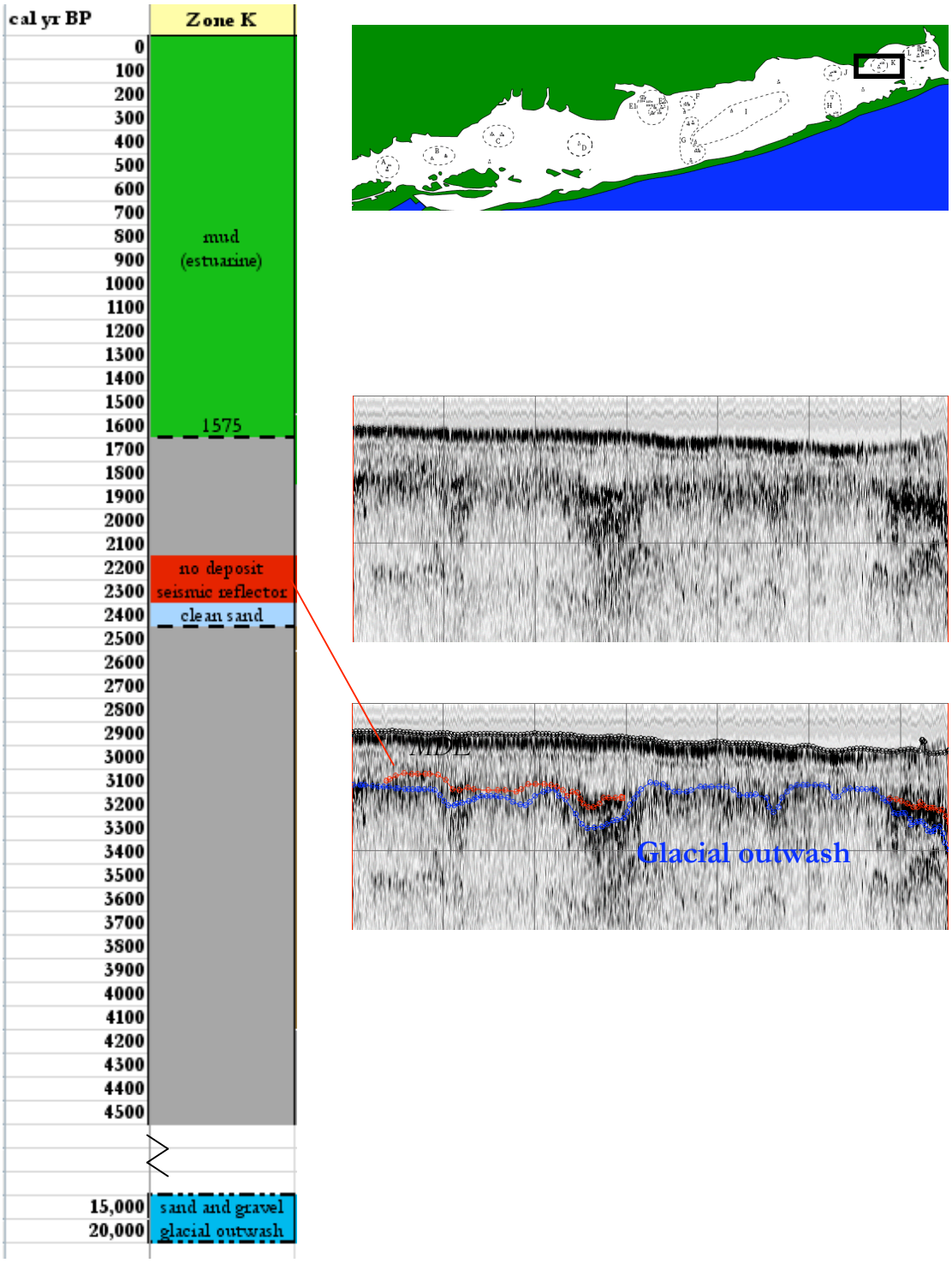

Figure 27: Zone K chronostratigraphy.

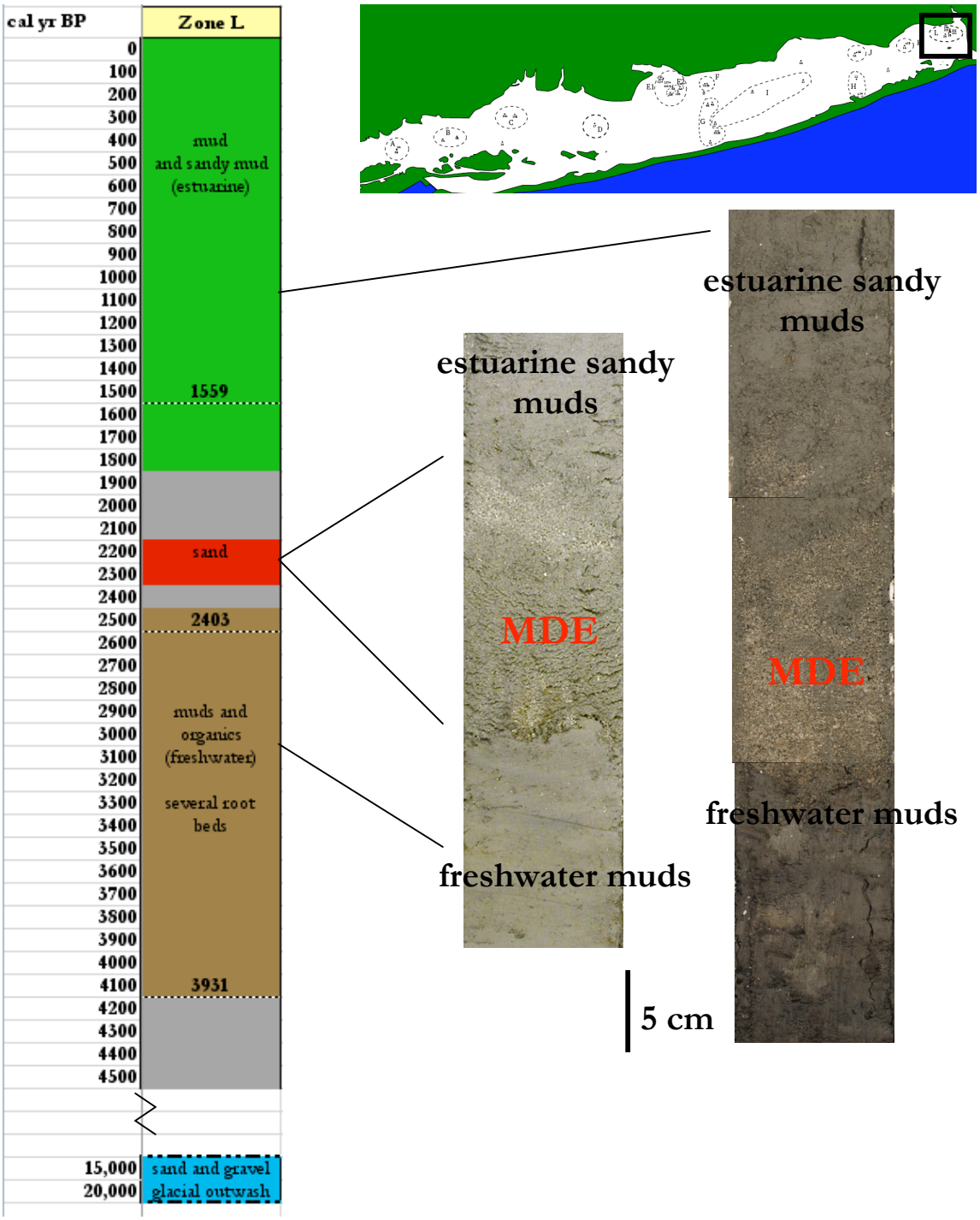

Figure 28: Zone L chronostratigraphy and images of the sandy MDE deposit from cores 2A and 2B. Slight color difference in portions of the core is a camera artifact. As in zones E2 and J, the freshwater environment was established early in the estuary's history in this area. Cores 102 and 104 also are located in zone L, contain the MDE layer and can be seen in Figure 7.

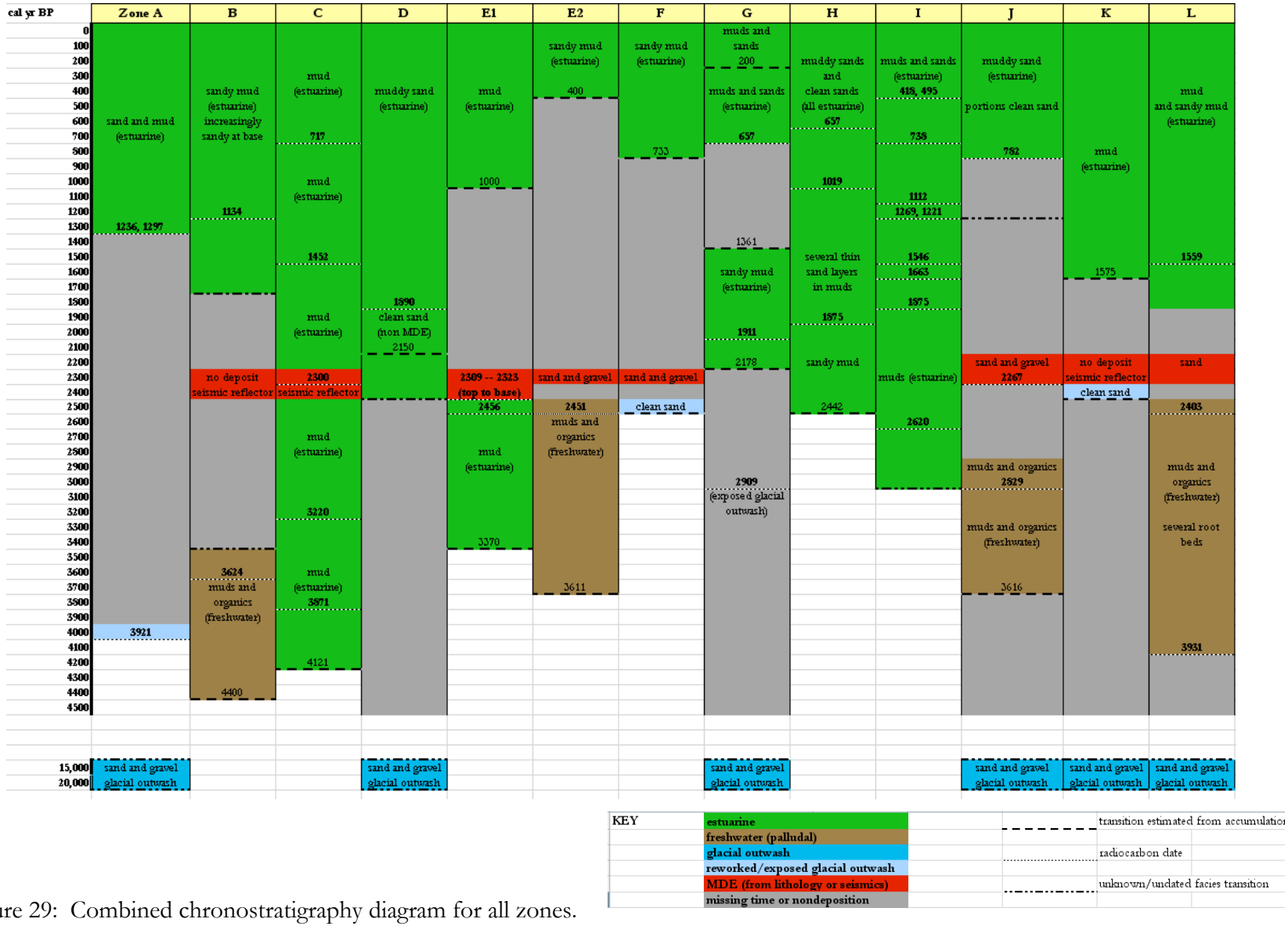

Figure 29: Combined chronostratigraphy diagram for all zones.

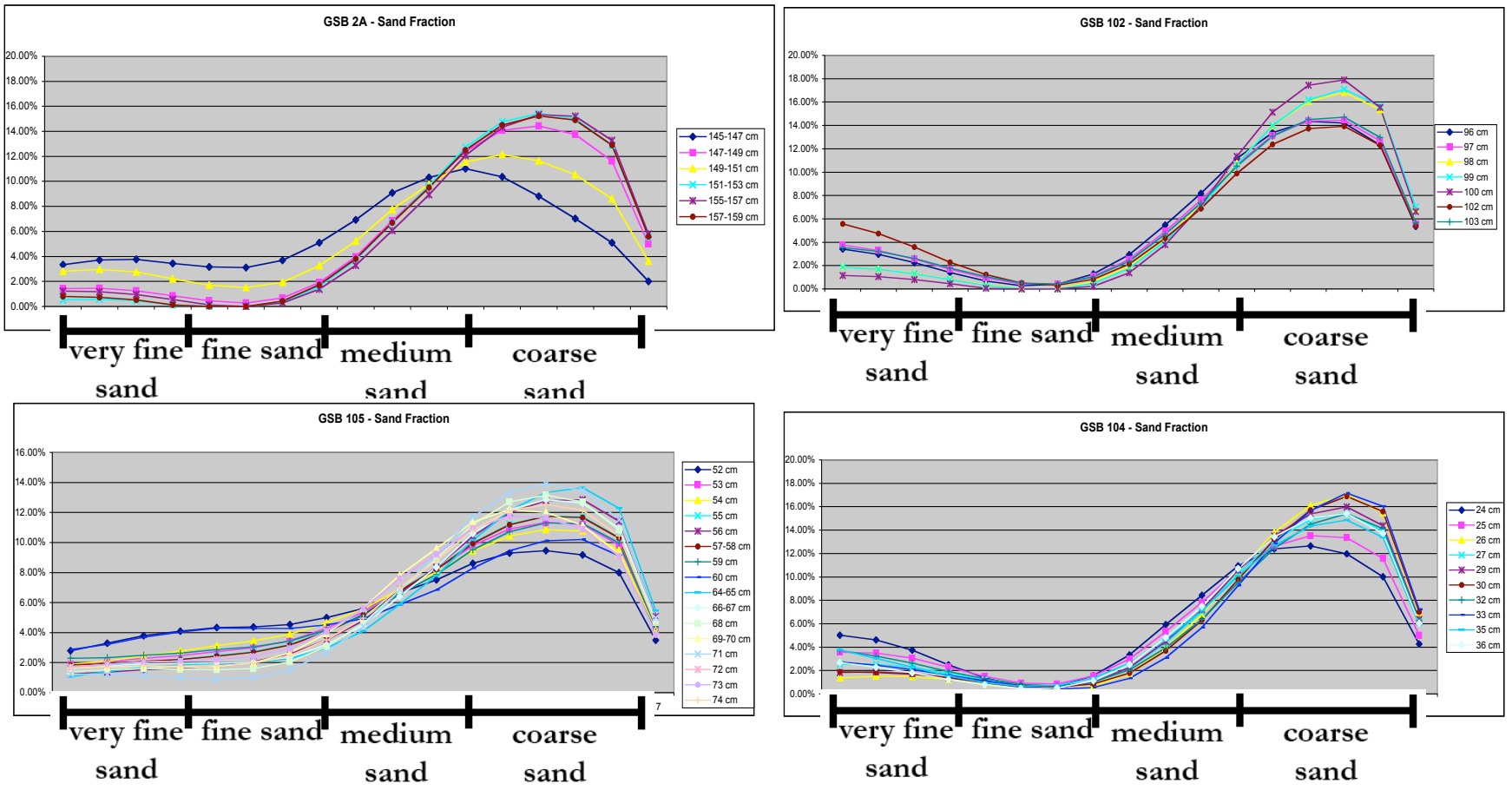

Figure 30: Sand grain size data for select samples of the MDE. In the sand fraction, the deposit appears relatively homogenous with slight fining up trends seen. Sand size distribution also appears consistent with modern and paleo sand samples in the estuary (Figure 33), indicating the deposit was likely quite locally sourced.

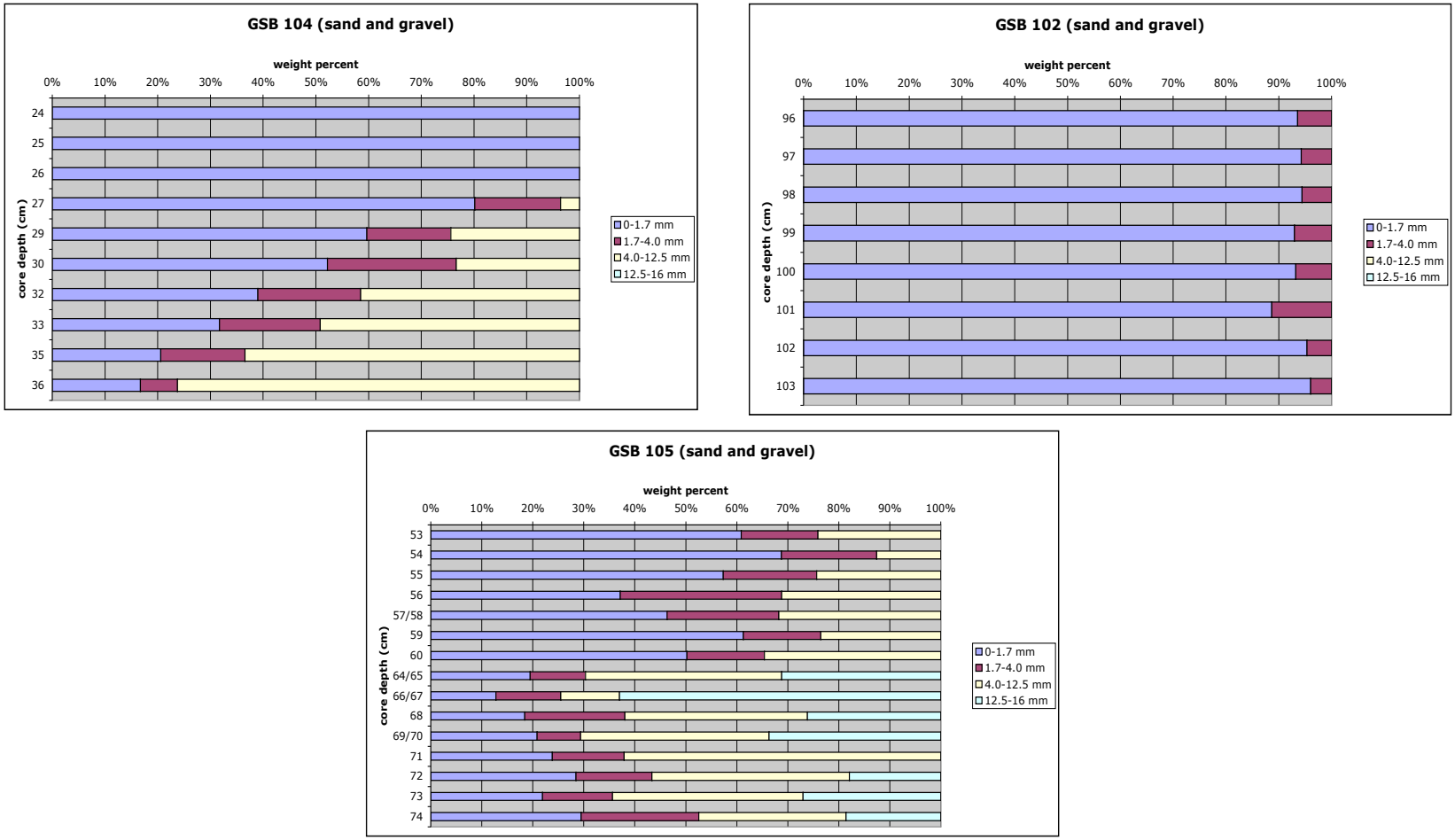

Figure 31: Sand and gravel grain size data for select MDE samples. While medium and coarse sands dominate the sand fraction, a more distinct fining up pattern is visible in cores such as GSB 104, when both sands and gravels are considered. Other cores, such as GSB 102 and GSB 105 however show slight to no fining.

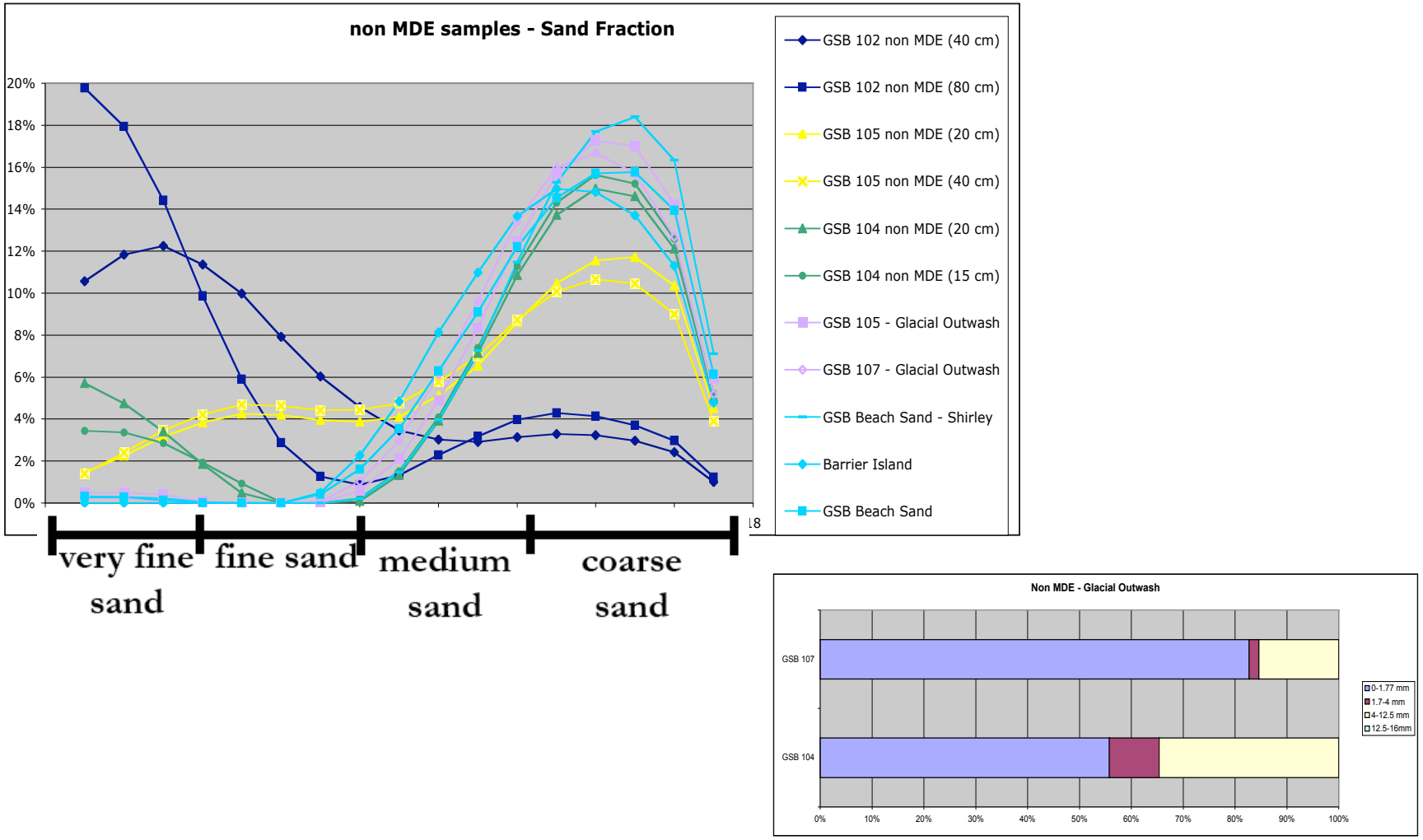

Figure 32: Grain size data for non-MDE sand samples as well as the sandy and gravelly glacial outwash. Sand samples from throughout the estuary are dominated by medium and coarse sands, with the exception of a sand sample from GSB 102 which contained finer materials.

DISCUSSION

What mechanism or process formed the MDE layer?

The characteristics and distribution of the MDE deposit in the Great South Bay that were detailed in the previous section provide key information for determining the origin of the layer. From the introduction, the three most plausible theories for the deposit's formation are:

- Transgressive lag layer
- Storm or hurricane
- Tsunami

While the storm and tsunami are instantaneous events in geologic time, a transgressive lag layer is the result of sea-level rise over hundreds to thousands of years and the lag deposit formed from the process. The first step is to determine whether the MDE was formed rapidly as an event layer or is time-transgressive and formed over 100s of years.

Transgressive lag layer

Figure 33 shows an example of a continuous, clear segment of the MDE reflector in the seismic record. As was shown earlier in Figures 9 and 14, the distribution of the deposit was mapped in that record. Discrete segments of the mapped deposit were also analyzed for their length, range of depths covered, and location (Appendix B). In this analysis, however, there was greater variability in the orientation of seismic lines than in the MDE spatial data; thus any statistical analyses would be more reflective of trends of acquisition than of trends in the data. Nevertheless, clear, continuous segments such as the one shown in Figure 33 provide crucial information to understanding the origin of the MDE.

Transgressive deposits, or transgressive lags, are newly flooded coastal surfaces of coarse sediments formed by landward translation of the shoreface, and they tend to be highly variable depending upon local topography and sediments(Cattaneo and Steel 2003). In estuaries, transgressive deposits generally are complex due to both marine and fluvial processes and often infilling channel segments but show an overall landward and upward trend of movement as sea level rises and overtops the shoreface (Dalrymple 1992). As illustrated earlier, the MDE deposit in Great South Bay extends across extensive topography, often as a contiguous layer. If the deposit is related to sea level during the Holocene, its elevation should roughly track the rate of rise of approximately 1 mm/yr (Varekamp 1992). , and the MDE deposit in the Great South Bay does gain in elevation landward (Figure 11). However, the key diagnostic feature of a transgressive lag deposit in an environment such as the Great South Bay is an unconformable contact between non-marine and marine deposits with the potentially coarse lag deposit separating them (Cattaneo and Steel 2003).

The example in Figure 33 rises from 3.2 to 0.9 m below the sea bed, a change of approximately 2.3 meters. For this continuous segment to have formed from transgressive processes, tracking sea level as it rose, it would take (2300 mm) / (1 mm/yr) or 2,300 years to accumulate. This substantial time span is not evidenced by basal radiocarbon dates of the MDE, which, error included, encompass at most hundreds not thousands of years. Although the visual and stratigraphic character of the MDE deposit could be consistent with a transgressive lag deposit, none of the 6 radiocarbon dates taken near the base of the deposit, nor the multiple dates taken near its top, show the immense time that would be needed to develop the deposit via sea level processes. The deposit is instead consistent with a single high-energy event striking the estuary.

Even in areas where both sea-level change and tsunami events are known and well constrained, sand and gravel deposits may be misinterpreted (Bondevik 1998). In the Bondevik study, previously published works had misidentified a tsunamigenic deposit from the 7000 yr BP

Storegga tsunami in Norway. While both tsunami and lag deposits were present in the study area, all had been attributed to transgressive lag layers due to Holocene sea-level rise. The major defining characteristic between the two was found to be the erosive basal surface of the tsunami deposit, a feature that was lacking in the lag layers. A tsunami will have a much higher energy than the waters from rising sea levels, ripping up sediments and redepositing them. As all instances of the MDE deposit in Great South Bay , basal contact is a sharp, irregular rip-up surface, sometimes including rip-up clasts. Thus, its similarity to the tsunamigenic deposits in Norway is suggestive of formation via a high energy event rather than the ongoing process of sea level rise.

Differentiating storm and tsunami deposits

Although spatial and lithologic characteristics suggest that a single event formed the MDE deposit, the specific type of event remains to be determined. Large storm events as well as a modest tsunami are both plausible as sources. Due to their inherent similarities, such as the reworking of local sediments, many studies have been undertaken to establish criteria to distinguish coastal storm deposits from tsunamigenic deposits (e.g. Tuttle 2004; Morton 2007; Kortekaas 2007).

Differences between storm and tsunami deposits may be subtle but result from hydrodynamic differences in the processes that form them. Storms are high energy and can potentially entrain and transport gravel-sized sediments, but they do so via short-period waves where the principal mode of transport is as bedload. Short-period storm waves also do not extend far landward, rather dissipating their energy rapidly at the shoreface.

Tsunamis are also high energy events that may transport large particles, but they have a very long period and transport the majority of their sediment as suspended load (Morton 2007). As the tsunami wave reaches peak inundation and its velocity slows, the suspended load, usually sands, will settle from suspension. Heavier particles will begin to settle at higher wave velocities while finer

sediments remain in suspension, thus these particles tend to form a fining up sequence (Jaffe 2007). In the case of the Great South Bay, the MDE deposit shows only modest fining in its sand sequences. As the MDE deposit and other sand deposits in the estuary are highly concentrated with coarse sands, this lack of fining in the MDE sands is likely a result of the source material rather than its transport mechanism. Although not conclusive, the grain size data from the MDE deposit suggest that it could have been formed by sediment falling out of suspension during a tsunami .

When the long period tsunami wave inundates the coastal area, it floods the coast and inland, ripping up existing topography as it first hits the coast and depositing it further inland (Jaffe and Gelfenbaum 2007; Gelfenbaum and Jaffe 2003). Rip-up clasts formed in the erosion zone from this process are found exclusively in tsunami deposits rather than layers formed from a storm (Goff 1998; Kortekaas 2007). These different zones of erosion and deposition also tend to create tsunami deposits that drape over existing topography as the MDE reflector is seen to do, rather than truncate it (Morton 2007).

When applied to the MDE layer, six of seven of the major deposit characteristics used to differentiate tsunami deposits from storm deposits match (Table 4), indicating that the MDE layer is consistent with a tsunamigenic deposit. Although storm and tsunami deposits share many common characteristics, the presence of rip up clasts as well as a draped landscape conformity suggest the MDE deposit is more in line with characteristics of a tsunami deposit rather than a storm layer.

Table 4: Comparison of tsunami and storm deposit characteristics (summarized from Morton et al. 2007, Kortekaas et al. 2007, and Goff et al. 2001)

Deposit Characteristic	**Tsunami Deposits**	**Storm Deposits**	**MDE deposit**
Lower contact	Erosional and/or unconformable	Erosional and/or unconformable	Erosional and unconfomable (~100 yrs)
Deposit thickness	Usually <25 cm	Usually >30 cm	5-30 cm
Rip-up clasts	Present	Absent	Present
Grain size	Muds to boulders	Sands, occasionally gravel	Sands and gravel
Landscape conformity	Mimics or drapes existing landscape	Fills lows and levels landscape	MDE seismic reflector drapes over existing topography (glacial outwash reflector)
Sorting	Inland fining	No trend or inland fining	Slight inland fining
Shell beds	Shell-rich units common and shells are often articulated	Individual broken shells common	Dense, articulated bivalve bed (*Gemma gemma*)

How does the MDE deposit fit into the geologic history of the Great South Bay through the late Holocene transgression?

Chronostratigraphic context of MDE layer

The chronostratigraphy of Great South Bay suggests that most areas of the estuary share a generally similar sedimentary succession through the Holocene transgression, changing from a braided outwash plain to freshwater and brackish marshes to finally the modern estuarine environment (Figure 29). However, despite the bay's small size, the different areas of the bay seem to be extremely heterogeneous in the evolution and duration of these different facies depending upon location.

Areas of higher elevation, whether on the banks of an incised channel, or slightly further inland contain muds and organics from fresh to brackish marshes that are not found in deeper and more seaward portions of the bay. Areas nearer to the modern barrier island, which presumably formed by at least 4000 yr BP, also contain layers of clean sandsrelated to inlet migrations, barrier breachings, and storm overwashes. In every zone except E1, the MDE also divides the organic intertidal muds from the modern subtidal estuarine muds. Cores from E1 are located in one of the deepest sections of paleochannel in the estuary and likely infilled earlier than areas with shallower glacial-outwash basement , making it logical that the estuarine sequence preceded the 2300 yr BP MDE. In every zone, however, after 2300 yr BP the estuarine system fails to revert back to the pre-2300 depositional environment, indicating the possibility that the origin of the MDE deposit could be the cause of the environmental changes.

Bay wide depositional hiatus post-MDE

In addition to potentially causing the shift in the depositional environment of the estuary, the MDE is also correlated with a 1000-2000 yr distinct period of non-deposition in the estuary's

history. Zones containing the MDE deposit (B, C, E1, E2, F, J, K, and L) as well as zone A show visible unconformities and significant gaps based upon radiocarbon dating. The other 3 zones (D, H, and I) do not show an unconformity in the chronostratigraphy chart because no visible stratigraphic unconformity was seen in cores. However, these latter 3 zones contain a depositional hiatus revealed through analysis of sedimentation rates, so although it was not resolvable in the sediment record, they do not appear to be exempt from bay wide patterns.

The MDE, therefore, is strongly correlated with a period of great change in the sedimentological history of the Great South Bay centered around 2300 yr BP. Perhaps the event was not influential enough to drastically alter the existing landscape, because the underlying glacial outwash topography is never seen to be truncated, but it is sufficiently influential to change it just enough to alter the depositional regime. This suggests a high sensitivity of the Great South Bay system to such an event. As its sedimentological characteristics are consistent with a tsunami strike, and the coast is still vulnerable to tsunami, understanding its impact on such a system is critical and requires further scrutiny that is not addressed in this study.

Related Studies

Evidence from several independent studies also shows a distinct change at the 2300 yr BP period of the Holocene (Figure 34) in the New York – New Jersey coastal region. Geologic evidence seems to show that the potentially tsunamigenic ~2300 yr BP event had a considerable and enduring impact on the coastal system.

Tappan Zee, NY

Sub-bottom reflection data and cores show a prominent unconformity of several hundred years in the Tappan Zee area of the Hudson River estuary (Carbotte 2004). The unconformity is onlapped by deltaic deposits from the nearby Sparkill Creek and date to 2200 cal yr BP (Carbotte 2004; Slagle 2006). Cores in the area also show several distinct woody debris layers dated to a similar age. Sedimentation rates in the area have consistently been within a few mm/yr during the late Holocene (Carbotte 2004, Pekar 2004) making deposits of this thickness highly anomalous. Fragments from the woody layer date to 1999, 2215 and 2355 cal yr BP. The deposit is potentially resultant of sediment and debris liberated from a coastal tsunami strike and carried upstream.

Sandy Hook, NJ

Two sediment cores taken from the protected Sandy Hook area of Raritan Bay document a 50-cm thick mass wasting event dated to 2210 cal yr BP at its base. The deposit shows overturned beds and clasts of terriginous muds mixed with estuarine mollusks. At this time, this portion of the bay was open to the Atlantic, as the Sandy Hook spit did not develop until 1500 yr BP. Cores in this area show the period from the 2300-yr BP event until ~1600 yr BP as a period of non-deposition.

Deposit characteristics such as the terriginous clasts are often characteristic of tsunami deposits (Morton 2007).

ODP Site 1073

On the nearby upper slope of the New York – New Jersey continental shelf, a sandy mass flow deposit is seen, its base dated at 2120 yr BP (McHugh and Olson 2002). The stratigraphy well documented in the ODP cores in the area indicate that, with the exception of the Hudson Canyon system, storms rarely transport sediments to this point on the continental shelf (Moore 2002; McHugh 2004). The anomalous mass flow deposit appears to be related to the same high energy event responsible for the MDE emplacement.

Newburyport, MA

Evidence of a late Holocene tsunami is also seen further north in the Newburyport, Massachusetts. As described in a USGS technical report (Tuttle 2008), liquefaction features related to probable paleo-seismicity as well as a sandy deposit is seen in the coastal marshes. In one location the sand layer truncates a killed tree. The sand layer fines upwards and is described as similar in size, location, and lithology to sand deposits seen from the 1929 Grand Banks tsunami and has been described as potentially tsunamigenic. Five calibrated radiocarbon dates from the paleosols immediately below the sand layer, the killed tree, and the overtopping sediments constrain the date of the event to approximately 2300 yr BP. The nature of the deposit as well its location and correlation of dates with the MDE suggest a potential emplacement by the same event. A prior segment of the same USGS study also found distinctive sand layers in coastal marshes of New Hampshire as well and noted that they were also possibly tsunamigenic.

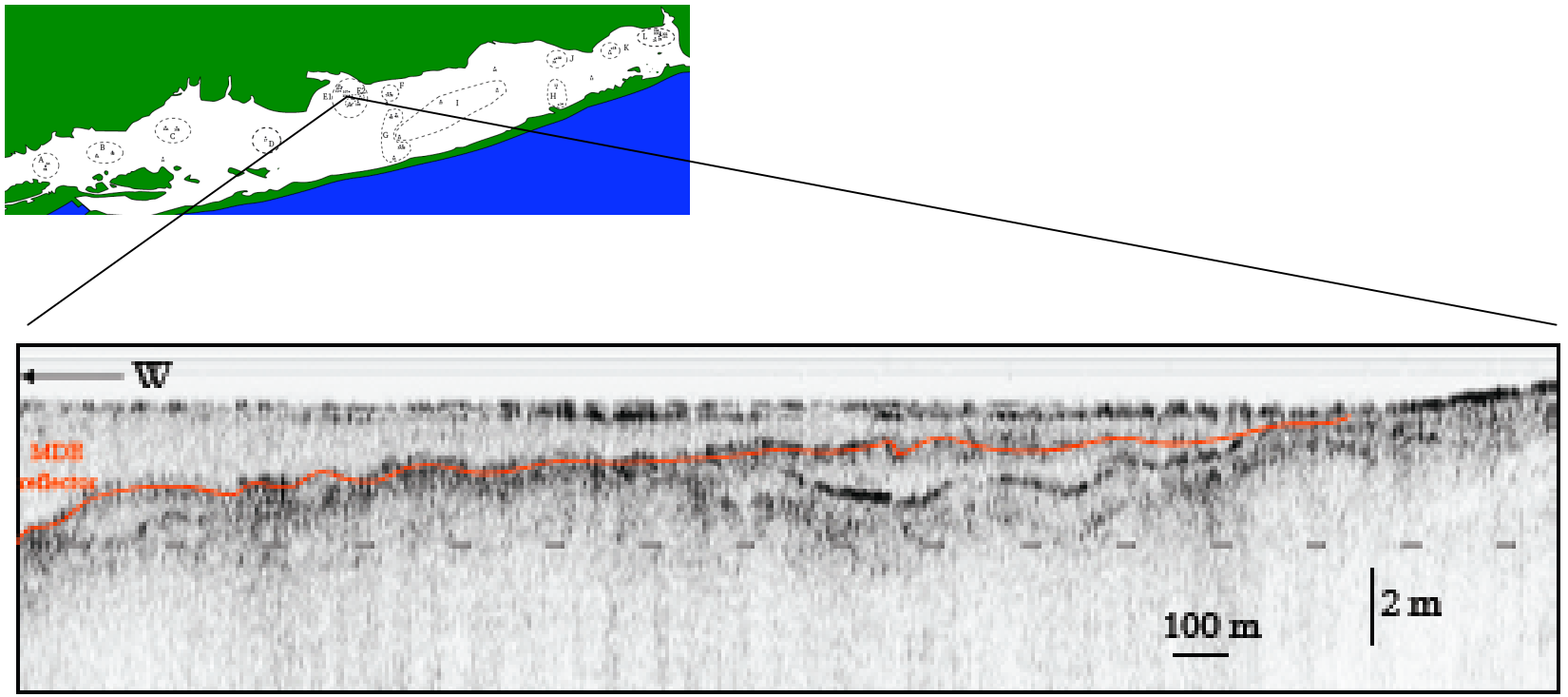

Figure 33: Map and segment of MDE reflector in seismic record showing a continuous 2.3 m change in elevation over approximately 2 km.

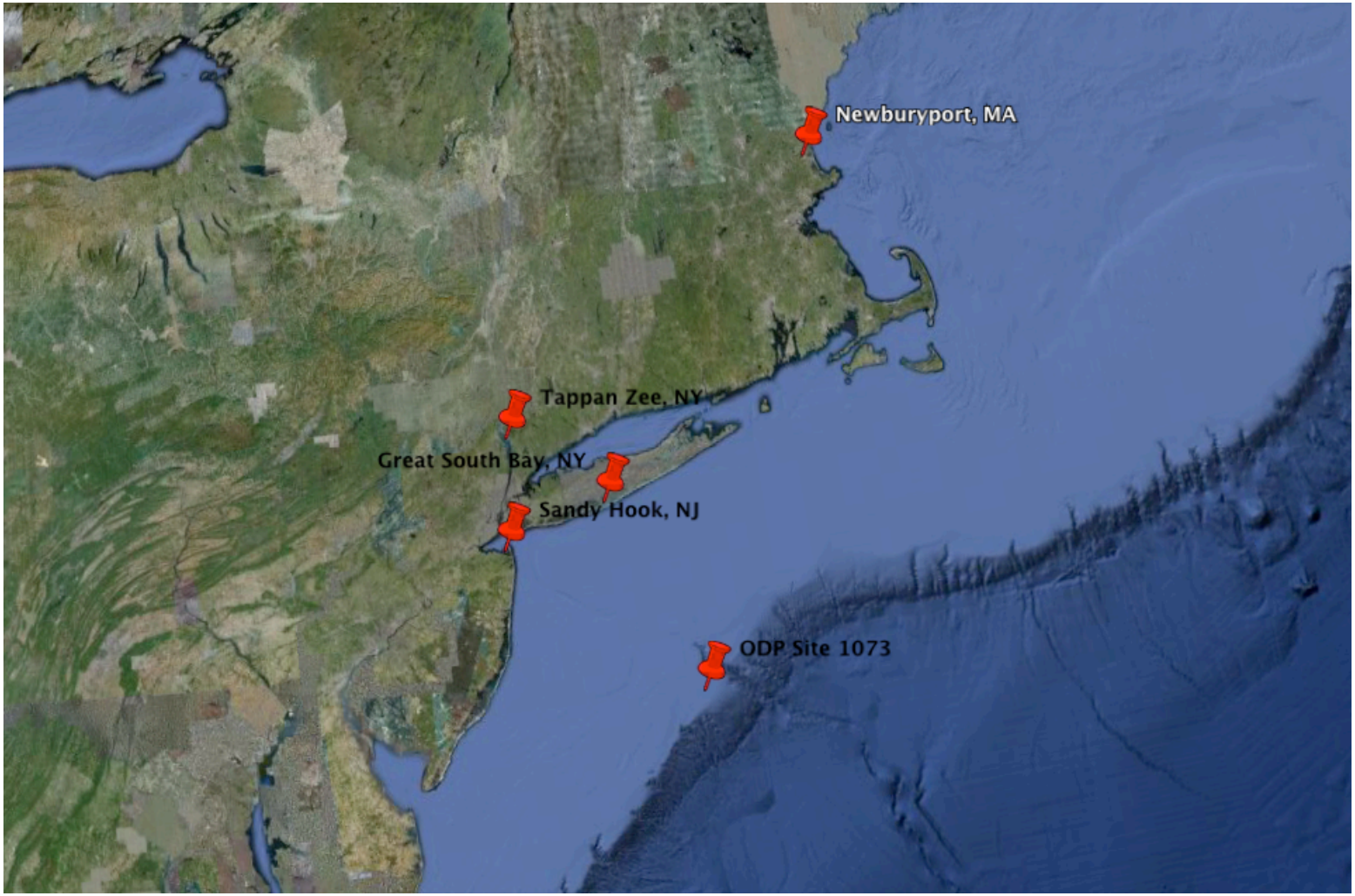

Figure 34: Locations of other related studies on the Atlantic coast showing evidence for an influential high-energy event 2200-2400 yr BP. Great South bay has been highlighted for reference.

CONCLUSIONS

Sedimentological characteristics as well as deposit distribution are all consistent with a tsunami event occurring between 2200 and 2400 yr BP in the New York and New Jersey region. Basal dates from the MDE layer bay wide are strikingly close in age, indicating the MDE was formed by a geologically instantaneous event rather than by processes related to sea level rise and coastal transgression. The event appears to reflect an abrupt and unique transition in the geologic history of the bay. As the New York – New Jersey coast is one of significant human population, understanding the recurrence and impact of such an event is critical and further fieldwork and analyses are required to fully constrain the parameters of the event and its cause. For all of the independent studies detailed, further work is needed to conclusively correlate them to the MDE seen in the Great South Bay. However, there is a remarkable parallel between deposit type, location, and radiocarbon dates that suggests something significant and unique occurred not only in the Great South Bay but along the northern Atlantic coastal system 2300 yr BP.

APPENDICES

Appendix A: All radiocarbon dates and related information from Great South Bay Study

Core	Calibrated Age	Depth (cm below sea level)	Radiocarbon age	Type	Stratigraphic Position
GSB 2A	**1559**	295	2100	Mollusk	mud-dog whelk above MDE
GSB 2A	**2403**	325	2380	Plant/Wood	freshwater organics just below MDE
GSB 2A	**3931**	440	3620	Plant/Wood	wood fragments from freshwater just above outwash
GSB 3A	**2267**	395	2700	Mollusk	articulated shell at base of MDE
GSB 3B	**782**	335	1340	Mollusk	shell from top of gravelly sand MDE
GSB 3B	**2829**	363	2710	Plant/Wood	3 cm below MDE contact into freshwater muds
GSB 4B	**1911**	595	2400	Mollusk	estuarine mud 30 m below transition into sand
GSB 4B	**2909**	643	3230	Mollusk	base of estuarine muds above outwash
GSB 6A	**0**	353	480	Mollusk	clean, non articulated shells above MDE
GSB 6A	**2451**	380	2430	Plant/Wood	1 cm below MDE in freshwater sediments
GSB 8A	**1236**	311	1310	Plant/Wood	
GSB 8A	**1297**	424	1850	Mollusk	10 cm below estuarine muds
GSB 8A	**3921**	461	3504	Plant/Wood	from muddy gravelly sands
GSB 9B	**1134**	411	1680	Mollusk	base of 40 cm thick sand layer within estuarine muds
GSB 9B	**3624**	504	3380	Plant/Wood	upper side of thin sand layer within freshwater sediments
GSB 10B	**717**	366	1260	Mollusk	
GSB 10B	**1452**	439	2010	Mollusk	base of fossiliferous sediments, no shells above 320 cm
GSB 10B	**2300**	494	2283	Plant/Wood	top of non-fossiliferous bed
GSB 10B	**3220**	574	3460	Mollusk	top of fossiliferous sediments
GSB 10B	**3871**	634	4000	Mollusk	base of estuarine muds
GSB 11	**1663**	560	2190	Mollusk	center of 10-cm thick shell layer within estuarine muds
GSB 11	**2629**	730	2970	Mollusk	center of 40 cm thick shell layer within estuarine muds
GSB 12	**753**	268	1310	Mollusk	base of 100-cm thick sand layer within estuarine muds
GSB 12	**1875**	450	2370	Mollusk	top of muddy sand, base of alternating mud and sand layers
GSB 14	**1019**	280	1570	Mollusk	base of 150-cm clean sand unit overlying estuarine muds
GSB 17	**1890**	328	1940	Plant/Wood	top of thick clean sand unit

GSB 18	**657**	370	1200	Mollusk	top of fining up sand, base of mud to surface
GSB 20	**2309**	410	2730	Mollusk	top of MDE, articulated shell
GSB 20	**2323**	425	2740	Mollusk	base of MDE, articulated shell
GSB 20	**2456**	445	2382	Plant/Wood	in estuarine muds below MDE
GSB 22	**738**	400	1290	Mollusk	top of thick shell layer with serpulid worms
GSB 22	**1221**	445	1770	Mollusk	base of thick shell layer
GSB 22	**1112**	445	1660	Mollusk	base of thick shell layer
GSB 22	**1875**	612	2370	Mollusk	near top of basal clean sands, below estuarine sequence
GSB 23	**418**	374	890	Mollusk	abundant Mulinia community
GSB 23	**495**	425	980	Mollusk	shell layer of reefal community
GSB 23	**1269**	548	1920	Mollusk	small shell layer
GSB 23	**1546**	730	2090	Mollusk	top of basal sand/gravel underlying estuarine muds

Appendix B: Full spatial analysis of MDE reflectors. Due to differing orientations of seismic lines as well as gaps in penetration related to sediment type and other interference, reliable statistical analysis could not be performed. Each 'segment' is a discrete, continuous portion of the MDE reflector. Left and right edges indicate orientation of the reflector viewed on screen, not necessarily correlating to east-west.

file name (Triton)	total # of 'segments' in file	minimum depth (m)	maximum depth (m)	depth at 'left' edge (m)	depth at 'right' edge (m)	length of segment (m)	ping at 'left' edge (Triton pings)	ping at 'right' edge (Triton pings)	gradient (from 'left' to 'right')	maximum vertical change (m)
P0	1	1.2	2.04	1.2	2	43	921	1399	0.020	2.040
P1	0									
P2	2	1.54	1.92	1.68	2	140	1168	1479	0.000	1.920
		1.03	1.46	1.27	1	131	2970	3261	0.001	1.460
P3	1	0.94	2.23	1.5	1	1645	all	all	0.000	2.230
P4	1	1	2.72	2.61	1	1635	4320	390	-0.001	2.720
P5	0									
P6	0									
P7	1	1.32	2.16	2.16	2	107	1523	1742	-0.004	2.160
P8	1	0.85	1.56	0.99	1	545	0	1010	0.000	1.560
P9	1	1.15	1.94	1.94	1	110	2177	2405	-0.007	1.940
P10	0									
P11	1	0.96	1.81	1.44	1	346	0	321	-0.001	1.810
P12	0									
P13	4	0.44	1.93	1.93	2	206	1350	1730	-0.002	1.930
		1.89	3.13	2.45	2	164	2569	2879	-0.005	3.130
		1.12	2.13	2.13	2	579	3216	4329	0.000	2.130
		1.73	2.29	1.97	2	175	4610	4943	0.002	2.290
P14	2	2.33	3.32	2.72	3	175	2322	2609	0.003	3.320
		2.38	3.56	2.92	3	185	2945	end	-0.001	3.560

P15	0									
P16	0									
P17	0									
P18	0									
P19	2	0.75	2	1.94	1	500	8190	7244	-0.002	2.000
		0.46	3.19	3.19	1	777	5816	4269	-0.003	3.190
P20	0									
P21	0									
P22	0									
P23	0									
P24	0									
P25	0									
P26	0									
P27	0									
P28	0									
P29	1	1.65	2.15	1.8	2		3620	4067		2.150
P30	0									
P31	0									
P32	0									
P33	0									
P34	0									
P35	0									
P36	0									
P37	0									
P38	0									
P39	0									
P40	0									
P41	0									
P42	0									
P43	0									
P44	0									

P45	0									
P46	0									
P47	0									
P48	0									
P49	0									
P50	0									
P51	0									
P52	0									
P53	0									
P54	0									
P55	0									
P56	1	0.52	2.23	2.23	1	725	2692	3933	-0.002	2.230
P57	0									
P58	0									
P59	0									
P60	0									
P61	0									
P62	0									
P63	0									
P64	5	2.02	2.02	2.02	2	76	2731	2852	0.000	2.020
		0.56	1.44	1.19	1	329	2948		0.001	1.440
		1.13	1.44	1.44	1	58.5	4896	5103	-0.005	1.440
		1.28	4	1.28	4	366	5605	6797	0.007	4.000
		1.5	1.85	1.85	2	62	8382	8583	-0.006	1.850
P65	0									
P66	0									
P67	0									
P68	0									
P69	0									
P70	0									

REFERENCES

Bondevik, S., Svendsen, J.I. and Mangerud, J., 1998. Distinction between the Storegga tsunami and the Holocene marine transgression in coastal basin deposits of western Norway. Journal of Quaternary Science 13, 529-537.

Bonisteel, J.M., Peters-Snyder, M. and Zarillo, G., 2004. Barrier Island Migration and Morphologic Evolution, Fire Island Inlet, NY. Shore and Beach 72, 1-25.

Carbotte, S., Bell, R.E., Ryan, W.B.F., McHugh, C.M.G., Slagle, A., Nitsche, F., and Rubenstone, J., 2004. Environmental change and oyster colonization within the Hudson River estuary linked to Holocene climate. Geo-Marine Letters 24, 212-224.

Cattaneo A., and Steel, R.J., 2003. Transgressive deposits: a review of their variability. Earth-Science Reviews 62, 187-228.

Dalrymple, R.W., Zaitlin, B.A., and Boyd, R., 1992. Estuarine facies models: conceptual basis and stratigraphic implications. Journal of Sedimentary Petrology 62, 1130-1146.

Dyke, A.S., Andrews, J.T., Clark, P.U., England, J.H., Miller, G.H., Shaw, J., and Veillette, J.J., 2002. The Laurentide and Innuitian ice sheets during the Last Glacial Maximum. Quaternary Science Reviews 21, 9-31.

Geist, E.L., and Parsons, T.A., 2009. Assessment of source probabilities for potential tsunamis affecting the U.S. Atlantic coast. Mar. Geol, in press.

Gelfenbaum, G., and Jaffe, B., 2003. Erosion and sedimentation from the 17 July 1998 Papua New Guinea tsunami. Pure and Applied Geophysics 160, 1969-1999.

Goff, J., Crozier, M., Sutherland, V., Cochran, E., and Shane, P., 1998. Possible tsunami deposits from the 1855 earthquake, North Island, New Zealand. Geol. Soc. London Spec. Pub 133, 353-374.

Goff, J., Chague-Goff, C. and Nichol, S., 2001. Palaeotsunami deposits: a New Zealand perspective. Sedimentary Geology 143, 1-6.

Goodbred, S., Cerrato, R., and Cochran, J.K., 2007. Geological and Environmental History of Great South Bay, New York. Umpublished Final Report, New York Sea Grant. Stony Brook, NY, 10 p.

Heezen, B.C., and Ewing, M., 1952. Turbidity currents and submarine slumps and the 1929 Grand Banks earthquake. American Journal of Science 250, 849-873.

Jaffe, B., and Gelfenbaum, G., 2007. A simple model for calculating tsunami flow speed from tsunami deposits. Sedimentary Geology 200, 251-265.

Kortekaas, S. and Dawson, A.G., 2007. Distinguishing tsunami and storm deposits: An example from Martinhal, SW Portugal. Sedimentary Geology 2007, 208-221.

LoCicero, P.V.R., 2006. The history of benthic habitat and associated mollusk assemblages in Great South Bay, New York. Unpublished M.S. thesis, Stony Btook University, 192 p.

McHugh, C.M.G., and Olson, H.C., 2002. Pleistocene chronology of continental margin sedimentation: New insights into traditional models, New Jersey. Marine Geology 186, 389-411.

McHugh, C.M.G., Pekar, S.F., Christie-Blick, N., Ryan, W.B.F., Carbotte, S., and Bell, R., 2004. Spatial variations in a condensed interval between estuarine and open marine settings: Holocene Hudson River Estuary and adjacent continental shelf. Geology 32, 169-172.

Morton, R.A., Gelfenbaum, G. and Jaffe, B.E., 2007. Physical criteria for distinguishing sandy tsunami and storm deposits using modern examples. Sedimentary Geology 200, 184-207.

Morton, R.A., Gelfenbaum, G., and Jaffe, B.E., 2007. Physical criteria for distinguishing sandy tsunami and storm deposits using modern examples. Sedimentary Geology 200, 184-207.

O'Reilly, C., Macaulay, P., and Parkes, G, 2007. Atlantic Storm Surge and Tsunami Warning System. Report, Le GéoCongrès international, Quebec, 11/2/2007, 8 pages.

Pekar, S.F., McHugh, C.M.G., Christie-Blick, N., Jones, M., Carbotte, S.M., Bell, R.E., and Lynch-Stieglitz, J., 2004. Estuarine processes and their stratigraphic record: paleosalinity and sedimentation changes in the Hudson Estuary (North America). Marine Geology 209, 113-129.

Rampino, M.R. and Sanders, J.E., 1980. Holocene Transgression in South-Central Long Island, New York. Journal of Sedimentary Petrology 50, 1063-1080.

Schubel, J.R., T.M. Bell and H.H. Carter (Editors), The Great South Bay. State University of New York Press, Stony Brook, NY, pp. 107.

Scileppi, E., and Donnelly, J. P., 2007. Sedimentary evidence of hurricane strikes in western Long Island, New York, Geochemistry Geophysics Geosystems 8, Q06011

Slagle, A.L., Ryan, W.B.F., Carbotte, S.M., Bell, R., Nitsche, F.O., and Kenna, T., 2006. Late-stage estuary infilling controlled by limited accommodation space in the Hudson River. Marine Geology 232, 181-202.

Stuiver, M., Reimer, P. J., and Reimer, R. W. 2005. CALIB 5.0. [WWW program and documentation].

Tuttle, M.P., Ruffman, A., Anderson, T. and Jeter, H., 2004. Distinguishing tsunami from storm deposits in eastern North America: The 1929 Grand Banks tsunami versus the 1991 Halloween storm. Seismological Research Letters 75, 117-131.

Varekamp, J.F., Thomas, E., and Van de Plassche, D., 1992. Relative sea-level rise and climate change over the last 1500 years. Terra Nova 4, 293-304.